

Quantitative Bioprocess Containment Validation

**A thesis submitted for the degree of Doctor of Philosophy
to the University of London
by**

Michael Ian Bradley

Department of Biochemical Engineering
University College London
London
WC1E 7JE

August 1999

ProQuest Number: 10609416

All rights reserved

INFORMATION TO ALL USERS

The quality of this reproduction is dependent upon the quality of the copy submitted.

In the unlikely event that the author did not send a complete manuscript and there are missing pages, these will be noted. Also, if material had to be removed, a note will indicate the deletion.



ProQuest 10609416

Published by ProQuest LLC (2017). Copyright of the Dissertation is held by the Author.

All rights reserved.

This work is protected against unauthorized copying under Title 17, United States Code
Microform Edition © ProQuest LLC.

ProQuest LLC.
789 East Eisenhower Parkway
P.O. Box 1346
Ann Arbor, MI 48106 – 1346

Out of this nettle, danger, we pluck this flower, safety.

Henry IV, Part 1 act 2, sc. 3

William Shakespeare, 1564-1616.

Abstract

The safe use of genetically modified micro-organisms (GMMOs) for the industrial manufacture of therapeutic and other products depends on the design, implementation and validation of effective containment principles. This project has established a test method that can generate quantitative data on bioprocess releases that can be used to validate the containment of bioprocess equipment. A standard tracer gas leak test has been correlated with a quantitative polymerase chain reaction (QPCR) assay for the detection of GMMOs. The QPCR assay for *Escherichia coli* RV308 pHKY531 has been shown to be specific and have a low limit of detection (less than 50 cells in 10 μ L) with a range of 6 orders of magnitude and an error of ± 0.11 logs. This assay has been used to analyse bioaerosol samples collected by an Aerojet General Cyclone.

Throughout the course of the project, work has been carried out to improve the collection efficiency of a cyclone sampler and to investigate the effects of various approaches to bioaerosol sampling in a process environment. Using this method a good correlation has been observed between the spatial location of the release point and the collection efficiency of the cyclone.

The release of aerosols from leaks in bioprocess equipment has been simulated by capillary tubes of various diameters and lengths. From the data presented here a value below $6 \times 10^{-6} \text{ cm}^3 \text{ min}^{-1} \text{ SF}_6$ would be recommended for an acceptable level for a piece of bioprocess equipment at a differential pressure of 2 bar. For a 5 mm leak this value is equivalent to a 3 μ m diameter hole, which has been shown not to transmit a suspension of micro-organisms. The implications of these findings are discussed in relation to the validation of bioprocess containment.

Acknowledgements

I would firstly like to thank Professor Mike Turner for his supervision of this project and appraisal of this document. I am grateful for the assistance Dr. Will Cook of Eli Lilly & Co. gave to the research, through providing access to his production facilities and financial support.

I would like to give a special mention to the other members of the Biosafety team at UCL, Michael Noble, Paula Aggutter, John Ley, they each helped in different ways, thank you for your patience. I must also thank all of the ACBE staff, particularly Stuart Pope and Clive Osborn, and my friends from the Vineyard office.

Finally and not least, I would like to thank my parents for their continuous support of my academic endeavours. Sometimes saying thank you doesn't seem enough.

Table of Contents

ABSTRACT	3
ACKNOWLEDGEMENTS	4
TABLE OF CONTENTS	5
LIST OF FIGURES	10
LIST OF TABLES	13
LIST OF EQUATIONS	14
ABBREVIATIONS	15
NOMENCLATURE	17
1. INTRODUCTION	18
1.1 Biosafety Regulations And Guidelines	18
1.1.1 The Development Of Biosafety Legislation	19
1.1.2 Current Regulations On The Contained Use Of GMMOs	26
1.1.3 The Impact Of Biosafety Regulations On Bioprocesses	28
1.2 The Release Of Micro-organisms From Bioprocesses	29
1.2.1 Bioprocess Containment Design	29
1.2.2 Incidental And Accidental Releases From Processes	30
1.2.2.1 The Release Of Aerosols	31
1.2.3 Hazards Associated With Bioprocess Releases	33
1.2.4 Bioprocess Release Research	34
1.3 Methods Of Aerosol Sampling	36
1.3.1 Passive Aerosol Sampling	36
1.3.2 Active Aerosol Sampling	37
1.3.2.1 Impactors	37
1.3.2.2 Impingers	38
1.3.2.3 Other Sampling Devices	38

1.4	Cyclone Design And Application	40
1.4.1	Models Of Cyclone Behaviour	41
1.4.1.1	Critical Diameter, Timed Flight Models	41
1.4.1.2	Critical Diameter, Static Particle Models	42
1.4.2.3	Fractional Efficiency Models	42
1.4.2	Experimental Performance Of Cyclones	42
1.4.3	Optimisation Of Cyclones For Bioaerosol Sampling	44
1.5	Methods To Quantify Micro-Organisms	46
1.5.1	Polymerase Chain Reaction	47
1.5.1.1	Quantitative PCR	48
1.6	The Application Of Leak Detection To Bioprocesses	50
1.6.1	Methods Of Leak Detection	51
1.6.1.1	Pressure Tests	51
1.6.1.2	Bubble Tests	52
1.6.1.3	Penetrant Methods	52
1.6.1.4	Tracer Gases	52
1.6.1.5	Alternative Methods	53
1.6.2	Flow Through And Categories Of Leaks	54
1.6.2.1	Permeation Leaks	55
1.6.2.2	Molecular Flow Leaks	56
1.6.2.3	Transitional Flow Leaks	56
1.6.2.4	Viscous Flow Leaks	58
1.6.2.5	Leak Blockage	59
1.6.3	Leak Detection Research	60
1.7	Research Objectives	62
2.	MATERIALS AND METHODS	64
2.1	Microbiological Methods	64
2.1.1	Micro-Organism Details	64
2.1.2	Culture And Maintenance Of Micro-Organisms	64
2.1.2.1	<i>Escherichia coli</i> JM107 pQR701	65
2.1.2.2	<i>Escherichia coli</i> RV308 pHKY531	65
2.1.3	Microscopic Cell Counts	65
2.1.4	Optical Density Measurements	66
2.2	Quantitative PCR Assay	67
2.2.1	Precautions To Prevent PCR Contamination	67
2.2.2	PCR Sample Preparation	67

2.2.2.1	Cell Lysis	68
2.2.2.2	Extracellular Plasmid Filtration	68
2.2.3	Stock Reagents	68
2.2.4	PCR Primer Details	68
2.2.5	PCR Cycle Protocols	69
2.2.5.1	pQR701 Amplification Parameters	69
2.2.5.2	pHKY531 Amplification Parameters	69
2.2.6	Internal Standard	70
2.2.6.1	Internal Standard Generation	70
2.2.6.2	Internal Standard Isolation	71
2.2.6.3	Internal Standard Purification	71
2.2.6.4	Internal Standard Quantification	72
2.2.6.5	Internal Standard Storage	72
2.3	Analysis Of the PCR Product	73
2.3.1	Agarose Gel Electrophoresis	73
2.3.2	Gel Densitometry And Analysis	73
2.4	Aerosol Containment, Generation and Collection	74
2.4.1	Contained Cabinet Operation	74
2.4.1.1	Bassaire Cabinet	74
2.4.1.2	UCL Contained Cabinet	75
2.4.2	Atomiser Operation	75
2.4.2.1	Atomiser Preparation	76
2.4.2.2	Atomiser Cleaning	76
2.4.3	Aerojet General Cyclone Operation	76
2.4.3.1	Cyclone Preparation	77
2.4.3.2	Cyclone Cleaning	78
2.5	Leakmeter 200 Operation	79
2.5.1	Leakmeter 200 Calibration	80
2.6	Model Leak System	81
2.6.1	Model Leak System Design	81
2.6.1.1	Construction Of Capillary Leaks	81
2.6.2	Model Leak System Operation	83
2.6.2.1	Validation Of The Model Leak System	83
2.6.2.2	SF ₆ Releases	83
2.6.2.3	Liquid Releases	83
2.6.2.4	Simulating Aerosol Impacts	84
2.7	Particle Counting Devices	86

2.7.1	TSI Incorporated LPC 7450	86
2.7.2	Malvern Instruments 3600 E Type	86
2.8	Shear Devices	87
2.8.1	Instron Shear Device	87
2.8.2	Rotating Disc Shear Cell	88
2.8.3	Analysis Of Shear Damaged Cells.	88
3.	DEVELOPMENT OF QPCR ASSAY FOR <i>E. COLI</i> RV308 PHKY531	89
3.1	PCR Primer Selection	89
3.2	QPCR Calibration Curve Generation	90
3.2.1	Quantification of <i>E. coli</i> RV308 pHKY531 Whole Cell Samples	93
3.3	Accuracy of <i>E. coli</i> RV308 pHKY531 QPCR Assay	94
3.4	Considerations for bioaerosol samples	96
4.	AEROSOL SAMPLING WITHIN CONTAINED CABINETS	97
4.1	Cyclone Sampling Optimisation	97
4.2	Particular, Temporal And Spatial Aerosol Effects	102
4.3	Release Impacts And Its Effect On Secondary Aerosolisation	108
5.	AN EVALUATION OF THE TURBOSEP'S MICROBIAL HANDLING	111
5.1	Experimental Details	112
5.2	Results And Discussion Of Turbosep Performance	114
6.	BIOPROCESS LEAK SIMULATIONS	118
6.1	Model Leak System Design And Validation	120
6.2	The Behaviour Of Leaks	122
6.2.1	SF ₆ Leaks	122
6.2.2	Aqueous Leaks.	125
6.2.3	Microbial Leaks	127
6.2.4	Comparison of SF ₆ and Microbial Leaks	132
6.3	The Effect of A Surfactant On Leak Transmission.	137

6.4	Effect Of Shear On Cells Transmitted Through Capillary Leaks	140
7.	DISCUSSION OF BIOPROCESS LEAK DETECTION AND CONTAINMENT VALIDATION	145
	APPENDIX 1 LIST OF SUPPLIERS	151
	APPENDIX 2 AEROJET GENERAL CYCLONE DIMENSIONS	153
	APPENDIX 3 CALCULATION OF PHKY531 CONCENTRATION	155
	Agarose gel electrophoresis	155
	Densitometry Analysis	155
	Calculation of the pHKY531 concentration	156
	APPENDIX 4 PARTICLE SIZE ANALYSIS OF SHEARED CELLS	157
	APPENDIX 5 PARTICLE SIZE CALCULATIONS	159
	Calculation of the d_{50}	159
	Calculation of the Sauter Mean Diameter (SMD)	159
	REFERENCES	161

List of Figures

Figure 1	A simplified vertical section of a cyclone, showing the bulk phase flows.	40
Figure 2	Schematic representation of one PCR amplification cycle.	47
Figure 3	Typical flow regimes of capillary leaks, where Kn and Re are the Knudsen and Reynolds number respectively.	55
Figure 4	The relationship of total cell count to measured optical density. Each point is the mean of 5 samples with their standard deviation.	66
Figure 5	Schematic representation of the generation of the internal standard for <i>E. coli</i> RV308 pHKY531.71	
Figure 6	Bassaire cabinet showing dimensions (m), location of ports (both on same face of cabinet) and direction of airflow through HEPA filters (hashed areas).	74
Figure 7	UCL contained cabinet showing dimensions (m), location of ports and direction of airflow through HEPA filters (hashed areas).	75
Figure 8	Schematic cross section of the Warren Spring atomiser.	76
Figure 9	Schematic diagram of the Aerojet General Cyclone set-up for sampling.	77
Figure 10	A schematic of the model leak system.	81
Figure 11	A schematic of the attachment of a micropipette to a luer lock hub. The luer hub is represented at the very left with the PTFE tubing shown in grey. The micropipette passes through the hub and has a flame polished end shown in bold.	82
Figure 12	The layout of equipment for the sampling of liquid releases using the aerojet general cyclone in the UCL contained cabinet. Where 1 represents the model leak, 2 the LPC and 3 the cyclone connected to the cabinet.	84
Figure 13	The layout of equipment for the sampling of aerosol impacts using the aerojet general cyclone and the LPC in the UCL contained cabinet. Where 1 represents the model leak, 2 the LPC and 3, target location and 4 the cyclone connected to the cabinet.	85
Figure 14	Gel showing the co-amplification of IS(B)3 and pHKY531 to generate a calibration curve. Where the pHKY531 concentration (molecules $10 \mu\text{L}^{-1}$) was:	91
Figure 15	Calibration curves for pHKY531, showing upper and lower 95% confidence limits (dotted lines) of linear regression (solid lines).	92
Figure 16	The response of the QPCR protocol to <i>E. coli</i> RV308 pHKY531 whole cells. Each point shows the mean of duplicates with their standard deviation.	93
Figure 17	Direct (○) and indirect (□) capture of micro-organisms by an Aerojet general cyclone, where each point is the mean of two samples with their standard deviation.	98
Figure 18	Aerojet general cyclone collection efficiency of micro-organisms (●), particles $> 0.5 \mu\text{m}$ diameter (▼) and particles $> 5.0 \mu\text{m}$ diameter (▲), where each point is the mean of two (●) or thirty (▼, ▲) samples with their standard deviation.	100
Figure 19	Atomisation and capture of micro-organisms from Luria broth (▲) and TRS (●) within the Bassaire cabinet. The means and \pm standard deviation are shown. Previous data (Ferris, 1995) on TRS suspended bioaerosols is shown (○).	102

- Figure 20 Settling time of an *E. coli* RV308 pHKY531 bioaerosol (5×10^7 cells mL⁻¹) within the UCL contained cabinet, where each point shows the mean of duplicate samples with their standard deviation. 104
- Figure 21 Anisokinetic sampling effects on cyclone collection efficiency, where the angle from the cyclone to the release point was 0° (◆), 5° (●), 25° (▼), 35° (▲) and 55° (■). Each point shows the mean of duplicate samples with their standard deviation. 106
- Figure 22 The maximum, minimum and mean number of particles > 0.5 μm in diameter generated by impact with a shaped target or from atomisation. 109
- Figure 23 The maximum, minimum and mean number of particles > 5.0 μm in diameter generated by impact with a shaped target or from atomisation. 109
- Figure 24 The effect of Turbosep differential pressure on exhaust gas microbial load, showing means and ± standard deviation. 114
- Figure 25 The measured pressure drop in an LH 450 L bioreactor over 2 hours for capillary leaks of various sizes. 119
- Figure 26 The theoretical 1 % SF₆ flow rates for different flow regimes (···), compared with empirical values (Δ), for a capillary leak 65 mm long and 50 μm ID. 123
- Figure 27 The SF₆ flow rate for 65 mm long leaks of various diameters (10 μm (□), 25 μm (○), 50 μm (Δ), 75 μm (▼) and 100 μm (◇)), correlated with the theoretical transitional gas flow (···) expressed by equation 2 (Baram, 1991). 124
- Figure 28 The Water flow rate for 10 mm long leaks of various diameters (127 μm (■), 254 μm (●), 508 μm (▲) and 1066 μm (▼)), correlated with the theoretical laminar liquid flow (···) expressed by equation 5 (Tilton, 1997). 125
- Figure 29 The Water flow rate for 5 mm long leaks of various diameters (127 μm (■), 254 μm (●), 508 μm (▲) and 1066 μm (▼)), correlated with the theoretical laminar liquid flow (···) expressed by equation 5 (Tilton, 1997). 126
- Figure 30 The theoretical flow of water (···) as expressed by equation 5, and the actual flow of *E. coli* RV308 pHKY531 cells (8×10^3 cells mL⁻¹ (■), 8×10^{10} cells mL⁻¹ (●)) through 50 mm long leaks of various diameters at 2 bar ΔP. 127
- Figure 31 The actual flow of *E. coli* RV308 pHKY531 cells through 50 mm long leaks of various diameters at 0.5 bar ΔP. 128
- Figure 32 The actual flow of *E. coli* RV308 pHKY531 cells through 50 mm long leaks of various diameters at 1.0 bar ΔP. 129
- Figure 33 The actual flow of *E. coli* RV308 pHKY531 cells through 50 mm long leaks of various diameters at 2.0 bar ΔP. 129
- Figure 34 The maximum *E. coli* RV308 pHKY531 cell concentration that can flow through a 50 mm long leak without blocking at various ΔP (0.5 bar (◇), 1.0 bar (□) and 2.0 bar (○)). 130
- Figure 35 The effect of leak length on the flow of 1 % SF₆ (5 mm (Δ), 10 mm (▼) and 50 mm (◇)) and 8×10^3 cells mL⁻¹ *E. coli* RV308 pHKY531 (5 mm (▲), 10 mm (▼) and 50 mm (◆)) at 1.0 bar ΔP. 133

- Figure 36 The effect of pressure (ΔP) on the flow of 1 % SF₆ (□), 1.0 bar (▽) and 2.0 bar (○) and 8×10^3 cells mL⁻¹ *E. coli* RV308 pHKY531 (0.5 bar (■), 1.0 bar (▼) and 2.0 bar (●)) through 10 mm leaks. 134
- Figure 37 The flow of 1 % SF₆ (○) and 8×10^3 cells mL⁻¹ *E. coli* RV308 pHKY531 (●) through 10 mm long leaks of various diameters at 2 bar ΔP , compared with the theoretical flow of 100 % SF₆ (···) expressed by equation 2 (Baram, 1991) at various ΔP . The theoretical flow data is shown only for the Leakmeter 200 SF₆ range of detection 135
- Figure 38 Particles > 0.5 μm diameter of a suspension of *E. coli* RV308 pHKY531 cells (8×10^9 cells mL⁻¹) with 0 % (○), 0.01 % (▽) and 0.1 % (△) Tween 80 (v:v) generated by passing through a capillary 50 mm long and 254 μm diameter. 137
- Figure 39 Particles > 5.0 μm diameter of a suspension of *E. coli* RV308 pHKY531 cells (8×10^9 cells mL⁻¹) with 0 % (●), 0.01 % (▼) and 0.1 % (▲) Tween 80 (v:v %) generated by passing through a capillary 50 mm long and 254 μm diameter. 138
- Figure 40 The rotating disc shear-induced cell breakage of an *E. coli* RV308 pHKY531 cell suspension (2×10^8 cells mL⁻¹). 141
- Figure 41 The shear-induced breakage of a suspension of *E. coli* RV308 pHKY531 cells (8×10^5 cells mL⁻¹) passed through 100 μm (◇, ◆, ♦), 150 μm (○, ⊕, ●) and 200 μm (□, ⊠, ■) diameter capillaries. Each point is the mean of triplicate samples with the error bars showing the standard deviation of that mean. The flow characteristic based on Reynolds number is shown as laminar (◇, ○, □), transitional (◆, ⊕, ⊠) or turbulent (♦, ●, ■). 1st order exponential growth is represented by the dotted lines (···) 142
- Figure 42 The effect of shear rate (unsheared control (■), 3.24×10^6 s⁻¹ (○), 9.59×10^5 s⁻¹ (△) and 4.05×10^5 s⁻¹ (▽)) on the particle size distribution of a suspension of *E. coli* RV308 pHKY531 cells (2×10^8 cells mL⁻¹). 144
- Figure 43 Diagram of an Aerojet General Cyclone (all dimensions in mm). The shading represents the air inlet of the cyclone which rises 50 mm from the plane of the page and terminates with a female BS32/29 quick-fit adapter. 153
- Figure 44 Cross section of the wash liquid injection attachment, connected to the aerojet general cyclone via a male B32/29 quick-fit adapter (all dimensions in mm). 154
- Figure 45 Agarose gel showing the results of a QPCR of a sample containing an unknown concentration of pHKY531. Lane 1 contains IS(B) 1 and the sample, Lane 2 contains IS(B) 2 and the sample, Lane 3 contains the molecular weight marker (PCR Marker, Sigma). 155
- Figure 46 The particle size distribution for an *E. coli* RV308 pHKY531 cell suspension (2×10^5 cells mL⁻¹) passed through a 100 μm diameter capillary at various flow rates. 157
- Figure 47 The particle size distribution for an *E. coli* RV308 pHKY531 cell suspension (2×10^5 cells mL⁻¹) passed through a 150 μm diameter capillary at various flow rates. 158
- Figure 48 The particle size distribution for an *E. coli* RV308 pHKY531 cell suspension (2×10^5 cells mL⁻¹) passed through a 200 μm diameter capillary at various flow rates. 158

List of Tables

Table 1	OECD Containment Levels (from OECD, 1986).	24
Table 2	Criteria for classifying group I GMMOs (taken from 94/51/EC).	27
Table 3	Potential routes and activities which may contribute to a release from a bioreactor.	31
Table 4	Common impactor sampling devices.	37
Table 5	Common impinger sampling devices.	38
Table 6	Methods of microbial quantification.	46
Table 7	Leak detection method sensitivity, from McMaster (1982).	51
Table 8	Details of Micro-organisms used.	64
Table 9	Stock Reagents used in the PCR.	68
Table 10	<i>E. coli</i> primers used in this project.	69
Table 11	Capillary size and material details for leak simulations	82
Table 12	Shear rates developed by the Instron shear device for various capillary attachments.	87
Table 13	Details of IS(B) and pHKY531 used in co-amplification trials.	90
Table 14	IS(B) concentrations used to produce calibration curves.	91
Table 15	Parameters of IS(B) linear regression analysis.	92
Table 16	Accuracy and error of the QPCR assay.	94
Table 17	Inoculation times and duration of each growth stage.	112
Table 18	<i>E. coli</i> concentration after 12 hours fermentation.	115
Table 19	Details of the model leak system integrity validation.	121
Table 20	The time (s) taken for a 50 mm long capillary to become blocked by a suspension of cells at 1 bar ΔP . Each sample is the mean of duplicates.	131
Table 21	The time and relative size of peak particle generation from a suspension of <i>E. coli</i> RV308 pHKY531 cells (8×10^9 cells mL ⁻¹) passing through a capillary 50 mm long and 254 μm diameter in the presence of Tween 80.	138
Table 22	The failure probabilities of some industrial items and operations.	148
Table 23	Potential technical improvements to the methods used in this research project.	150
Table 24	Densitometry analysis of lane 1 (Figure 45).	156

List of Equations

Equation 1	Molecular gas flow through a capillary.	56
Equation 2	Transitional capillary flow throughput.	57
Equation 3	Calculation of Reynolds number through a leak with circular cross-section.	58
Equation 4	Average velocity during laminar and turbulent flow.	58
Equation 5	Laminar fluid flow through a capillary.	59
Equation 6	The pressure required to overcome surface tension in a fully wetted capillary leak.	59
Equation 7	Static particle prediction of d_{50}	159
Equation 8	Calculation of the SMD from empirically derived parameters	159
Equation 9	Solution of Equation 8 for typical operational parameters	160

Abbreviations

µg, mg, g, Kg	microgram, milligram, gram, kilogram
µL, mL, L	microlitre, millilitre, litre
nm, µm, mm, m	nanometer, micrometer, millimeter, meter
mM, M	millimolar, molar
A ₂₆₀	absorbance at 260 nm
A ₂₈₀	absorbance at 280 nm
APS	aerodynamic particle sizer
ATP	adenosinetriphosphate
bp	base pair(s)
BST	met-asp-bovine somatotropin
DMSO	dimethylsulfoxide
DNA, dsDNA	deoxyribonucleic acid, double stranded deoxyribonucleic acid
RNA, mRNA	ribonucleic acid, messenger ribonucleic acid
dNTP	deoxynucleotide triphosphate
dATP	deoxyadenosine triphosphate
dTTP	deoxythymidine triphosphate
dCTP	deoxycytosine triphosphate
dGTP	deoxyguanosine triphosphate
GILSP	good industrial large scale practice
GMMO	genetically modified micro-organism(s)
GMO	genetically modified organism
HEPA	high efficiency particulate air filter
HSC	health and safety commission
HSE	health and safety executive
ICSI	intracellular sperm injection
ID	internal diameter
LBB	leak-before-break
MHz	mega hertz
OAF	open air factor
PCR	polymerase chain reaction
PTFE	polytetrafluorethane
QPCR	quantitative polymerase chain reaction

RMM	relative molecular mass
rpm	revolutions per minute
s, min, h	second, minute, hour
SCADA	supervisory control and data acquisition
SOP	Standard Operating Procedure
SF ₆	sulphur hexafluoride
SMD	sauter mean diameter
SROW	sterile reverse osmosis water
TRS	thiosulphate ringers solution
UV	ultra-violet
VMD	volume mean diameter
(v/v)	volume:volume ratio
(w/v)	weight:volume ratio

Nomenclature

Symbol	Definition	Units
T	absolute temperature	K
p'	average pressure across leak	bar
U	average velocity	m s^{-1}
A	cross-sectional area	m^2
ρ	density	Kg m^3
D	diameter	m
d	diameter	μm
μ	dynamic viscosity	Pa s
R	ideal gas constant	J
Kn	Knudsen number	dimensionless
l	leak length	μm
L	leak length	m
M	molecular weight	Kg
π	Pi	dimensionless
Δp	pressure drop across leak	bar
ΔP	pressure drop across leak	Pa
r	radius	m
Re	Reynolds number	dimensionless
σ	surface tension	N m^{-1}
P_s	pressure to overcome surface tension	bar
G	volumetric flow rate	L min^{-1}
Q_l	volumetric flow rate (liquid)	$\text{m}^3 \text{s}^{-1}$
Q_m	volumetric flow rate (molecular)	$\text{Pa m}^3 \text{s}^{-1}$
Q_t	volumetric flow rate (transitional)	mbar L s^{-1}

1. Introduction

The safe use of genetically modified micro-organisms (GMMOs) for the industrial manufacture of therapeutic and other products depends on the design, implementation and validation of effective containment principles. This project aims to establish a test method that can generate quantitative data on bioprocess releases, that can be used to validate the containment of bioprocess equipment. To achieve a validated method a standard tracer gas leak test will be correlated with a quantitative polymerase chain reaction (QPCR) assay for the detection of GMMOs.

The QPCR protocol has been developed specifically for *Escherichia coli* RV308 pHKY531. A model system with variable orifice sizes and leak path lengths has been developed for the simulation of bioprocess releases. The data generated on the release of a microbial challenge through small orifices has been correlated with the response of the tracer gas detection system. The correlation of the data can be used to define limits on the permissible leak rates to aid the rational design of bioprocess equipment and containment regulations.

Throughout the course of the project, work has been carried out to improve the collection efficiency of a cyclone sampler and to investigate the effects of various approaches to bioaerosol sampling in a process environment.

1.1 Biosafety Regulations And Guidelines

There is a long history of man's involvement with biotechnology, from the brewing of beer to the baking of bread. Our knowledge of microbiology, biochemistry and genetics has brought us to a point in time where we can now engineer the genetic code of certain organisms. Biotechnology exploits and optimises the potential offered by biological systems through the use of modern genetic engineering techniques. This technology has enabled the use of GMMOs in the large scale processes of today's bioindustry.

The use of GMMOs has always been subject to a high degree of concern since their inception (Singer and Soll, 1973). The concerns arising from the application of GMMOs vary, and are intimately connected to the procedures, reagents, products and waste

associated with the process. Hence the risk of any bioprocess can be seen as an objective view of the nature (real or potential), extent (low or high probability), and impact (adverse effects) of the process hazards. Modern regulations must provide the necessary legislation to ensure the adequate protection of health and the environment, whilst at the same time allowing an innovative atmosphere that encourages the exploitation of biotechnology.

1.1.1 The Development Of Biosafety Legislation

Current UK regulations on the use of GMMOs date back to the early 1970's when two formative reports were published, one in the UK by Lord Robens (Robens' Report, 1972) and the second in the USA (Singer and Soll, 1973). The Robens' Report provided a turning point for safety legislation in the UK as it was critical of the retrospective approach to safety regulations. The report made two important recommendations in its summing up; the first requesting a unified administrative framework to be established. This would provide a comprehensive structure for future legislation. Today the HSC and HSE are responsible for the health and safety of all employees in Great Britain. The HSE advises the HSC on the shaping of policy and is responsible for its implementation. Lord Robens second recommendation was that a comprehensive health and safety act should be passed which would be supported by expert working parties who would provide technical specifications for codes of practice and regulations. Both these recommendations were taken into account when the Health and Safety at Work etc. Act (HSW, 1974) was published. The HSW Act (1974) is the blueprint for safety regulations in the UK. Of particular note are two key clauses outlining the legal requirement of employers and manufacturers in industry.

“...the provision and maintenance of a working environment for their employees that is, so as is reasonably practicable, safe without risks to health and adequate as regards facilities and arrangements for their welfare at work.”

[para. 2(1)]

“...to carry out or arrange for the carrying out of any necessary research with a view to the discovery and, so far as is reasonably practicable, the elimination or minimisation of any risks to health and safety to which the design or article may give rise.”

[para. 6(2)]

These statements require facilities and products to be designed so that the possibility of any risk to health or welfare to be accounted for in advance, and for it to be minimised.

A similar feeling was embodied in the report of the Gordon Research Conference on Nucleic Acids reported by Singer and Soll in 1973. This pivotal conference on molecular genetics recognised that it was possible to form hybrid DNA and transfer it between different organisms. This was acknowledged to herald the beginning of a new level of understanding of fundamental biological processes and human health problems. The enthusiasm for the new possibilities provided by recombinant DNA experiments was tempered with an intelligent degree of caution. Although no hazard had been identified there was a request for a study committee to be established to consider the hazards created by this new scientific advance. The Committee on Recombinant DNA Molecules was set up by the US National Academy of Sciences in 1974. The immediate effect of this was the voluntary embargo of certain types of DNA manipulations (Berg *et al.*, 1974). Among the embargoed experiments were those that would confer antibiotic resistance to bacterial strains not known to carry these traits. This represented the first classification of recombinant DNA experiments into two broad groups. However this first step was only a voluntary guide to safer practice and clarification of the hazards involved in recombinant DNA work was requested (Berg *et al.*, 1974).

The following year at the Asilomar Conference on Recombinant DNA Molecules the first steps to create formal safety guidelines for genetic engineering were made. The biggest conclusion drawn from the conference was that the potential risk of recombinant DNA technology should be balanced by physical and biological containment measures. A hierarchy of containment levels were drawn up (Berg *et al.*, 1975) to match the level of risk posed by any recombinant DNA experiment. These started with good laboratory practice through to the engineering of biological barriers. The new biological barriers to an engineered organisms survival were described in two forms. Firstly fastidious hosts that would be unable to survive outside of the laboratory environment. And secondly fastidious vectors which would be non-transmissible, except in well specified host organisms. The use of physical containment methods was recommended, such as a negative pressure working environment. There were concerns that large-scale

experiments would be inherently more hazardous than small-scale work. To this end an arbitrary upper limit of 10 L was put on the scale of laboratory experiments.

Following the Asilomar conference in 1978 the HSE published the first UK specific regulations on the use and handling of GMMOs, the Health and Safety (Genetic Manipulation) Regulations 1978. These were based on a voluntary code of conduct and were supported by a set of guidance notes. Then in 1984 the Advisory Committee on Genetic Manipulation (ACGM) was formed. The ACGM is a tripartite committee consisting of an independent chairman, representatives of the employer and employee organisations, and scientific and medical specialists. It advises the HSC, HSE and other government departments on the human health and environmental aspects of the contained uses of GMMOs. This came to fruition in 1988 when the ACGM published a method for assessing the hazard posed by GMMOs (ACGM, 1988). The potential hazard associated with the experiment was derived from three component factors, access, expression and damage. These factors were assessed and scored on the Brenner scale from 12 (low risk) to 1 (high risk). The product of the three factors score was then used to assign a level of containment for that experiment.

In addition to the HSW Act of 1974 and the guidelines for the categorisation of genetic manipulation experiments (AGCM, 1988), the Control of Substances Hazardous to Health (COSHH) Regulations of 1988 (HSC, 1988) require that a risk assessment of experimental operations should be carried out prior to commencing any work. This was a broad legislative move to anticipate any hazards posed principally by chemicals in an experimental procedure and ensure measures were taken to reduce them.

Guidance on work with biological agents is provided by the Advisory Committee on Dangerous Pathogens (ACDP). Their guidelines categorise naturally occurring micro-organisms into four hazard groups based on their pathogenicity. They also describe appropriate levels of containment to minimise infection when handling these organisms.

The Organisation for Economic Co-operation and Development (OECD) has always expressed a degree of concern over the development of biotechnology. In 1983 at the recommendation of the Committee for Scientific and Technological Policy, an *ad hoc* group of government experts was created to review the safety policy employed by

OECD member countries on the use of GMMOs. The groups aims were to look at legislation in the industrial, agricultural and environmental sectors, to identify monitoring or authorisation criteria which have or may be adopted, and to explore ways of monitoring the future production and care of GMMOs. The committee published its findings in 1986 in their handbook, Recombinant DNA Safety Considerations (OECD, 1986). In this handbook the committee developed the idea of Good Industrial Large Scale Practice (GILSP), according to which it was recommended that for organisms considered to be of low risk only minimal controls on containment procedures were necessary. It was recognised that some industrial applications would use micro-organisms which do not meet the specified criteria for GILSP and that some products and processes may require special considerations when applying GILSP. Thus GILSP is not a biological or physical method of containment in its own right, rather an acknowledgement that the vast majority of organisms used in modern bioprocesses can be regarded as safe. This assumed safety stemmed from an extensive knowledge of the organisms use and a clear definition as to the form and function of any inserted DNA. From this base line of GILSP the OECD handbook then goes on to develop safety guidelines for applications other than those covered by GILSP. The guidelines resulting from this were particularly relevant for large-scale operations and described by three levels of containment (Table 1). However from an inspection of the criteria for OECD containment category 1 it can be seen that the operator is asked to minimise the release of viable organisms and not to prevent them. The uses of qualitative terms such as “minimise release” and “prevent release” that are used in these regulations can not be directly translated into mechanical engineering design. So how can OECD containment category 1 and GILSP be seriously considered containment strategies if there is no requirement to prevent release from a closed system? This indicates a release is considered permissible even when basic containment measures appropriate to the organism are in place, such as engineered biological containment in the form of lethal genes. This would suggest that for certain organisms biological containment would be sufficient and complete physical containment is therefore unnecessary.

The work of the OECD (OECD, 1986) formed the basis for the UK guidelines for the large-scale use of genetically manipulated organisms (ACGM, 1987a & b). The structuring of containment levels is three tiered increasing in stringency with a good large-scale practice equivalent to GILSP. The Royal Commission on Environmental

Pollution Report (RCEP, 1989) stated that organisms with simple engineered gene deletions could not be considered safe when released into the environment. Because of this the deliberate release of GMMOs should only be permitted on a case by case basis after reviewing the experiments risk. This now creates an inconsistency in what is perceived to be a safe release into the environment, and highlights a fundamental difference in the regulatory controls imposed on GMMOs by different regulatory bodies.

Table 1 OECD Containment Levels (from OECD, 1986).

Specifications	Containment Category		
	1	2	3
1. Viable organisms should be handled in a system which physically separates the process from the environment (closed system)	Yes	Yes	Yes
2. Exhaust gases from the closed system should be treated so as to:	Minimise release	Prevent release	Prevent release
3. Sample collection, addition of materials to a closed system and transfer of viable organisms to another closed system, should be performed so as to:	Minimise release	Prevent release	Prevent release
4. Bulk culture fluids should not be removed from the closed system unless the viable organisms have been:	Inactivated by validated means	Inactivated by validated chemical or physical means	Inactivated by validated chemical or physical means
5. Seals should be designed so as to:	Minimise release	Prevent release	Prevent release
6. Closed systems should be located within a controlled area	Optional	Optional	Yes, and purpose built
(a) Biohazard signs should be posted	Optional	Yes	Yes
(b) Access should be restricted to nominated personnel only	Optional	Yes	Yes, via an airlock
(c) Personnel should wear protective clothing	Yes, work clothing	Yes	A complete change
(d) Decontamination and washing facilities should be provided for personnel	Yes	Yes	Yes
(e) Personnel should shower before leaving the controlled area	No	Optional	Yes
(f) Effluent from sinks and showers should be collected and inactivated before release	No	Optional	Yes
(g) The controlled area should be adequately ventilated to minimise air contamination	Optional	Optional	Yes
(h) The controlled area should be maintained at an air pressure negative to atmosphere	No	Optional	Yes
(i) Input and extract air to the controlled area should be HEPA filtered	No	Optional	Yes
(j) The controlled area should be designed to contain spillage of the entire contents of the closed system	No	Optional	Yes
(k) The controlled area should be sealable to permit fumigation	No	Optional	Yes
7. Effluent treatment before final discharge	Inactivated by validated means	Inactivated by validated chemical or physical means	Inactivated by validated chemical or physical means

The regulations on contained use are administered by the HSE, whilst the Department of the Environment (DOE) is responsible for legislation on deliberate releases. The two sets of regulations implement parallel European Commission Directives 90/219/EEC and 90/220/EEC respectively (EC, 1990b & c), and both are designed to ensure the protection of human health and the environment. The difference between these two regulatory controls can be summarised by noting that the regulations on contained use are designed to ensure that any release to the environment of GMMOs is minimised and prevented if possible by both physical and biological methods. Whereas the DOE regulations allow the deliberate release of GMMOs into the environment. And any GMMO deliberately released, may only have minimal biological containment.

In 1992 the Genetically Modified Organisms (Contained Use) Regulations were published (HSE, 1992). The designation “contained use” in the title of the document covers any operation where organisms are genetically modified, or in which GMMOs are cultured, stored, used, transported, destroyed or disposed of. The requirements expected from anybody working with GMMOs were extended to include;

- A recorded assessment of the risks to human health and the environment.
- The establishment of a local genetic modification safety committee to advise on risk assessments.
- The classification of all activities and organisms used according to a prescribed scheme.
- The notification of the HSE of the intention to use premises for genetic modification work for the first time and for certain subsequent activities, and to await specific consent from the HSE before starting the work if so directed.
- The adoption of controls including suitable containment measures.

The GMMOs used should also be classified according to one of two groups. The location of a GMMO in either group was based on two main criteria. The host organism must be non-pathogenic and have an extended history of safe use; the vector/insert must be well characterised and poorly mobilisable. If either of these conditions is not true then the GMMO is classed as group II and considered hazardous to man and/or the environment, compared with Group I GMMOs which are considered low risk. It is conceivable that a GMMO could be classed in Group II on environmental grounds

alone, irrespective of its health risk. To make classification simpler and more logical, guidance was provided in the ACGM/HSE/DOE Note 7 (ACGM, 1993). A comparable classification of the unit operations to be carried out is also made, dividing teaching, R&D and non-commercial work below 10 L in scale into one group (Type A) and all other unit operations as Type B. It is then expected that from these two classifications an appropriate level of containment can then be assigned for the planned process. However, some definitions are not clear and these could create problems. First it may be difficult to define an operation (*i.e.* one experiment, a series of experiments, or a whole research program). Second, the definition of type A and B operations is vague. The third problem is the classification of micro-organisms themselves.

The containment levels required for a process are linked to the hazard classification of the micro-organism used. The containment levels are designated as B1 to B4 and follow the OECD guidelines for GILSP through to OECD level 3 respectively. So B1 is seen to equivalent to GILSP and B3 equivalent to OECD level 2. For Type B unit operations involving Group II GMMOs the containment should be B2 at least, but may be higher. The final level of containment implemented will then be appropriate to the GMMO used and the potential risk to health and the environment.

1.1.2 Current Regulations On The Contained Use Of GMMOs

New COSHH regulations came into force on 16 January 1995 (HSC, 1994) and apply amongst other things to biological agents. These agents are defined as micro-organisms, cell cultures, or human endoparasites, including any which have been genetically modified, which may cause an infection, allergy, toxicity, or otherwise create a hazard to human health. Additionally new regulations governing the contained use of GMMOs came into force on the 27 April 1996 which amend the 1992 Contained Use Regulations (HSE, 1992). The amendments implement EC directive 94/51/EC (EC, 1994) and address some difficulties which have arisen in the practical application of the 1992 Regulations which were based on the earlier EC directive 90/219 (EC, 1990a). For example under the 1992 regulations a person undergoing gene therapy would be classified as a GMO and subject to containment. Under the amendments people are no longer regarded as GMOs when undergoing gene therapy treatment. A new and simpler system for classifying GMMOs has been implemented which details more stringent

criteria for classifying a GMMO as a group I organism (Table 2) as previously detailed under EC directive 90/219/EC.

Table 2 Criteria for classifying group I GMMOs (taken from 94/51/EC).

Criteria to fulfil	
1	the recipient or parental micro-organisms is unlikely to cause disease to humans, animals or plants.
2	the nature of the vector and insert is such that they do not endow the genetically modified micro-organism with a phenotype likely to cause disease to humans, animals or plants, or likely to cause adverse effects in the environment.
3	the genetically modified micro-organism is unlikely to cause disease to humans, animals or plants and is unlikely to have adverse effects on the environment.

With the advent of genetically engineered consumer products, such as tomato puree, new safety legislation is required to adapt. Now certain marketed products which have been cleared through the relevant product legislation become exempt from containment legislation. The 1992 regulations remain unchanged with regard to risk assessment, control measures to protect health and the environment and the disclosure of information to the public. The new regulations now address the problem of classifying a micro-organism as either group I or group II, which was an area of contention under the 1992 guidelines.

In order to provide environmental and human safety, public acceptance, and open access to a world market for products obtained through genetic modification, biosafety regulation needs to be controlled by competent authorities. Regulations are still being passed retrospectively to accommodate shortcomings in existing legislation. In order to attain efficiency, flexibility and control in the regulating authorities, a simplification of the essential legislative requirements is required. The EC and UK governments are taking the right steps to create biosafety legislation that will foster the development of an effective and productive biotechnology industry. The most recent UK legislation does simplify essential criteria and provide scope for technological advances. But the reporting systems in place are still complex, in need of harmonisation and neglect the industry's views (Dickson, 1996).

1.1.3 The Impact Of Biosafety Regulations On Bioprocesses

The notification, reporting and inspection required by a production plant using GMMOs can demand many hours of management time. As a result of this it is not uncommon to have a department that deals with all aspects of regulatory affairs, from initial notification through to product licensing.

At the design and operational levels the most significant regulatory impact on a bioprocess is the necessity in some cases for the use of high (B3 and 4) containment measures to prevent the release of the process organism. The application of high containment to a bioprocess to meet regulatory requirements increases the cost of equipment and the complexity of the unit operations. It has been estimated that basic bioreactor costs would increase by at least 30 % for each increase in the applied containment level (Pennman, 1989). This in itself may make a process undesirable to run. The addition of containment measures is to increase the safety of the system. But any change to a process has the potential to introduce new failure modes and risks (Dowell and Hendershot, 1997). A more complex system could produce greater incidents of operator error which could result in more serious accidents than if a simple less well-contained piece of equipment was being used.

1.2 The Release Of Micro-organisms From Bioprocesses

In any processes there is always the chance of a fault occurring. However a well-designed process minimises the probability of such an event. A fault in the containment of a bioprocess could then logically cause a release of the process material at the point of failure. This could take the form of a drop of microbial broth on a leaking flange to an over pressure vessel rupturing. Clearly there is a difference between the scale of these two events, yet both are theoretically possible. A containment strategy must take both extremes into account. This has a fundamental effect on the design and cost of the process. The hazard posed by any anticipated release is then of primary concern and this becomes the factor driving the process design.

1.2.1 Bioprocess Containment Design

Industrial bioprocesses can be seen as a series of unit operations that take raw materials and process them into a purified product. A process can then be seen as the discrete unit operations and the engineering linking them. In terms of the process safety, each unit operation and the pipe work integrating them may pose different hazards that need to be considered individually. Therefore it is essential to specify the unit operation for a chosen task on safety grounds as well as its overall performance (Dowell and Hendershot, 1997).

Typically the product from a biological system will be produced intracellularly or extracellularly. This simple difference in product expression has massive implications on the downstream processing required to purify the product. An intracellular product requires a mechanism to free the product from the cell before the purification process can take place. However extracellular products are often simpler to purify as there are no cell debris or enzymes to be removed prior to the product purification. Therefore the complexity of the downstream processing depends very much on the product and how it was produced. A complex system is more likely to create the opportunity for operator error, and be more difficult to contain as a result of this.

There are two broad categories of process containment. Primary containment of an operation should provide the protection of personnel and the immediate vicinity of the

process from exposure to process materials. This should be achieved by specification of appropriate equipment for the operation and the implementation of standard operating procedures. Secondary containment is in effect the protection of personnel and the environment external to the processing facility from exposure to process materials. This secondary level should be provided by a combination of building design and good manufacturing practices. A process which has a connection to the external environment can be considered open as opposed to a closed system which has no connections to the external environment. Turner (1989) has discussed the design of closed systems with primary and secondary containment in place. He concludes that complete closure of a process is difficult if not impossible to achieve, because the resources required to completely close a system are complex to install and operate. In practice this means that processes should have a high level of primary containment thereby reducing the demands of secondary containment. This should then create a system closed to the egress of the process organism and the ingress of contaminating organisms or materials.

1.2.2 Incidental And Accidental Releases From Processes

Principally there are two types of release from a bioprocess, incidental and accidental. The incidental release of micro-organisms from a process results from less than perfect containment. The accidental release of micro-organisms into the environment from a process results from an unforeseen event. As it has already been stated (Turner, 1989) that containment can not be absolute, it follows that any bioprocess will release biological material into the environment during its operation. Therefore the containment principles applied to a process need to balance these two types of release realistically. This is difficult to do in practice as there is no reliable method of quantitatively assessing bioprocess containment. The result of this is that one often over-engineers the containment precautions irrationally in order to achieve a perceived level of containment. Miller and Bergmann (1993) also suggest that over-specifying your process containment shows a lack of confidence in your process and facility. This then sends a conflicting signal to a public which may not know about the GMMO's safety. An example of this over-engineering might be the use of two HEPA filters on an exhaust gas stream and less attention paid to the release generated by opening a sample port or washing a process area.

Accidents are always unexpected but it is essential that the risk from each type of accident should be assessed and measures put in place to prevent the event occurring. In the bioprocess industry fluids moved in pipelines or held in vessels are usually aqueous, non-corrosive and at low temperatures and pressures. Some unit operations such as homogenisation and centrifugation do have to handle high pressures and pose additional problems for process containment (Kastelein *et al.*, 1989; Tinnes and Hoare, 1992). Therefore in the majority of unit operations the statistical chance of equipment failure is far less significant than the probability of an accident occurring. The potential for an accident leading to a release can then be statistically analysed by using methods such as fault tree analysis (Jefferis & Schlager, 1986). This type of analysis can also highlight the events and avenues of escape which may lead to an incidental release (Table 3). Leaver and Hambleton (1992) state that the bioreactor is the most likely point in a bioprocess at which significant amounts of biological material could be released.

Table 3 Potential routes and activities which may contribute to a release from a bioreactor.

Routes	Activities
Drive shaft seals	Inoculation
Valve glands	Sampling
Probe ports	Harvesting
Pipe flanges	Cleaning
Exhaust gas	

The type of release is dependant on the nature of the material breaking the containment and the manner in which the containment is breached. Most releases will involve a process fluid that is released into the atmosphere. Depending on the size of the hole, the velocity of the escaping fluid and any obstructions to the flow path, an aerosol may be formed. Because aerosols can be produced from simple manipulations as well as through incidental leaks, they are considered the commonest form of release from bioprocesses (Hambleton *et al.*, 1992).

1.2.2.1 The Release Of Aerosols

Aerosols are suspensions of liquid particles in gases. The focus of aerosol science is generally on the behaviour of the particles rather than on the influence of the particles on the gas. The mechanisms of particle formation and growth, sedimentation

phenomenon, and the effects of particles on human health and the environment are all commonly addressed research topics. Aerosolised particles provide an effective mode of transport for a wide range of minute particles of dust, minerals, trace elements, and micro-organisms attached to the surface or incorporated into the liquid droplet. The theory of aerosol behaviour originated with studies of atmospheric particles, beginning with Aitken's work in the 19th century (Podzimek, 1989).

Almost any operation manipulating a microbial suspension can result in the generation of an aerosol (Norris, 1994). However the physical characteristics of an aerosol and the environment in which it was formed predominantly determine the distance that it will travel and the form it will take. Generally large particles will travel a shorter distance and sediment more rapidly compared to small particles. Within any aerosol the particle size distribution will be a factor of the manner of the release and the characteristics of the original liquid (Szewczyk *et al.*, 1991). Hage and Wessels (1980) investigated the number of bacteria present in varying sizes of aerosol droplets. An aerosol containing 2×10^9 bacteria mL⁻¹ would produce droplets of 5 μm radius that would contain 1 bacterium. Larger droplets of 100 μm radius would contain in the region of 8000 bacteria. The larger particle of 100 μm radius was shown to sediment about 100 times quicker than the smaller 5 μm particle. The number of bacteria present in a release will depend on where they are being released from. In a freshly inoculated bioreactor there will be significantly fewer bacteria present than in the liquor removed in an early downstream processing operation. Ashcroft and Pomeroy (1983) performed small scale experiments that showed an aerosol of bacteria would contain a fraction (10^{-6}) of the total number of bacteria present in the escaping liquid. This data does provide a good first approximation to quantify the hazard posed by the release of an aerosol.

The interaction of the environmental factors and the physical characteristics of the aerosol will determine the duration that a micro-organism will survive in an aerosolised state. Over the years a great deal of research has been done investigating the survival of airborne bacteria much of it based on work by Harper *et al.* (1958), Cox (1966) and Ehrlich *et al.* (1970). The actual generation of the aerosol may produce sufficient energy to rip apart many bacteria and account for a sizeable proportion of the 10^{-6} drop in number seen by Ashcroft and Pomeroy (1983). Environmental factors such as relative humidity and temperature will form the largest stresses on cells in an

aerosolised state (Cox, 1989). These factors will bring about a decrease in cellular water content that will damage metabolism and membranes in all aerosolised micro-organisms. Another factor identified by Cox (Cox, 1989) was the “Open Air Factor” (OAF). The OAF was the effect that olefin-ozone reaction products had on micro-organisms. When indoor air was examined micro-organisms survived longer on microthreads than identical particles exposed to outdoor air. It has also been shown that the survival of micro-organisms is dependent on the suspending medium (Marthi *et al.*, 1990). When a bacterium is aerosolised in a typical broth the media components act as foci for bacterial adhesion. This results in larger aerosol droplets and in such an arrangement bacteria are more likely to survive aerosolisation. Cells on the periphery will probably die but they will act as a barrier to dehydration for cells on the interior. In an aerosol of cells suspended in buffer the protective effect will be minimised and higher cell mortality will be reported (Marthi *et al.*, 1990). All of these factors need to be considered when designing a method for sampling airborne bacteria. The assessment of bioaerosols was the subject of a critical review by Griffiths and DeCosemo (1994) investigating current techniques available for sampling and detection and considering the problems inherent in dealing with bioaerosol systems.

1.2.3 Hazards Associated With Bioprocess Releases

Although bioprocesses are generally considered safe the main hazards arising from the uncontrolled release of micro-organisms and their products in biotechnology operations are from inhalation, ingestion and by skin contact (Norris, 1994). The latter two routes can be avoided through suitable protective clothing and training. The hazards remaining with the inhalation of micro-organisms or their products can be split into five categories (Bennett, 1994):

1. infection by a pathogen;
2. allergic reaction to viable or non-viable micro-organism;
3. allergic reaction to a product;
4. reaction to endotoxin;
5. toxic reactions.

As most bioprocesses use non-pathogenic organisms the first hazard is not as serious as public perception would believe. Far more common is the allergic response to an

organism or a bioproduct. The first symptom of an allergenic response is the loss of lung capacity. Because there is a lack of quantitative information on airborne levels of micro-organisms in bioprocessing there are no threshold limit values for acceptable exposure. This is not the case with endotoxin, which is far more well characterised. Endotoxin is a term used interchangeably with lipopolysaccharide, a major component of Gram-negative bacteria cell walls. Dunnill (1982) describes symptoms similar to influenza lasting 24 hours in workers exposed to *Pseudomonas aeruginosa*. As many Gram-negative bacteria produce intracellular enzymes their extraction often requires the use of high pressure homogenisation to break the cells. It is this sort of operation which can produce the most significant bioaerosol release. Workers may also suffer other toxic effects from unprotected exposure to micro-organisms, products or by-products. This is particularly true for people working with antibiotics.

There could also be environmental hazards associated with the uncontrolled release GMMOs from a bioprocess. If as a result of an accident there was a release of GMMOs from a processing suite the organisms would have to breach the secondary containment features of that room before they could escape to the external environment. This highlights the need for appropriately designed secondary containment around a processing area.

1.2.4 Bioprocess Release Research

There is an increasing understanding of the deliberate release of GMMOs to the environment for agricultural, biopesticide and bioremediation tasks. However there is little quantitative data on the release of GMMOs from contained bioprocesses. The difficulty of quantification and the assumption that a contained design will be contained in practice have resulted in sporadic investigations on the incidental and accidental release of micro-organisms.

Dunnill (Dunnill, 1982) has shown that after whole cells were discharged from a disc stack centrifuge high levels of micro-organisms could be detected. Tinnes and Hoare (Tinnes and Hoare, 1992) refined this experiment and monitored the release of supernatant from a centrifuge. A silt sampler and settle plates were used to monitor the release of micro-organisms from the deliberately leaking centrifuge. The use of settle

plates confirmed that some micro-organisms had been transported far from the leak. Investigations into the transport of microbial particles has been carried out by a variety of researchers, notably Lighthart and Kim (1989) and Bae *et al.* (1998).

Beyond simple monitoring experiments there has been a lack of quantitative data generated, mainly due to the difficulty in quantitatively collecting airborne micro-organisms. Cameron *et al.* (1987) attempted to quantify the number of spores released from a valve opening by using a slit sampler. Tuijnenburg Muijs *et al.* (1987) used active sampling and settle plates to investigate the air and surface contamination resulting from microbiological processing. By using a cyclone collection device and direct counting Ferris (Ferris, 1995 a & b) showed that aerosols can be sampled quantitatively. Approximately 40 % of the total number of cells released into a 0.36 m³ cabinet were captured by the cyclone which sampled the air at 360 Lmin⁻¹. The work of Ferris showed that it was possible to count cells once captured and relate this number to the number present in the air during the sampling period. This method was effective as it removed the uncertainties and low estimates resulting from quantification through culturing cells. Previously data on micro-organism levels in aerosols was at best an estimate of the true number. The work by Ferris was further developed by Noble (1996) and improved by the use of a quantitative polymerase chain reaction method for the measurement of genetically modified *E. coli* cells in fermenter exhaust gas. The technique employed enabled a detection limit of approximately 10 cells per litre of air sampled.

A recent review by Crook and Cottam (1996) showed that within the UK biotechnology industry bioprocess release monitoring does take place in well-defined strategies. The sampling methods employed by the companies questioned in the review varied and a need for further identification of typical background levels and sampling methods was desired. The variety of methods used are an example of poorly described specifications for bioprocess containment. The pursuit of absolute containment is purely an academic endeavour. Practically, what is required is a more or less stringent degree of containment selected according to the application requirements. Therefore it is necessary to establish a practical release rate that is acceptable to the bioindustry as a whole.

1.3 Methods Of Aerosol Sampling

The delicate nature of airborne micro-organisms makes them hard to sample and assay quantitatively. Methods for collecting microbial aerosols are similar to those for collecting other airborne particles. However the processing and analysis of the samples after collection requires greater attention to detail. Detecting viable micro-organisms usually requires that the collected cells be allowed to multiply to readily observable numbers, through culturing. The literature on sampling airborne micro-organisms is extensive. Reviews have been written which discuss the selection of specific types of samplers and the limitations of various sampling devices (May, 1980; Fannin, 1981; Benbough *et al.*, 1993; Griffiths and DeCosemo, 1994). Upton *et al.* (1994) evaluated three types of collection device comparing their collection efficiency with regard to sampling bioaerosols. Much of the technology for collecting airborne microbes was developed by medical researchers and by microbiology laboratory personnel. This probably stemmed from a desire to protect their patients health as well as their own.

There are a number of forces or mechanisms which are employed for the collection of aerosols. Most often gravitational and inertial forces are used to settle particles and filters are commonly used to trap aerosols. Since many collectors utilise more than one of these factors, aerosol sampling devices can be classified into several categories. Some devices have been designed with sampling bioaerosols in mind and others are more general in their application.

1.3.1 Passive Aerosol Sampling

The passive sampling techniques rely upon gravity to cause aerosol particles to settle on to a sampling surface. The surface may be an open Petri dish, an adhesive coated surface, or a collecting liquid. The problem with these types of methods is that the collection is biased towards large particles that settle rapidly close to the source of emission. This creates a skew in any data as the number of cells collected will be under-reported. Additionally to assess the viability of cells a culturing step is required, incorporating all the uncertainties of plate counting methods. Hence quantitative measurements of bacterial loading are hard to perform with passive sampling regimes.

Nonetheless passive sampling could be used for collecting aeroallergens for microscopic identification, and is also useful for the long term collection of more hardy organisms.

1.3.2 Active Aerosol Sampling

To collect micro-organisms consistently and to remove the uncertainties of passive sampling, active sampling devices enable the air flow through the device to be measured allowing quantitative particle collection. The method of airflow manipulation and the variety of collection surfaces employed provides a variety of different samplers.

1.3.2.1 Impactors

Impactor samplers operate by causing aerosol particles to deposit on to solid or semi-solid surfaces. The air is usually pumped so that a change in its direction of flow causes a collision with the collection surface. The biggest difference between an impactor and a settle plate is that the impactor device has a forced air flow, yet in all other respects the method employed is the same. The sample is collected and then cultured directly off the collection media. Some impactor collection equipment does allow information on the particle size distribution of the aerosol to be determined, compared with simpler forced impaction devices (Table 4).

Table 4 Common impactor sampling devices.

Device	Particle Size Information	Sampling Air Velocity	Notes	Reference
Anderson Microbial Sampler	✓	28 L min ⁻¹	8 stage particle separation	Anderson, 1958
Marple Personal Cascade Impactor	✓	2 L min ⁻¹	8 stage particle separation	Macher & First, 1984
Casella Slit Sampler	×	30-700 L min ⁻¹	Collection on rotating agar plate	Lundholm, 1982
Biotest RCS	×	40 L min ⁻¹	poor collection of particles < 4µm diameter	Hambleton <i>et al.</i> , 1992

1.3.2.2 Impingers

An impingement separator is a sampling device in which the particle laden gas is caused to pass through a jet or slit which increases the velocity of the air and the inertial velocity of particles being carried. The greater inertia of the suspended particles results in their deposition in the collecting liquid. Many impingers were originally designed to simulate the air flow through nasal and bronchial passages, and operated by drawing air into a liquid medium. The advantages of sample collection in a liquid medium are that large particles containing more than one cell can be separated and you have a more flexible starting point for further analysis. There are impingers that give limited particle size information upon collection and impingers that will not segregate the particles in a sample (Table 5). Cyclone sampling devices are commonly used where a large volume of air has to be sampled, as they have a high sampling velocity and can be run for 20-30 minutes without overloading the collection.

Table 5 Common impinger sampling devices.

Device	Particle Size Information	Sampling Air Velocity	Notes	Reference
Swirling Aerosol Collector	*	12.5 L min ⁻¹	Combines impaction and centrifugation	Willeke <i>et al.</i> , 1998
May Three-Stage Impinger	✓	Low	3 stage particle separation	May, 1966
Porton All Glass Impinger	*	12.5 L min ⁻¹	two common configurations	Zimmerman <i>et al.</i> , 1987
Cyclone collectors	*	≈ 750 L min ⁻¹	variety of designs	Errington & Powell, 1969

1.3.2.3 Other Sampling Devices

There are many variations on a theme for impaction and impinging samplers, slight changes in the device geometry can cause very different collection characteristics (Grinshpun *et al.*, 1997). Because of this other methods of microbial capture from air tend to be for more specialised applications. For the collection of sub-micron particles electrostatic precipitation samplers can be used (Stetzenbach *et al.*, 1992). But the

exposure to a high electric charge may also produce high local concentrations of ozone and nitrogen oxides, all of which reduce microbial viability. And as the precipitation velocity is low in this type of device they are only useful at very low flow rates. The collection of airborne bacteria using small cassette filters and high volume filter devices has also been tried. However there is a significant loss of viability (Neef *et al.*,1995) due to the desiccation caused by the filtering technique. The filter type samplers are relatively inexpensive and portable which tends to make them useful for the monitoring of airborne allergens, such as endotoxin.

1.4 Cyclone Design And Application

In 1969 Errington and Powell (Errington and Powell, 1969) used a cyclone separator for aerosol sampling. They recognised the potential of a cyclone as a collection device for micro-organisms despite no coherent theory existing for their design. Cyclones were originally used as simple dedusting devices for the chemical industry, and still find use in that role today.

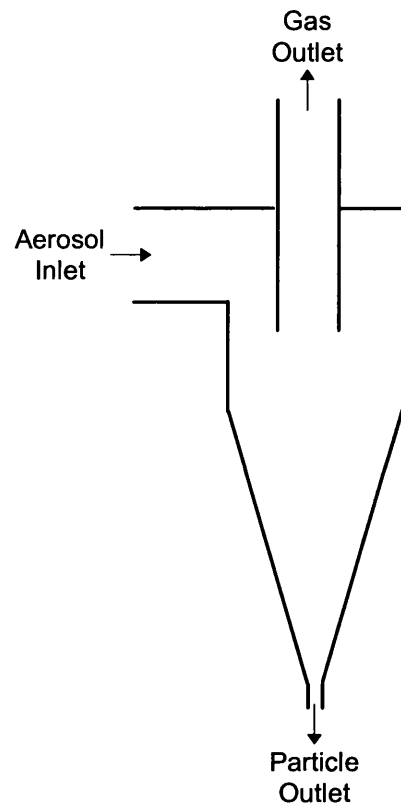


Figure 1 A simplified vertical section of a cyclone, showing the bulk phase flows.

Cyclones generally consist of two sections (Figure 1), an upper cylindrical section and a lower conical section. The gas flow enters the upper section tangentially and exits axially through an exhaust tube in the centre of the upper section. Separation of particles in a cyclone is due to the centrifugal force caused by the spinning gas stream; this force throws particles outward and into the cyclone wall. Opposing this outward particle motion is an inward drag force caused by gas flowing towards the axis of the cyclone prior to its discharge.

1.4.1 Models Of Cyclone Behaviour

As many different types of cyclone have been built it is important to characterise a cyclone when attempting to improve existing designs or model it effectively. There are eight common dimensions used to characterise cyclones, often expressed as a ratio to the cyclone body diameter. Standard cyclone designs exist but there is no reasoning to prove that they operate optimally. This is where the real value of modelling appears, as a good model could predict changes in dimensions and operation that should improve performance.

Cyclone collection efficiency is defined as the fraction of particles of a given size that are retained by the cyclone. The first model attempting to describe cyclone efficiency was proposed by Rosin in 1932. Since then many theories have been developed to predict the performance of a cyclone. Researchers tend to agree that operating parameters should be used to predict performance, as well as particle and gas characteristics. An area of debate are the effects of cyclone dimensions and geometry with varying numbers of cyclone dimensions included in predictive models.

All cyclone theories aim to create a force balance between the outward centrifugal force and the inward drag force. There are three general approaches taken to predict cyclone efficiency, however it is unrealistic to expect that one model will predict collection efficiency for all applications.

1.4.1.1 Critical Diameter, Timed Flight Models

This method assumes that particles enter the cyclone at a certain radial distance from the cyclone axis. Particles must then travel outwards from this point to the cyclone wall where they are impacted. The critical diameter in these models is the particle size that travels exactly this distance during its residence time in the cyclone. This theory was first proposed by Lapple (1950) and was used as a starting point for more widely used models.

1.4.1.2 Critical Diameter, Static Particle Models

The static particle models determine the particle diameter for which centrifugal force is exactly balanced by the drag force. These theories predict that there is a critical particle size which will spin indefinitely about the cyclone core, below the gas exhaust. The models assume that the critically sized particle will have a collection efficiency of 50%, and hence the critical particle diameter is referred to as the d_{50} . The static particle approach predicts a sharp increase in cyclone efficiency from zero for particle smaller than the d_{50} to unity for larger particles. This sharp discrete separation is never seen in practice due to variations in radial and tangential gas velocities over the height of the cyclone. This type of theory was first developed by Stairmand in 1950, and later refined by Barth (1956). According to this theory the d_{50} can be calculated for any cyclone and operating conditions if the tangential velocity at the core and core length are known.

1.4.2.3 Fractional Efficiency Models

Cyclone theories now assume that gas turbulence mixes uncollected particles in any plane perpendicular to the cyclone axis. This allows the entire fractional efficiency curve to be determined without resorting to a generalised curve based on a critical particle diameter. This theory was first proposed by Leith and Licht (1972). The description of the fractional collection efficiency is more complex for this model as it incorporates all eight cyclone dimensions and includes a modified inertia parameter to compensate for particle and gas properties. This theory does suffer from a simplified handling of the gas mixing which was refined by Dietz in 1981.

1.4.2 Experimental Performance Of Cyclones

An empirical approach to cyclone design has been adopted by some designers (Swift, 1986) but most mechanical engineers develop a model then test it experimentally with reference to other existing models (Dirgo and Leith, 1985a and b; Iozia and Leith, 1989, 1990; König *et al.*, 1991; Moore and McFarland, 1993). A number of papers have focused on the separation of particles in cyclones and the best way to design experiments and collect data (Bürkholz, 1985; Kim & Lee, 1990). Computational fluid

dynamics (CFD) has also been used to examine the correlation between models and experiments (Griffiths & Boysan, 1992; Griffiths & Boysan, 1996).

What is clear from the models proposed for predicting cyclone efficiency is that each of them works best under certain conditions specific to the type of cyclone and the operating conditions. Some experiments are carried using heterodisperse aerosols and some with homogenous aerosols. The heterodisperse experiments can not be accurately duplicated and as a result make drawing conclusions between models difficult. With particle sizes from 1 μm to 10 μm discrepancies among theories and differences between results are the greatest. The particles at this size are most likely to be affected by small variations in the internal gas dynamics than larger particles, hence attempting to model them is all the more difficult.

Moore and McFarland (1993) recommend that a designer should start with a cyclone following the dimensions laid down by Stairmand (1956) as there is the greatest information on this design. Iozia and Leith (1990) present their modified Barth (1956) model and prove that it gives the best correlation to recent experiments and competing models. Although this method may predict efficiency significantly better than other methods there is still a great deal of scatter about the results. Some of this will result from experimental errors and some will be due to shortcomings in the model.

Most importantly when looking at the experiments performed and the performance achieved with cyclones it is important to note the scale of the experiment and the aerosol used. Industrial cyclones are designed to collect dust and are built on a much larger scale than the sampling cyclones used for collecting micro-organisms from aerosols. It has been shown that small scale cyclones do have higher collection efficiencies (Kim & Lee, 1990). The treatment of the aerosol is important as it greatly affects the particle characteristics; the difference between a sphere of water and a solid dust particle can not be stressed enough when comparing experimental data.

1.4.3 Optimisation Of Cyclones For Bioaerosol Sampling

From the literature it is clear that there is still a great deal of uncertainty over the best way to optimise the cyclone design, and it is also clear that the cyclone can be used to collect airborne micro-organisms (Errington & Powell, 1969; Hambleton *et al.*, 1992). Therefore the best approach for a microbiologist to optimise the recovery of airborne micro-organisms is to look at the operation of the sampling cyclone rather than to look at modifying the cyclone itself.

A liquid rinsed cyclone for collection of the microbial sample is crucial, by collecting into a liquid you can disperse large agglomerates of cells and use this liquid for culturing inocula and other forms of assays. But in using a liquid to rinse the surfaces of the cyclone you introduce two sources of sample loss. Firstly, precession currents will develop at the top of the cyclone body and cause a frictional effect on the liquid flow. The increased friction causes an increase in the inwards drift of the liquid rinse which will then creep over the roof of the cyclone and the outside of the gas exhaust tube till it is lost on the lip of the exhaust tube. In order to reduce this effect with washed cyclones some are fitted with a serrated skirt that is fixed to the roof of the cyclone (Swift, 1986). The skirt flares out at about 30 ° so that any liquid following a precession current will travel down it and then at the serrated edge form a droplet and fall back into the vortex. Secondly the higher air velocities will increase evaporation of the liquid rinse. This can be significant as there will be a thin layer of liquid covering most of the cyclone surfaces, providing a large area for evaporation to take place. To overcome this is difficult, but precautions can be taken to prevent excess sample loss, such as keeping the sampling time short. To increase the removal of impacted cells from the walls of the cyclone Errington and Powell (Errington & Powell, 1969) briefly investigated the use of surfactants. Their results showed conclusively that by adding a surfactant you could improve the collection efficiency of the cyclone. They suggest the use of a non-ionic surfactant as they are generally chemically inert, which is important when performing assays on the sample liquid, particularly PCR reactions. The sampling rate is also important as cyclones can be operated at high and low air throughputs. The higher the sampling rate the greater the efficiency of collecting small particles, but cyclones can be run at a lower velocity if isokinetic sampling is important. Sampling indoors requires less attention to air velocity because the velocities expected are low. It has been shown that considerable variation is tolerable in the design of the inlet to

samplers for small particles. May and Druett (1953) have shown that particles below 7.5 μm diameter are not affected greatly by anisokinetic sampling conditions. On the other hand if the aerosol particles are large and being carried in an air stream at over 2 ms^{-1} isokinetic sampling should be used.

1.5 Methods To Quantify Micro-Organisms

The optimal bioaerosol sampling device will have a high collection efficiency and deliver a sample that can be assayed by a number of different methods. There are many different methods available for the detection of micro-organisms. They range from simple colony counting to sophisticated molecular biology techniques. Some methods are specifically designed for the detection of GMMOs within the natural environment (Steffan and Atlas, 1991). Methods used for the quantification of GMMOs must function at the genomic level to truly distinguish between strains. Whilst a simple plate count can quantitate the number of culturable cells, it can not distinguish between genetically modified and wild type strains in a mixed culture. This is the limitation of phenotypic methods of microbial quantification. The application of quantitative methods to the enumeration of micro-organisms in bioaerosols is more complex, as the environment imposes metabolic and physical stresses. This may damage the cells or kill them, which raises the issue of distinguishing between viable cells, viable but non-culturable cells and dead cells (Colwell *et al.*, 1985; Islam *et al.*, 1993). As a result of this not all methods in existence are suitable for quantifying the microbial load in bioaerosols. Techniques that have been applied are outlined in Table 6.

Table 6 Methods of microbial quantification.

Method	Sensitivity	Specificity	Speed	Quantification	Example
Colony Counts	Low	Low Phenotypic	Days	Culturable cell count	Errington and Powell, 1969
Microscopy	Low	Low Phenotypic	Minutes	Total count	Ferris <i>et al.</i> , 1995
Bioluminescence	Low	None Phenotypic	Minutes	Viable count	Stewart, 1990
Immunoassays	Relatively	High Phenotypic	Hours	Total count	Colwell <i>et al.</i> , 1988
Gene Probes	Relatively	High Genotypic	Hours	Total count	Neef <i>et al.</i> , 1995
PCR	High	High Genotypic	Hours	Total count	Nugent <i>et al.</i> , 1997

1.5.1 Polymerase Chain Reaction

Of all the techniques available there has been a rapid development in the application of the polymerase chain reaction (PCR) to bioaerosol samples and environmental monitoring. The advent of PCR allows the selective amplification of specific DNA sequences which, then at high concentrations can be easily detected. The PCR technique uses an enzymatic amplification of specific DNA sequences, using two oligonucleotide primers that hybridise to opposite strands and flank the region in the target DNA to be synthesised.

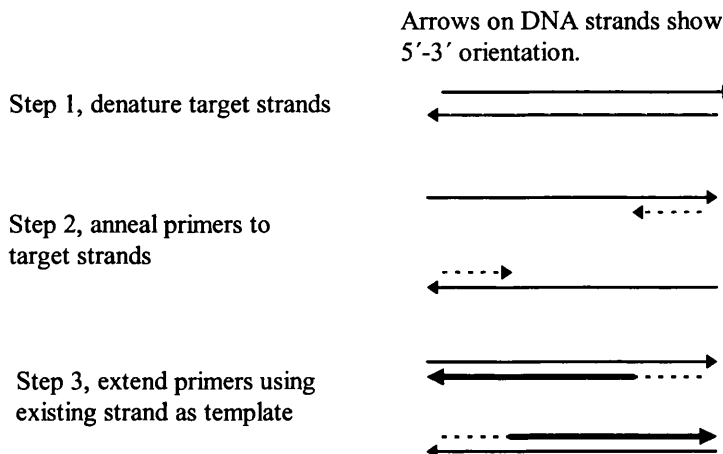


Figure 2 Schematic representation of one PCR amplification cycle.

The enzymatic amplification is controlled by cycling the temperature of the reaction mixture causing, template denaturation, primer annealing, and primer extension. The products of one round of amplification can then serve as the template in the next giving a doubling of target DNA in each round (Figure 2). Therefore 30 cycles of amplification can theoretically yield a billion fold (2^{30}) amplification of the target sequence.

Once the PCR has been performed there are a number of methods available for the identification of the amplified DNA. The simplest method is to run the DNA on an agarose gel and measure the size of the fragments. The identity can be confirmed with labelled DNA probes or other techniques.

PCR has a number of advantages over traditional methods for the detection of GMMOs;

- detection is based on the presence of a nucleotide sequence, hence there is no prerequisite for the expression of a marker compound;
- the selectivity of the technique allows the distinction between the target organism and closely related strains;
- the technique is very sensitive and can in theory detect a single organism.

1.5.1.1 Quantitative PCR

Much of the work on detection of specific micro-organisms by PCR has been concerned with the qualitative detection of a micro-organism. The problem in trying to obtain quantitative data from PCR assays is inherent in the amplification process. Because the amplification results in an approximately exponential growth (Ferre, 1992) in the concentration of the target DNA, small differences in the reaction can become significant sources of error. The careful control of chemical and physical parameters involved in the reaction is essential to prevent a high degree of variation between samples (Gilliland *et al.*, 1990b). As the number of cycles of amplification increases the rate of product accumulation decreases, resulting in a plateau for the PCR where an increase in cycle number does improve product yield. This makes the correlation of product and initial target concentration difficult (Gause and Adamovicz, 1994). To establish the initial target concentration there are three approaches that can be used.

1. The measurement of products during the linear section of the PCR, which requires extremely sensitive product detection methods as the amplification is considerably lower than normal (Gause and Adamovicz, 1994). Equally this approach can suffer from high variation between samples if there are any inhibitors of the PCR which is possible when dealing with a “dirty” environmental sample (Jansson, 1995).
2. The use of a limiting dilution principle as demonstrated by Picard *et al.* (Picard *et al.*, 1992). Through the use of amplified dilution series and statistics a quantification of the initial target concentration can be achieved.
3. The use of a competitive internal standard for quantitative PCR (QPCR) methods overcomes many of the problems associated with the alternative methods (Gilliland *et al.*, 1990a; Forster, 1994; Jansson, 1995). The internal standard normally used is a section of DNA that has been constructed (McCulloch *et al.*, 1995) and co-amplified

with the target DNA. Because the amplification takes place in the same reaction the product accumulation is proportional to the initial starting concentrations of the standard and the target sequence (Gilliland *et al.*, 1990). The ratio of the two products can be measured by, for example gel electrophoresis, and by comparison with standards the initial starting concentration of target DNA can be quantified. Initially when QPCR was first attempted there was a great deal of scepticism (Ferre, 1992) over the technique. Since then there has been extensive development of the technique resulting in a range of methods now available (Radich, 1996).

The detection and quantification of PCR products is the final stage in the quantitative analytical procedure. Non-specific methods of detection commonly used include electrophoresis (Gebhardt *et al.*, 1994) and high performance liquid chromatography (HPLC) (Chan *et al.*, 1994). Gel electrophoresis can, with the inclusion of an image analysis or densitometry step, allow the quantification of DNA bands present (Sundfors and Collan, 1996). The use of nucleic acid probes enables the specific detection of PCR products, which can improve the specificity and sensitivity of the assay (Reischl and Kockanowski, 1995). This is an area of ongoing development with many alternative methods of direct and indirect identification of the PCR product available (Kricka, 1995).

1.6 The Application Of Leak Detection To Bioprocesses

As has been previously stated (section 1.2.2) accidental releases can not be prevented, but they can be anticipated and the process design and operation structured to minimise their occurrence. Incidental releases are most likely to result from a failure in the design or maintenance of the process and will most often be manifested in the form a leak. In process plants over 40 % of leaks can come from faulty valves and 25 % from faulty pumps (Bello & Siegell, 1997). Large leaks are often easily located by eye, but small leaks require sensitive equipment to locate, which is often a time-consuming exercise. For example, when constructing a pressure vessel it is important to perform an integrity test to ensure that seals, joints, *etc.* do not have any imperfections which could result in a leak. Generally, welds are checked using x-ray analysis after manufacture for high specification vessels, and once complete, the vessels are leak tested.

Within the bioindustry where containment is a key issue, there are relatively few methods available to test the integrity of process components. The issue of containment in bioprocesses is whether an organism or contaminant can enter or leave the process via an uncontrolled route. Hence leaks in the bioprocess industry need to be measured absolutely with respect to a microbial release. Relative release rate specifications for process equipment are expensive, time consuming and open to misinterpretation unless precisely described. It has been suggested that, when specified, zero leakage be defined as a measurable quantitative value of leakage rate that is insignificant in the operation of the system (McMaster, 1982).

If the diameter of a leak can be established it could be compared with the process organism to determine a critical leak size through which that organism could not pass. This could then be used to provide realistic quantitative information on the process containment and the likelihood of a release. By simply pressurising a vessel and measuring the drop in pressure over time, a leak small enough to allow the release of a micro-organism may not be detected. To localise and quantify leaks large enough to allow the passage of a micro-organism more sophisticated methods of leak detection are required.

1.6.1 Methods Of Leak Detection

Leak detection can at its most simplistic be a visual inspection of a filled container, if you can see the contents escaping you have a leak. This basic form of leak detection is not quantitative and dependent on the inspector being able to see the release. There are a variety of more sophisticated approaches to leak detection available, with the most appropriate method for a given situation depending on the equipment under test, and the performance criteria of the method (Table 7).

Table 7 Leak detection method sensitivity, from McMaster (1982).

Method	Sensitivity ($\text{Pa m}^3 \text{s}^{-1}$)	Comments
Pressure hold test	Time limited	Only large leaks, slow, overall quantitative measure
Ultrasound	0.05	Only large leaks, rapid, leak location only
Chemical penetrants	10^{-4}	Simple, leak location only, may block, clean up required
Bubble tests	10^{-5}	Simple, leak location only, may block, clean up required
Thermal conductivity	10^{-6}	Simple, portable, inexpensive
Halogen detectors	10^{-10}	Portable, sensitive to ambient halide gases
Mass spectrometer	10^{-12}	Expensive, complex

Within the bioprocess industry all of the above methods (Table 7) could be used for leak detection. However by far the commonest methods used are pressure hold tests, chemical and liquid penetrants, bubble tests and halogen tracer gas detectors. The application of these techniques to bioprocesses is further discussed below.

1.6.1.1 Pressure Tests

A pressure hold test is a simple measure of the ability of a vessel to maintain a set pressure. By measuring the exponential pressure decay over a period of time it is possible to assign an overall leak rate for the vessel under test. If a vessel losses pressure it could signify a leak or poorly sealed connection. The disadvantage of this approach is that it is very dependent on sensitive pressure transducers and long run times to allow small leaks to become detectable. Nonetheless this method is widely

used for many vessels, particularly in small pilot plants where lag times for pressure drops are shorter in smaller vessels.

1.6.1.2 Bubble Tests

Bubble tests are simple and inexpensive to perform. Typically the equipment under test is pressurised and a low surface tension liquid detergent applied to the surface areas of examination, such as welds, flanges, *etc.*. The appearance of bubbles on the surface of the applied solution signifies a leak. The process of forming the bubbles is dependent on the pressure conditions, and the properties of the liquid film and the gas under pressure. If these conditions are standardised it is possible to approximate the leakage rate from the collection of a known volume of bubbles over a period of time (McMaster, 1982).

1.6.1.3 Penetrant Methods

Penetrant methods are more appropriately used for small pieces of equipment or pipework. The principle relies on the leakage of the penetrant through the fault where it can be detected on the surface. There are a variety of special coloured or fluorescent penetrants which can be detected by means of a developer or by direct viewing in darkness with the aid of ultra-violet (UV) light. The special properties of the penetrant substances include a low viscosity and surface tension and a highly sensitive dye material. This type of method is not quantitative and can only highlight leaks through which a low viscosity liquid could pass. This could leave leaks through which a gas could escape undetected.

1.6.1.4 Tracer Gases

The typical halogen leak detector system comprises a sensor, air pump, power supply and associated electronics to convert the sensors signal to a real value. Baram (1991) has proposed that only tracer gas techniques offer the reliability and ability to localise and quantify leaks in bioprocess equipment. The use of tracer gas based leak detectors began with the development of the atom bomb (Nerken, 1989). Part of the Manhattan Project required the separation of radioactive uranium-235 from uranium-238 which occurred as uranium hexafluoride. This separation took place in the vapour phase and

leaks from process equipment could not be tolerated. Consequently a leak detection device was required, the result was a leak detector based on a simplified mass spectrometer for helium gas. Since then the variety of detectors and tracer gases has increased.

Sulphur hexafluoride (SF₆) is most commonly used as an insulator for electrical switchgear and other high voltage power applications (Brüel & Kjær Innova, 1997). As SF₆ does not naturally occur in the environment and is a strongly electronegative gas it is widely used as a tracer gas. Because SF₆ is larger than helium (0.51 and 0.26 nm molecular diameter respectively) it is less likely to permeate through plastic and elastomer seal materials, which is an advantage to using it as a tracer gas in a bioprocessing environment. However the high molecular weight of SF₆ (146 Kg) may result in stratification of the gas after injection into a vessel if adequate mixing of the gas is not provided. This would then result in a lower resolution of leak detection. The majority of SF₆ leak detectors are based on an electron capture detector, as used in gas chromatography. These serve as the signal transducer and can give a sensitivity of 1 part of SF₆ in 10⁸ parts of air.

As a tracer gas SF₆ finds applications not only for leak detection (Seliverstov, 1992) but also for studying ventilation in buildings (Riffat & Cheong, 1992; Dols & Persily, 1995) and mines (US Bureau of Mines, 1995), nuclear reactor building integrity (Collins & Lafreniere, 1994.), and the environmental monitoring of pollutants (Horrell *et al.*, 1989). Although the SF₆'s chemical and physical properties make it very attractive for the applications above, it is one of the worlds most potent "Greenhouse" gases with a Global Warming Potential 25,000 times greater than that of carbon dioxide (Brüel & Kjær Innova, 1997). This may cause its use to be limited in the future with constraints on halogenated gas emissions increasing.

1.6.1.5 Alternative Methods

The use of leak detection techniques is very well established in the chemical and petrochemical sector. This has been driven by tightening environmental and safety regulations around the world as a result of high profile accidents such as the Piper Alpha disaster (Whaley and Ellul, 1994). The use of leak detection systems and supervisory

control and data acquisition (SCADA) programs are an integral part of modern pipeline operation. Equally popular are acoustic systems that can monitor a section of pipeline for leaks through pattern recognition of pressure fluctuations. There are model based methods that simulate fluid flow in real-time and compare this with the hydrodynamic data acquired from an array of sensors, these can provide an alternative and more accurate monitoring than SCADA systems. There is no published use of these systems applied to bioprocesses, probably because the scale of operation is too small and the sensitivity (0.38 L h^{-1} (Young, 1993)) not high enough.

1.6.2 Flow Through And Categories Of Leaks

All leak detection with tracer gases involves their flow from the high pressure side of a boundary through a presumed leak to the low pressure side. Depending on the pressure and the form of the release (liquid or gas) there are various relationships which can describe the flow of a fluid. All of these are derived from the macroscopic conservation equations of mass, momentum and energy (Tilton, 1997). The basic modes of fluid flow include viscous, transitional and molecular. Viscous flow may be further divided into laminar flow or turbulent flow. Depending on the pressure gradient, fluid characteristics and leak geometry any one of the flow types may result (Figure 3). Permeation of gases is not considered fluid flow as the process involves an number of interactions between the gas and solid. However this effect is of importance when considering leaks within bioprocessing equipment.

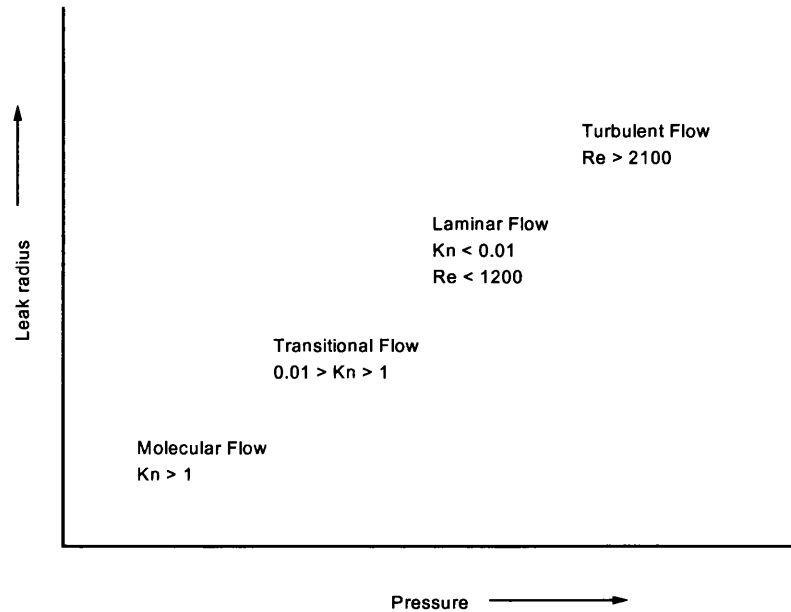


Figure 3 Typical flow regimes of capillary leaks, where Kn and Re are the Knudsen and Reynolds number respectively.

There are established theoretical relationships describing the behaviour of fluids within each flow regime. These relationships for the flow rate through a leak are a valuable tool when investigating a model system and comparing results with empirical findings. Additionally an understanding of fluid mechanics allows leak categories to be differentiated by the observation of the effects of time and pressure on a leaks magnitude (Beavis, 1970). This is of particular use when there is a molecular or permeation leak in the equipment under test.

1.6.2.1 Permeation Leaks

A permeation leak requires an interaction between the tracer gas and the solid through which it is passing. The interaction is in the form of a distortion or complete dissociation of the electron cloud from the atom of the molecular gas. The activation energy required to enable the distortion of the electron cloud must come from the environment. Beavis (Beavis, 1970) has cited hydrogen as an example of a gas that does not flow as a molecule but rather as an atom through metals. The molecular and atomic size of the tracer gas then become important factors in determining the likelihood of permeation leaks. For a system to be leak tested effectively with a tracer

gas, permeation of that gas through any test components should be ideally zero. However this will never be achieved as there will always be interactions at the atomic level that can not be prevented. As such permeation leaks through semi-permeable materials, such as plastics and elastomers used in flange seals, could contribute to background levels of tracer gas within a process area. To overcome this problem when leak testing, large molecular weight tracer gases should be used at lower test pressures. Additionally, areas of high permeability should be tested first whilst the gas is still being transmitted through the porous component.

1.6.2.2 Molecular Flow Leaks

A molecular leak occurs at low pressures and with leaks of a small bore, the assumption for this type of leak is that the mean free path of the gas molecules is larger than the cross sectional diameter of the leak ($Kn > 1$). This type of leak will be unlikely to allow the transmission of a liquid due to the effects of surface tension. The molecular flow of a gas through a capillary has been characterised (Equation 1) by Tilton (Tilton, 1997).

Equation 1 Molecular gas flow through a capillary.

$$Q_m = \left(\frac{\pi D^3}{8L} \sqrt{\frac{RT}{M}} \right) \Delta P$$

The flow rate of molecular leaks is very small and it is probable that tracer gas leaking through a hole will exhibit molecular flow at low pressures. The throughput of a molecular leak is proportional to the pressure difference applied across the leak. This relationship can be used to establish that the leak observed during a leak test is molecular in nature.

1.6.2.3 Transitional Flow Leaks

Transitional flow will typically occur when the gas mean free path is approximately equal to the cross sectional diameter of the leak. This type of flow is very complex as its behaviour is described by both molecular and laminar flow components. This combination of flow behaviours enabled Knudsen to derive an equation for the mixed flow through a long capillary, which Burrows (Burrows, 1961) later simplified. More

recently Dobrowolski (Dobrowolski, 1988) stated a poorly justified form of this equation, and Baram (Baram, 1991) provided a modified form of Knudsen's derivation for use in leak testing bioprocessing valves (Equation 2).

Equation 2 Transitional capillary flow throughput.

$$Q_t = 1 \times 10^{-9} \times \frac{d}{l} \Delta p \left[0.00245 \frac{p'd}{\mu} + 3.81 \sqrt{\frac{T}{M}} \left\{ \frac{\left(1 + 0.110 \sqrt{\frac{M}{T}} \frac{p'd}{\mu} \right)}{\left(1 + 0.124 \sqrt{\frac{M}{T}} \frac{p'd}{\mu} \right)} \right\} \right]$$

Both Burrows (Burrows, 1961) and Baram (Baram, 1991) made a number of assumptions in simplifying Knudsen's equation for transitional flow. The assumptions they made require that;

1. the capillary is long relative to its diameter (length ≥ 25 diameter);
2. the capillary has a uniform circular cross section;
3. the gas flowing is isothermal and incompressible over the length of the capillary;
4. the pressure loss over the length of the capillary is large compared with any entrance or exit losses;
5. the flow is not turbulent in any part of the capillary.

Equation 2 takes into account that there will be molecular and laminar flow within a capillary enabling it to be applied quite easily providing the assumptions can be met. Capillaries at low pressure have insignificant laminar flow and at high pressures molecular flow is close to zero. However there is a loss in accuracy due to the molecular slip occurring at the capillary wall during laminar flow. McMaster (McMaster, 1982) states that the effect of slip can change the predicted flow rate by about 20 %. The greatest error resulting from slip occurs when the majority of the flow is molecular. At higher pressures laminar flow predominates and molecular slip can be taken to be equivalent to the molecular flow at zero differential pressure (Burrows, 1961).

1.6.2.4 Viscous Flow Leaks

A viscous leak will typically occur above atmospheric pressure through a large diameter hole where the mean free path of a gas is significantly smaller than the cross section of the leak. Hence viscous flow is often found in systems where tracer gases are used for leak detection. The diameter of the leak and the kinematic properties of the liquid or gas escaping through it will determine whether the leak is turbulent or laminar in nature. The distinction between laminar and turbulent flow can be determined by the Reynolds number for the capillary leak (Equation 3) (Bowman and Davidson, 1972).

Equation 3 Calculation of Reynolds number through a leak with circular cross-section.

$$\text{Re} = \frac{\Delta P \rho r^4}{4L\mu^2}$$

Where:

Re < 2100	laminar flow
1200 < Re < 2100	either viscous flow regime could occur depending on the leak characteristics.
Re > 2100	turbulent flow

A leak in the laminar flow regime has a parabolic velocity distribution across its cross section. Turbulent flow within a leak is only generated by high velocity along the leak path. These velocities can be calculated from the leak characteristics and are shown in Equation 4 (Tilton, 1997). The high velocity results in the formation of eddies and vortices in the flow, creating an erratic flow path.

Equation 4 Average velocity during laminar and turbulent flow.

$$\text{Laminar flow} \quad U = \left(\frac{D^2}{32\mu} \right) \left(\frac{\Delta P}{L} \right)$$

$$\text{Turbulent flow} \quad U = \left(\frac{D^{0.714}}{0.351\mu^{0.143}\rho^{0.429}L^{0.57}} \right) \left(\frac{\Delta P}{L} \right)^{0.57}$$

The overall leak rate can be calculated by multiplying the average velocity by the cross sectional area of the leak. There are other approaches to the calculation of leak rate in the viscous flow regime that can be derived from the Hagen-Poiseuille equation (Tilton, 1997). This is shown in terms of the leak dimensions and pressure gradient in Equation 5.

Equation 5 Laminar fluid flow through a capillary.

$$Q_l = \frac{\pi \Delta P D^4}{128 \mu L}$$

All fluids flowing in the viscous regime exhibit viscosity and as a result of this their flow can also be influenced by the surface roughness of the material they are flowing through. There are well established relationships between the Fanning friction factor and the Reynolds number depending on the surface roughness of the material (Tilton, 1997). These two dimensionless numbers can be used to describe the pressure drop across a tubular leak.

1.6.2.5 Leak Blockage

Self-sealing or blockage of leaks will occur when the pressure difference across the leak is insufficient to overcome the surface tension of the leaking liquid. Burrows (Burrows, 1961) stated that if you assume that the liquid wets the leak wall completely, then the liquid in the leak will be held in place, effectively blocking it below a certain differential pressure (Equation 6).

Equation 6 The pressure required to overcome surface tension in a fully wetted capillary leak.

$$P_s = \frac{2\sigma}{r} \times 1 \times 10^{-5}$$

As water (surface tension, 0.072 N m^{-1}) can block a 1 micron capillary at up to 1.44 bar, vessels to be leak tested should be dried completely before testing.

1.6.3 Leak Detection Research

Since the beginning of research into fluid mechanics researchers have examined the behaviour of liquids and gases that flow through small capillaries as an approximation to a real leak. In 1961 Burrows (Burrows, 1961) published a paper on the flow through and blockage of capillary leaks which drew together earlier work on capillary flow mechanics. A number of papers published in the 1970's investigated the relationships between gas flow and leaks, particularly their detection and prevention in the vacuum industry (Beavis, 1970; Roth, 1972; Bloomer, 1973). Because of this much of the theoretical relationships between gas behaviour and leak rate have been established. Capillary tubes were commonly used as leak elements either for the calibration of leak detection equipment or for the controlled flow of gases into vacuum equipment (Burrows, 1961; Tison, 1993). Research Work by Stecklemacher and Rogal (Stecklemacher, 1978; Rogal, 1978) began to investigate the effect of leak geometry on the throughput of gases in leaks. This research has been extended and a number of papers now focus on defining flow through cracks (Narabayashi *et al.*, 1989; Matsumoto *et al.*, 1989; Matsumoto *et al.*, 1991; Grebner, 1995; Clarke *et al.*, 1997), which are considered more applicable to fatigue and failure studies than capillary simulations of leaks. The area of fatigue, particularly in the nuclear industry has been examined with the goal of developing leak-before-break (LBB) models. The use of LBB analysis to plants enables designers to eliminate pipe rupture hardware and the dynamic effects of pipe ruptures (Dwivedy, 1989). This enables more simple plant equipment to be developed with a better idea of the likelihood of a leak causing the rupture of a pipe under normal and extreme operating conditions (Chexal *et al.*, 1992). However there is no published information of the application of LBB methodology to the bioprocess industries.

What is clear from the published literature is that there are few examples of leak detection applied to bioprocesses. Yet the sensitivity and use of tracer gases are often described in papers (Reich, 1987; Seliverstov, 1992). Perkowski (Perkowski *et al.*, 1983) has described the use of a range of leak detection methods to identify a persistent contamination problem stemming from leaks in bioreactor cooling coils. After passing a hydrostatic test using a fluorescent dye and a ultrasonic test the vessel was still suffering contamination. The use of Freon 12 and a halogen leak detector did not show up any leaks either. To resolve the problem x-ray analysis of the welds was made which

showed “sugaring” due to the loss of the inert gas purge when the weld was formed. This example justifies the additional cost of x-ray validation of welds on new bioprocess equipment. But the use of tracer gases for the monitoring of equipment is considerably simpler than x-ray methods. Baram (Baram, 1991) provides specified limits for the release of helium from valves for bioprocesses and a discussion of the types of leaks. Carvell (Carvell, 1992) also stresses the usefulness of tracer gas leak tests when validating valve containment. It has been shown (Bello and Siegel, 1997) that valves can be the cause of a significant proportion of releases from process plants.

1.7 Research Objectives

This research project aims to establish a method for the generation of quantitative data on bioprocess releases. With quantitative data on bioprocess containment, processes equipment can be validated and designed rationally. The approach taken during the course of the project was to correlate a standard tracer gas leak test with the microbial release from model leaks.

The literature review carried out covers the research techniques used in this project. The three key tools used were the cyclone sampler, QPCR assay and the model leak system.

The cyclone sampler was used to collect bioaerosols from bioprocess environments. Throughout the course of the project, work was carried out to investigate the effects of various approaches to bioaerosol sampling in bioprocesses, with the aim of improving the collection efficiency of the cyclone sampler.

The QPCR protocol used was previously designed for the detection of another strain of *Escherichia coli*. This technique was taken and developed specifically for *Escherichia coli* RV308 pHKY531. Additionally modifications to the protocol were made with the aim of improving the techniques accuracy.

A model system with variable orifice sizes and leak path lengths was developed for the simulation of bioprocess releases. The objective of the model system was that it should be capable of simulating the release of gases, liquids and microbial suspensions. Once developed the aim of the research was to correlate the release of a microbial challenge through small orifices with the response of the tracer gas detection system. The correlation of the data can be used to define limits on the permissible leak rates, to aid the rational design of bioprocess equipment and containment validation regulations.

These three tools were also applied to a number of secondary research objectives. These were the investigation of

- the Turbosep foam breakage device as a tool for the removal of micro-organisms from fermenter exhaust gas.

- the impact of temporal and spatial effects on a cyclones bioaerosol collection efficiency.
- the effect of shear on microbial cells passing through small diameter capillaries.

The development and current use of the techniques applied within this research have been described in the previous sections of this chapter. There has been little published evidence (Section 1.6.3) that the correlation of a tracer gas leak tests with simulated microbial releases has been performed. Through the research presented here a method for the generation of quantitative data on bioprocess releases is described.

2. Materials And Methods

This chapter lists the materials and methods used during the course of this project. The equipment and consumables suppliers listed in this chapter can be found in Appendix 1.

2.1 Microbiological Methods

2.1.1 Micro-Organism Details

Two strains of *E. coli* were used during the course of this project (see Table 8). The first strain of *E. coli* (JM107 pQR701) was the target strain for which the QPCR technique had originally been developed (Noble, 1996). The second strain had been constructed and cloned by Eli Lilly and Company (Indianapolis, Indiana, USA). Where the host (RV308) is derived from the thiamine deficient *E. coli* K-12. The vector is a *rop*⁻ plasmid which expresses met-asp-bovine somatotropin (BST). It also contains genes for tetracycline resistance and the cI857 temperature sensitive repressor which controls BST expression.

Table 8 Details of Micro-organisms used.

Strain	Characteristics	Strain supplied by	Reference
E. coli JM107 pQR701	Km ^R , transketolase	Dr J. Ward [†]	French and Ward, 1995.
E. coli RV308 pHKY531	Tc ^R , met-asp-bovine somatotropin	Dr W. Cook [‡]	Cockshott, 1993

Km^R: kanamycin resistant; Tc^R: tetracycline resistant

[†] Department of Biochemistry and Molecular Biology, UCL, London. [‡], Eli Lilly & Co. Ltd., Speke Operations, Liverpool.

2.1.2 Culture And Maintenance Of Micro-Organisms

Triplicate master stock cultures of both strains were maintained in 20 % (w/v) glycerol solutions, and were stored at -70 °C. Duplicate working cultures were prepared every 4 weeks from a master stock and these were maintained on agar at 4 °C.

2.1.2.1 *Escherichia coli* JM107 pQR701

Solid cultures were maintained on 28 g L⁻¹ nutrient agar (Oxoid) which was supplemented with 20 µg mL⁻¹ filter-sterilised kanamycin (Sigma) after autoclaving.

The liquid media used for shake flasks was 25 g L⁻¹ nutrient broth (Oxoid) with the addition of 10 µg mL⁻¹ filter-sterilised kanamycin (Sigma) after autoclaving. Cultures were grown at 37 °C for 14 hours overnight in 50 mL volumes in a 250 mL shake flask on an orbital shaker (New Brunswick) at 200 rpm.

2.1.2.2 *Escherichia coli* RV308 pHKY531

Solid cultures were maintained on 28 g L⁻¹ Luria agar (Sigma) which was supplemented with 10 µg mL⁻¹ filter-sterilised tetracycline (Sigma) after autoclaving.

The liquid media used for shake flasks was 25 g L⁻¹ Luria broth (Sigma) with the addition of 2 µg mL⁻¹ filter-sterilised tetracycline (Sigma) after autoclaving. Cultures were grown at 28 °C for 14 hours overnight in 50 mL volumes in a 250 mL shake flask on an orbital shaker (New Brunswick) at 200 rpm.

2.1.3 Microscopic Cell Counts

The concentration of *E. coli* cells suspended in a sample was determined by microscopic counting using a Helber Bacteria Counting Chamber with Thoma rulings (Weber Scientific International Ltd.) viewed at × 400 magnification under phase contrast (Nikon Optipoint Microscope, Nikon). The total number of whole cells in the grid of 16 squares was counted and recorded. To convert the cells counted in the grid to the number of cells per mL a factor of 7.8×10^4 was used, which gave a lower limit of detection for this method equivalent to 1.25×10^6 cells mL⁻¹.

2.1.4 Optical Density Measurements

The optical density of broth cultures from shake flasks was routinely measured at 600 nm using a Beckman DU-64 spectrophotometer (Beckman Instruments). Cultures were diluted in sterile reverse osmosis water (SROW) to ensure that the reading was in the range 0.005-0.03 absorbance units (Figure 4). Sterile broth diluted in SROW was used as the blank.

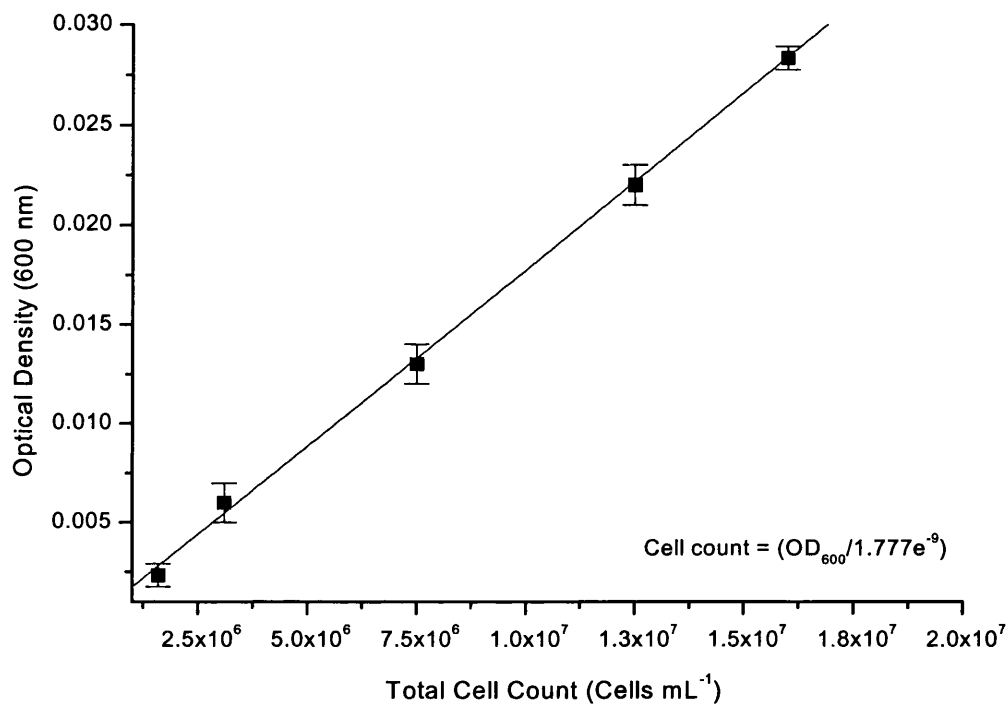


Figure 4 The relationship of total cell count to measured optical density. Each point is the mean of 5 samples with their standard deviation.

2.2 Quantitative PCR Assay

The method of QPCR used was based on the use of a competitive internal standard in the PCR (Janson, 1995). The ratio of standard to target product at the end of the PCR can then be used to deduce the initial amount of target DNA in the sample from the known concentration of internal standard added.

2.2.1 Precautions To Prevent PCR Contamination

The PCR technique for the amplification of DNA is very sensitive and can easily be contaminated by a lack of care during sample or reaction preparation and product analysis. To reduce the likelihood of sample contamination due to product carry over or standard contamination from target DNA certain procedures were rigorously adhered to (Sarkar and Sommer, 1990).

1. PCR preparation and product analysis were physically separated. Sample preparation was performed in a class II microbiological safety cabinet (Gelman) dedicated to PCR. No consumables were shared between the two areas. Gloves were worn at all times and changed between work areas.
2. All consumables were sterilised prior to use or were purchased sterile.
3. PCR reagents (primers, SROW, dNTP solutions, buffers and enzymes) were aliquoted from traceable batches and stored at -20°C.
4. All pipette tips (Anachem) used in setting up a PCR had a filter to prevent aerosols formed during the pipetting from being transferred between reagents, tubes or the pipette barrel.
5. The PCR mixture was made up for all tubes in a reaction and then dispensed. This reduced the use of consumables and reduced the number of steps performed.
6. Negative and positive controls were used in all QPCR assays.

2.2.2 PCR Sample Preparation

Samples collected in sterile thiosulphate ringers solution (TRS) can be used directly in the PCR assay. Alternatively samples were stored at -20 °C until required and then thawed at room temperature before analysis.

2.2.2.1 Cell Lysis

In cases where samples had a high cell concentration ($> 1 \times 10^8$ cells mL⁻¹) they were lysed by boiling in a water bath for 30 minutes. This was found to lyse the cells and leave the DNA intact for analysis by PCR (Noble, 1996).

2.2.2.2 Extracellular Plasmid Filtration

To distinguish between extracellular and intracellular plasmid, a 500 µL aliquot was transferred from a sample and was placed in a Costar spin-x tube (0.45 µm low DNA binding cellulose acetate filter, Costar). The spin-x tube was spun at 10,000 g for 2.5 minutes. The filtrate containing only the extracellular plasmid DNA was used directly in the PCR.

2.2.3 Stock Reagents

The stock reagents used in each PCR are shown in Table 9, and were prepared whilst following the guidelines described in section 2.2.1.

Table 9 Stock Reagents used in the PCR.

Reagent	Stock Concentration	Supplier	Diluent
<i>Taq</i> polymerase	5 Units µL ⁻¹	Gibco	
<i>Taq</i> polymerase buffer	200 mM Tris-HCl pH 8.4, 500 mM KCl	Gibco	
<i>Pfu</i> polymerase	2.5 Units µL ⁻¹	Stratagene	
<i>Pfu</i> polymerase buffer	10 × final	Stratagene	
dNTP mix (dATP, dTTP, dCTP, dGTP)	1.25 mM each	Pharmacia	SROW
Primers	20 µM	Pharmacia	SROW

2.2.4 PCR Primer Details

The primers used in the PCR are critical for the successful amplification of the target sequence. However there are no all-encompassing rules for the selection of suitable primer sequences and at best their selection is based on a knowledge of the sequence

under investigation and some informal guidelines (Steffan and Atlas, 1991). The primers used for each strain are shown in below.

Table 10 *E. coli* primers used in this project.

Strain			
E. coli	Plasmid	Primer	Sequence 5'-3'
JM107	pQR701	M13R1	GGA CCA AGC TAT GAC CAT G
		CMTA1	CGT CAA AGA GTG TAT TGA GG
		TK-LINKER	GTG TAT TGA GGG ATC GAT CAG GGC GTC TAT
RV308	pHKY531	P1	ATG GAT TTT CCG GCT ATG TCT
		P2	GTA CGT CTC CGT CTT ATG CAG
		BST-LINKER	TTC CAG CTC CCG CAT CAC GTA CGT CTC C

2.2.5 PCR Cycle Protocols

2.2.5.1 pQR701 Amplification Parameters

The PCR was carried out in 600 μ L reaction tubes containing 25 μ L reaction volume made up of 0.25 μ L *Taq* polymerase, 2.5 μ L of 10 \times *Taq* polymerase buffer, 0.75 μ L of 50 mM MgCl₂, 4 μ L of dNTP solution, 2.5 μ L of each primer (M13R1 and CMTA1), 1 μ L of internal standard (IS(T)), 1.5 μ L SROW, 10 μ L of sample and 25 μ L of light mineral oil (Sigma) to overlay the reaction mix.

The PCR was carried out in a Hybaid OmniGene (Hybaid) temperature cycler. The temperature program was 94 °C for 5 minutes followed by 30 cycles of: 94 °C for 30 seconds, 55 °C for 1 minute, 72 °C for 3 minutes; and finally 10 minutes at 72 °C. The whole PCR program took in the region of 3 hours to complete.

2.2.5.2 pHKY531 Amplification Parameters

The PCR was carried out in 600 μ L reaction tubes containing 25 μ L reaction volume made up of 0.5 μ L *Pfu* polymerase, 2.5 μ L of 10 \times *Pfu* polymerase buffer, 4 μ L of dNTP solution, 2.5 μ L of each primer (P1 and P2), 1 μ L of internal standard (IS(B)), 2 μ L SROW, 10 μ L of sample and 25 μ L of light mineral oil (Sigma) to overlay the reaction mix.

The PCR was carried out in a Hybaid OmniGene (Hybaid) temperature cycler. The temperature program was 94 °C for 5 minutes followed by 35 cycles of 94 °C for 30 seconds, 55 °C for 1 minute, 72 °C for 3 minutes; and finally 10 minutes at 72 °C.

2.2.6 Internal Standard

The internal standards used in this work were prepared according to the method described by Forster (1994). The internal standard used for *E. coli* JM107 pQR701 was constructed by Noble (1996), details of its construction are not shown. The construction of the internal standard for *E. coli* RV308 pHKY531 is presented here.

2.2.6.1 Internal Standard Generation

A schematic representation of the method of internal standard generation can be seen in Figure 5. The conditions for each of the PCR steps were those described in section 2.2.5.2. These conditions favour the binding of the primers P1 and P2, and were not optimised for the use of the BST-Linker primer. The first PCR produces a product of 527 bp with the primers P1 and P2 from a preparation of the plasmid pHKY531 purified by a wizard miniprep kit (Wizard DNA miniprep kit, Promega). The PCR product was visualised by using agarose gel electrophoresis under the conditions given in section 2.3.1. The size of the product was checked against a DNA marker ladder (PCR Marker, Sigma). The post PCR mix was then diluted in SROW by a factor of 10^4 . This was then used as the template for the next PCR step. The primers used in this PCR second step were P1 and BST-Linker. The BST-Linker has a 10 bp section of the primer P2 at its 5' end. The complimentary sequence then becomes incorporated into the PCR product during the primer extension in the PCR. The 416 bp product of this second PCR step was checked by agarose gel electrophoresis. The post PCR mix was diluted by a factor of 10^4 in SROW and used as the template for the final PCR step. The last PCR step uses the original primers P1 and P2 to produce a 426 bp product. This product was checked on an agarose gel and then purified prior to use as the internal standard IS(B).

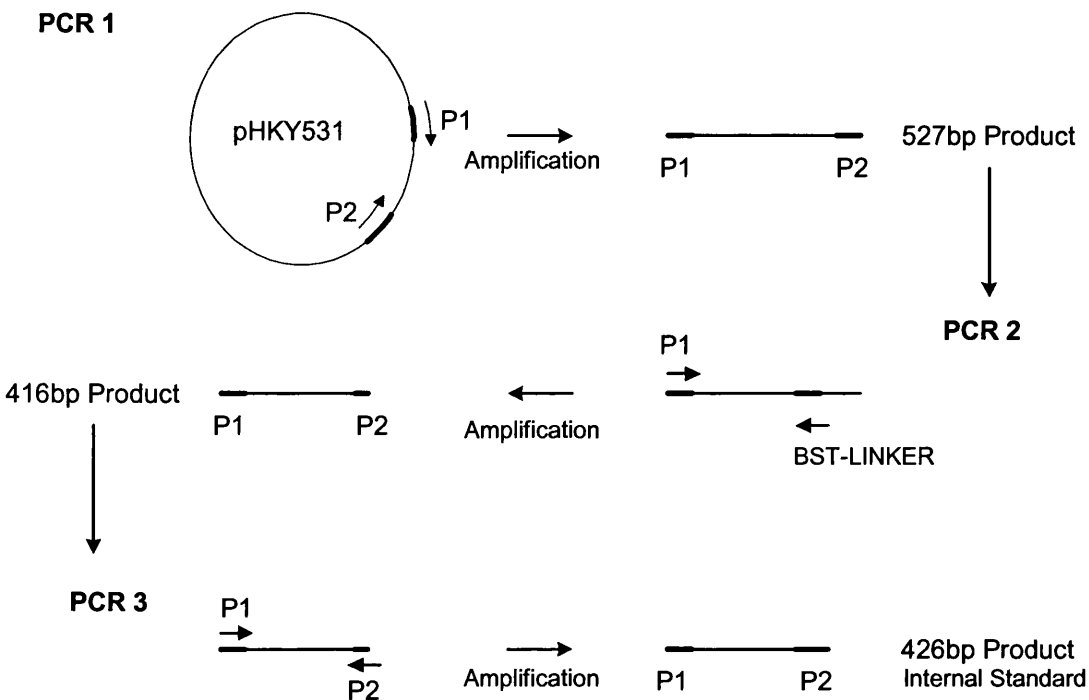


Figure 5 Schematic representation of the generation of the internal standard for *E. coli* RV308 pHKY531.

2.2.6.2 Internal Standard Isolation

The 426 bp product from the third and final PCR step was cut from the agarose gel under UV light. The DNA was isolated using Costar's Spin X method for the purification of DNA from agarose gels (Costar). A sample of the isolated DNA was checked by agarose gel electrophoresis prior purification.

2.2.6.3 Internal Standard Purification

The isolated DNA was further purified and concentrated by an ethanol precipitation step. Add 20 μL 3M sodium acetate pH 7.0 and 500 μL 100 % ethanol to the isolated DNA (225 μL). This was then mixed and stored at $-20\text{ }^{\circ}\text{C}$ overnight. This liquor was spun at 10000 g for 10 minutes and the supernatant removed with care so as not to disturb the pellet of DNA/salt. 100 μL 70 % ethanol was then added to the pellet, which was resuspended and the spun at 10000 g for 5 minutes. The supernatant was removed with care so as not to disturb the pellet which was left to air dry for 15 minutes. The dry pellet of DNA was finally resuspended in 75 μL SROW and then a sample was checked by agarose gel electrophoresis.

2.2.6.4 Internal Standard Quantification

The internal standard DNA was quantified by the measurement of the A_{260} and A_{280} using a Beckman DU-64 spectrophotometer (Beckman Instruments). The ratio of A_{260}/A_{280} is commonly used as a measure of protein contamination of DNA samples. This ratio had to exceed 1.7 for the internal standard DNA to be considered pure enough for quantification (Sambrook *et al*, 1989). The DNA concentration was calculated from the approximation that dsDNA at 50 mg mL^{-1} has an A_{260} of 1 (Sambrook *et al*, 1989).

2.2.6.5 Internal Standard Storage

The internal standard DNA was stored at $-70 \text{ }^{\circ}\text{C}$ as a concentrated stock prior to use.

2.3 Analysis Of the PCR Product

The analysis of all PCR products was performed by agarose gel electrophoresis.

2.3.1 Agarose Gel Electrophoresis

Agarose gel electrophoresis was performed as described by Sambrook *et al.* (1989). The running buffer used was 0.5× tris-borate ethylenediaminetetraacetic acid (disodium salt) (TBE) with 0.25 µg mL⁻¹ ethidium bromide. Aliquots of 7.5 µL of the PCR product were mixed with 2.5 µL gel loading solution (Sigma) and were run on horizontal 2 % agarose (Wide Range/Standard 3:1, Sigma) gels at 80 V for 3 hours at room temperature. The molecular weight marker used was PCR Marker (Sigma).

2.3.2 Gel Densitometry And Analysis

Gels were documented using a UV transilluminator and Gel Documentation System with ImageStore 5000 software (UVP Ltd.). The fluorescent detection system was sensitive to overloading from transmitted UV light, which was controlled by changing the aperture of the digital camera. The GelBase (UVP Ltd.) software measures the intensity of the DNA bands in each lane of the gel and produces the peak area or peak height for each band analysed. As the ratio of peak areas was used for the quantification of the DNA it was important that the peak areas were measured over a linear range of detection. To ensure this multiple images of the same gel were taken at various aperture settings for analysis using GelBase software. This would ensure that the band intensity in any lane would not be too low or saturating with reference to the other bands measured in the lane. The two criteria applied when recording the peak areas of bands are listed below.

1. A band peak area must be greater than 100 units.
2. A peak area ratio of any two bands from the same lane and for any set aperture must fall in the range of 0.05 to 20 units.

2.4 Aerosol Containment, Generation and Collection

Many of the experiments performed in this project required the production of a bioaerosol. This had to be carried out in a safe and reproducible manner. The following section details the methods used when dealing with artificially generated bioaerosols.

2.4.1 Contained Cabinet Operation

2.4.1.1 Bassaire Cabinet

The first cabinet used for aerosol spraying experiments was made by Bassaire Ltd., it has a total volume of 0.36 m^3 and can be seen in (Figure 6). The cabinet was fitted with variable air throughput HEPA filtered air inlet and outlets. After spraying a bioaerosol, the cabinet was flushed with a 1 % Tego (Th. Goldschmidt Ltd.) aerosol via the atomiser, which effectively wetted all the interior surfaces. This was left for 5 minutes then a side wall could be removed and the interior wiped dry. The wall was then reattached and the air outlet fan turned on for 30 minutes to ensure the cabinet surfaces were dry and that the air was clean and particle free within the cabinet. After this cleaning procedure the cabinet would be ready to receive another aerosol sample.

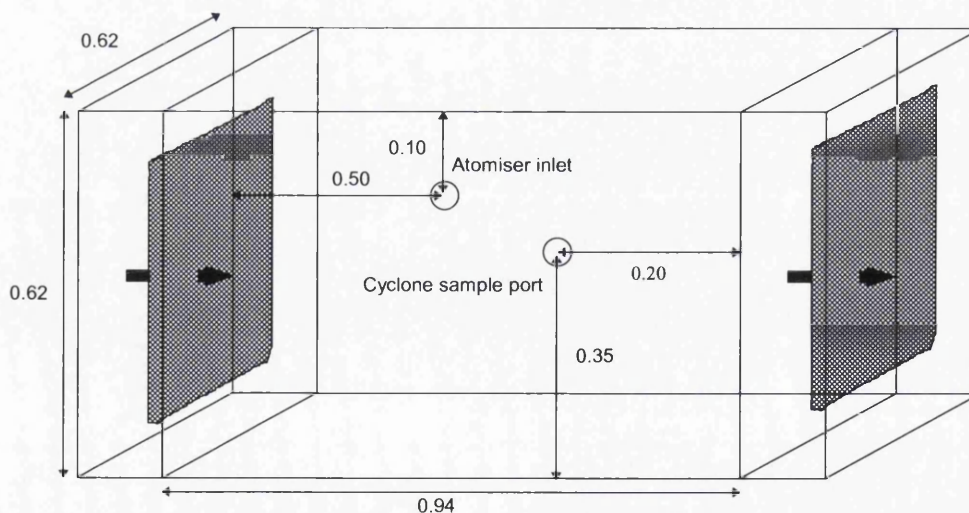


Figure 6 Bassaire cabinet showing dimensions (m), location of ports (both on same face of cabinet) and direction of airflow through HEPA filters (hashed areas).

2.4.1.2 UCL Contained Cabinet

The Bassaire cabinet was not ideally suited for the spraying and capture of aerosols, because the inlet and sample port are on the same face. A second cabinet was constructed in the Department that met the needs of aerosol release and capture via a cyclone. A diagram of this cabinet can be seen in Figure 7. The cabinet was cleaned using Aerocide 1 (Guardine Disposables Ltd.) and disposable disinfectant wipes (Agma plc) after the spraying of a bioaerosol. After the cleaning products were used the HEPA unit was turned on for 30 minutes to ensure the cabinet surfaces were dry and that the air was clean and particle free.

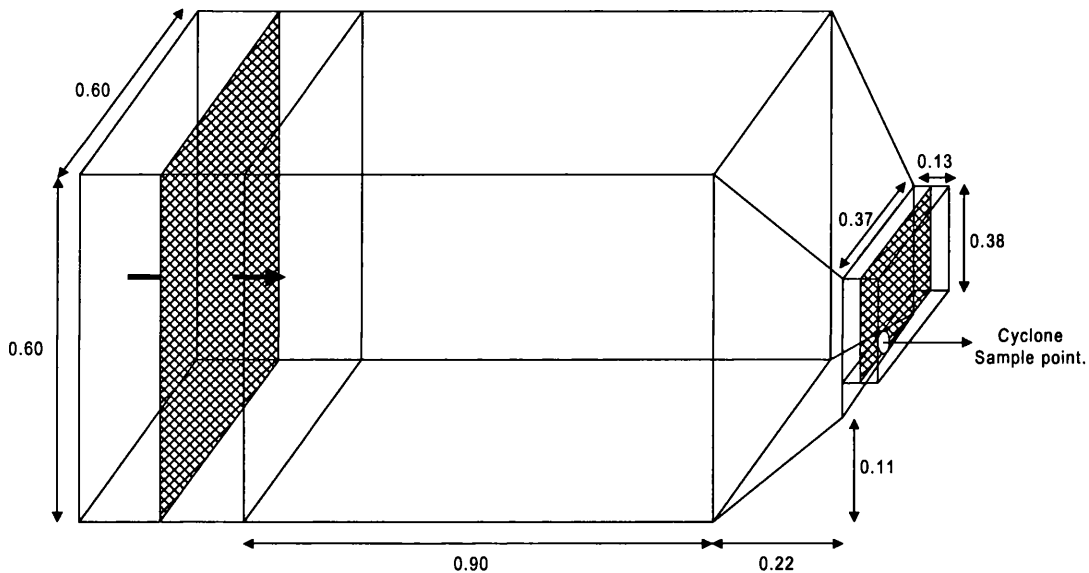


Figure 7 UCL contained cabinet showing dimensions (m), location of ports and direction of airflow through HEPA filters (hashed areas).

2.4.2 Atomiser Operation

Aerosols were generated in each experiment using an atomiser supplied by Warren Spring Laboratories. The particle size distribution generated by this atomiser for *E. coli* cell suspensions was previously characterised by Ferris (Ferris, 1995). It is apparently uniform from 1 μm to 15 μm diameter.

2.4.2.1 Atomiser Preparation

The atomiser (Figure 8) was connected to a compressed air supply set at 0.68 bar and the sample to be aerosolised was delivered at 1 mL min^{-1} via a peristaltic pump.

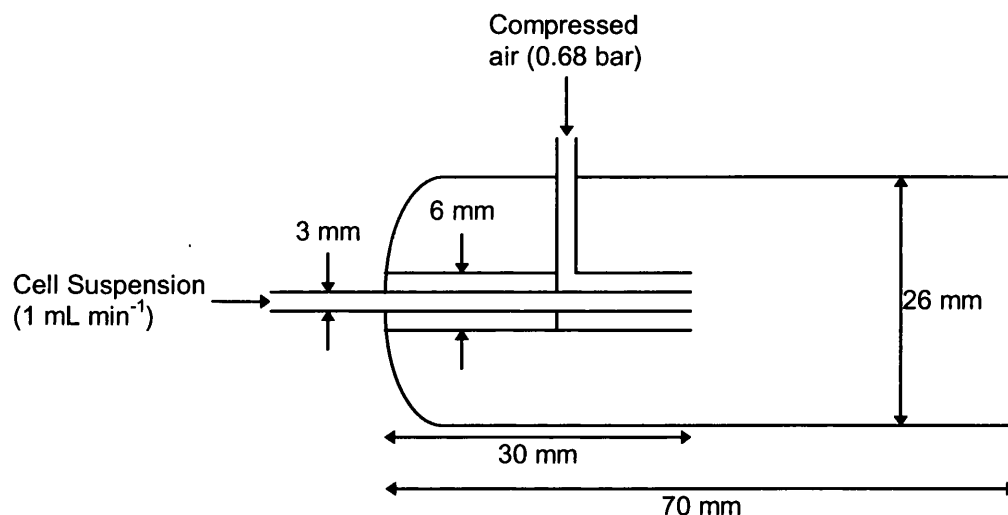


Figure 8 Schematic cross section of the Warren Spring atomiser.

Cell suspensions were serially diluted into either sterile TRS or sterile nutrient broth immediately before spraying. Either 15 mL or 18 mL of the cell suspension was aerosolised in the atomiser. A 5ml wash of sterile TRS was aerosolised immediately after the cell suspension, through the same spray line.

2.4.2.2 Atomiser Cleaning

After operation the tubing and atomiser head were soaked in 1 % Tego for 30 minutes then thoroughly rinsed in tap water for 2-3 minutes and then let to drip dry for 2-3 minutes.

2.4.3 Aerojet General Cyclone Operation

The cyclone air sampler used in these studies was an Aerojet General Cyclone (Soham Scientific) (Decker *et al.*, 1969, Upton *et al.*, 1994) which is based on an Errington-Powell Cyclone (Errington and Powell, 1969). The exact dimensions of the cyclone and attachment are given in Appendix 2.

2.4.3.1 Cyclone Preparation

The Aerojet cyclone was set up as shown in Figure 9. In the aerosol sampling experiments, air was drawn into the cyclone by an air pump (Air Control Installations) via the air inlet of the cyclone. When sampling from the Bassaire cabinet the air flow through the cyclone was 360 L min^{-1} and when sampling from the ACBE cabinet it was 375 L min^{-1} . The recirculating liquid was 80 mL sterile TRS, recirculated using a peristaltic pump (Watson-Marlow) at 20 mL min^{-1} . Sampling was carried out for 10-30 minutes and at the end of run the volume of TRS remaining was measured by weighing. Through normal operation it would be expected that 1 mL min^{-1} of TRS would be lost due to evaporation or precession (section 1.4.3). After collection the liquid sample can then be used in various quantification methods (QPCR and cell counts).

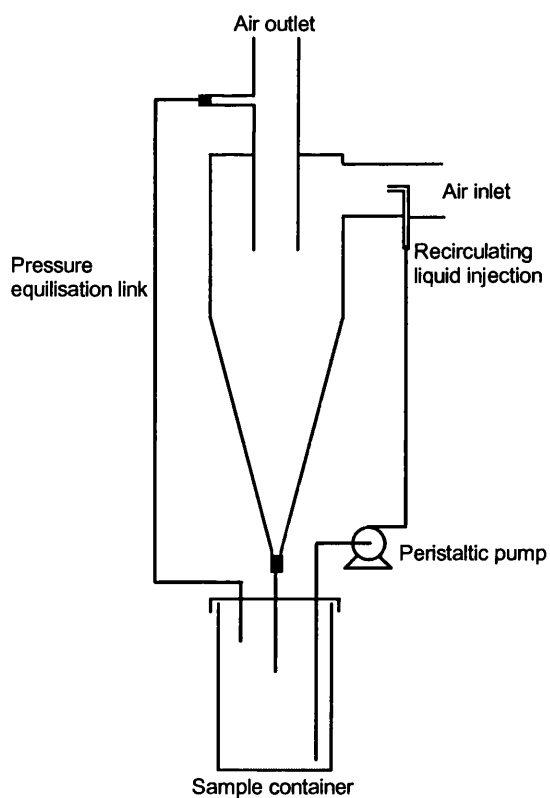


Figure 9 Schematic diagram of the Aerojet General Cyclone set-up for sampling.

2.4.3.2 Cyclone Cleaning

The cyclone was cleaned by immersion into a 5 L container of 1 % Tego solution (Th. Goldschmidt Ltd.) and allowed to stand for 30 minutes. It was inverted after 15 minutes to ensure all surfaces had been adequately wetted. All dedicated tubing was also flooded with 1 % Tego and soaked for 30 minutes. After the Tego soak the cyclone and tubing was thoroughly rinsed with tap water for 2-3 minutes and then allowed to air dry for a further 2-3 minutes.

The focus on cleaning and physically separated work areas (section 2.2.1) is an important consideration when attempting to minimise the contamination of samples, particularly negative or control measurements.

2.5 Leakmeter 200 Operation

The Leakmeter 200 (Ai Cambridge Ltd.), is a high sensitivity leak detector used to locate and quantify leaks with electron capturing trace gases. The detection principle is based on a single electron capture detector, and a low power radioactive source (^{63}Ni , 10 mCi). The ^{63}Ni sealed source ionises some of the carrier gas to produce a low current to flow between a biased pair of electrodes. When SF_6 molecules pass by the detector, they capture a proportion of the electrons and reduce the current measured between the electrodes. The drop in current is proportional to the SF_6 concentration.

The detector used in this project was specific for SF_6 and had a range of detection from $1 \times 10^{-7} \text{ mL SF}_6 \text{ s}^{-1}$ to $3.2 \times 10^{-4} \text{ mL SF}_6 \text{ s}^{-1}$. The leakmeter 200 was operated in strict accordance with the operating instructions, a summary of which follow.

1. After turning on the detector perform a calibration.
2. Present the hand held sniffer to the equipment to be checked for leaks. When searching a surface for a leak the sniffer should be held 1 cm above the surface and not moved across it quicker than 1 cm s^{-1} . When the detector was used to quantify the release of SF_6 from a capillary the nozzle of the sniffer unit was fixed 1 cm away from the end.
3. A 15 minute gap was left between each experimental run to minimise the background SF_6 in the following experiment.
4. To compensate for any increasing levels of SF_6 in the sampling environment during an experiment the detector was set to a slow background time averaging.
5. After all experimental work had been performed or after 4 hours of continuous use the detectors sinter was checked for a build-up of dirt. This was shown by a high ($> 10 \text{ MHz}$) signal frequency on the main unit. To clean the sinter the automated cleaning protocol was used. Particular attention was given to the sinter cleanliness as this could affect the sensitivity of the instrument.
6. After sinter cleaning the unit was shut down and stored until further use.

2.5.1 Leakmeter 200 Calibration

The calibration of the leakmeter 200 was carried out using a standard leak provided by Ai Cambridge Ltd.. The standard leak released 1×10^{-6} mL SF₆ s⁻¹ through a packed column of aluminium. The calibration program was run and when prompted the leakmeter sniffer was presented to the standard. The program would then perform the calibration against the standard leak. Once calibrated the leakmeter was ready for use.

2.6 Model Leak System

A system was developed that enabled leaks to be simulated through the use of capillary tubing of various lengths, internal diameters and materials of construction. Capillaries have been used for leak simulation by a number of researchers, notably Burrows (Burrows, 1961) and Tison (Tison, 1993).

2.6.1 Model Leak System Design

The system developed was conceptually very simple (Figure 10). A cylinder of 1 % SF₆ in nitrogen or a liquid sample was connected at point 1. The pressure in the system was controlled by the needle valve (2) and shown on the pressure indicator (3). The capillary leak was connected via the Luer lock fitting (4) and the release took place at the end of the capillary (5).

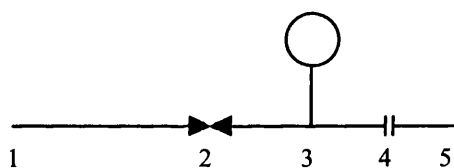


Figure 10 A schematic of the model leak system.

2.6.1.1 Construction Of Capillary Leaks

Two types of capillaries were used in the leak system, firstly stainless steel needles and then borosilicate glass micropipettes. Stainless steel needles were obtained in a range of internal diameters (ID) with metal (BDH) or Kel-F® (Anachem) Luer lock connections and a uniform cross-section. The manufacture of glass micropipettes is highly precise and very small tolerances can be achieved on tip internal diameter and length (Brown and Fleming, 1986). Because of this high reproducibility of manufacture and simplicity of design they were chosen as a model leak. The micropipettes used in this project were all manufactured by Research Instruments Ltd. and were made from borosilicate glass with an ID of 0.7 mm and an external diameter of 0.95mm. The tips were flame polished to increase the precision and strength of the final orifice ID. These micropipettes were connected to polytetrafluoroethylene (PTFE) Luer lock to tubing

connectors via a 1 cm piece of PTFE tubing (Figure 11). A table of the range of leak simulation capillaries is shown in (Table 11).

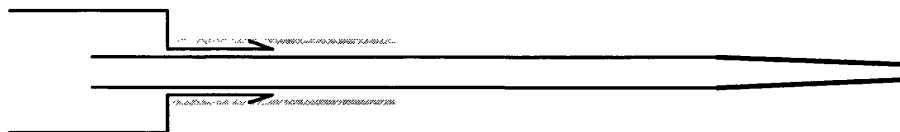


Figure 11 A schematic of the attachment of a micropipette to a luer lock hub. The luer hub is represented at the very left with the PTFE tubing shown in grey. The micropipette passes through the hub and has a flame polished end shown in bold.

Table 11 Capillary size and material details for leak simulations

Internal Diameter (μm)	\pm ID Tolerance (μm)	Luer Hub	Needle
1600	25	SS	SS
1190	12.5	SS	SS
1065	12.5	SS	SS
840	12.5	SS	SS
685	12.5	SS	SS
585	12.5	SS	SS
510	12.5	SS	SS
405	12.5	SS	SS
330	12.5	SS	SS
305	12.5	K	SS
255	12.5	K	SS
205	12.5	K	SS
180	12.5	K	SS
150	12.5	K	SS
125	12.5	K	SS
530	0.1	P	G
250	0.1	P	G
100	0.1	P	G
75	0.1	P	G
50	0.1	P	G
25	0.1	P	G
10	0.1	P	G
5	0.1	P	G
1	0.1	P	G

SS: stainless steel; K: Kel-F®; P: PTFE, G: borosilicate glass

2.6.2 Model Leak System Operation

The model leak system was used with gas and liquid samples, both within and outside of the UCL contained cabinet. Before the system was used for quantitative release experiments the system was validated to prove that it was itself leak tight. Once validated the system was set up with the specific conditions for each experiment.

2.6.2.1 Validation Of The Model Leak System

When monitoring the release of a gas or liquid from the model leak it was essential to prove that any release detected was produced from the terminal orifice of the capillary simulating the leak. The experiments conducted on releases were performed at up to 2 bar above atmospheric pressure. To prove the system did not leak any gas or liquid from any connections or joints a series of needles were prepared that had their terminal orifice sealed with an epoxy resin. These were then attached to the luer lock connection and the system was pressurised to 4 bar with SF₆. The model leak system was then scanned using the leakmeter 200 sniffer for any release of SF₆. At 4 bar there was no detectable release of SF₆ and the system was assumed to be leak-free. To prove that the system would leak SF₆, a series of the standard needles were connected and when SF₆ was passed through the system at 4 bar it was detected at the terminal orifice of the capillary by the leakmeter 200 sniffer.

2.6.2.2 SF₆ Releases

The leak system was positioned in a large well ventilated room and a cylinder of 1 % SF₆ in nitrogen (BOC) was connected. The system was left to equilibrate for 1 minute before commencing monitoring. The leakmeter 200 was positioned 1 cm from the terminal orifice of the capillary in use. Between each release of SF₆ a 15 minute period was left before performing a second sample to allow any released SF₆ to dissipate.

2.6.2.3 Liquid Releases

The leak system was connected to a 32 rpm peristaltic pump (Watson-Marlow) and the test liquid was pumped through the system. If the test liquid contained *E. coli* RV308 pHKY531 then all release experiments were performed in the UCL contained cabinet. When the test liquid was water the experiments were performed over a large sink. The

system was left to equilibrate for 1 minute before sampling was started. Liquid samples were collected over various time periods, by placing a container in the path of the released liquid, through the use of the aerojet general cyclone or the use of a TSI Incorporated model 7450 laser particle counter (LPC) (Figure 12). The samples collected in a container were weighed to provide a mass flow rate through the leak. Samples collected in the aerojet general cyclone were analysed using the QPCR assay. The LPC could be used to directly quantify the particles passing over the sampler.

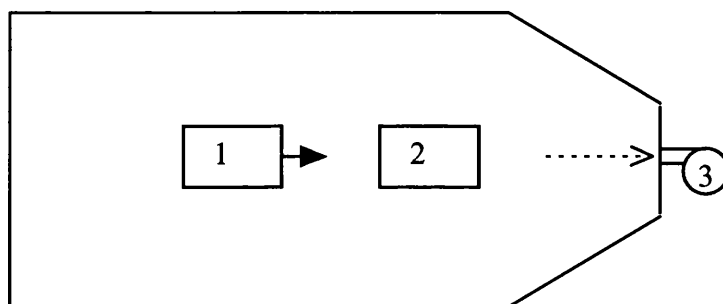


Figure 12 The layout of equipment for the sampling of liquid releases using the aerojet general cyclone in the UCL contained cabinet. Where 1 represents the model leak, 2 the LPC and 3 the cyclone connected to the cabinet.

The model leak system was cleaned by pumping a 1 % Tego solution through it for 30 minutes and then using compressed air at 2 bar to dry the system over a further 30 minutes. The UCL contained cabinet was flushed with air for 15 minutes in between each sample to reduce the background particle count within the chamber.

2.6.2.4 Simulating Aerosol Impacts

In order to simulate the effect of an aerosol impacting upon the surface of a piece of equipment the model leak system was set-up as shown in Figure 13. The LPC was located 15 cm from the release point and 10 cm below it. LPC samples were taken before the cyclone was running and during its sampling. The targets were flat (25 cm²), concave and convex pieces of Perspex, where the curved surfaces were half a cylinder of 6 cm diameter and 10 cm height. The targets were 30 cm from the release point, roughly the centre of the contained cabinet.

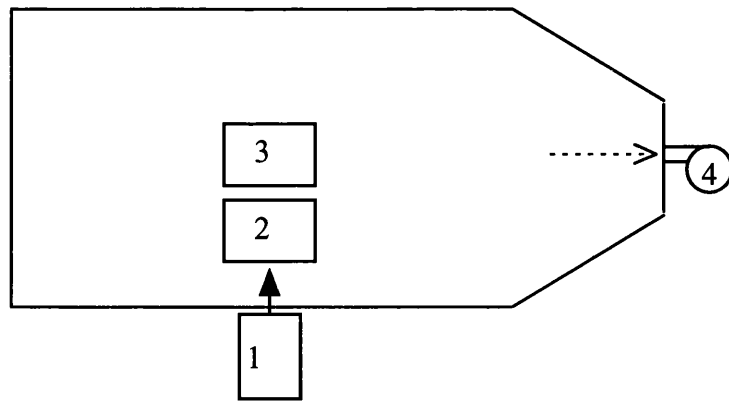


Figure 13 The layout of equipment for the sampling of aerosol impacts using the aerojet general cyclone and the LPC in the UCL contained cabinet. Where 1 represents the model leak, 2 the LPC and 3, target location and 4 the cyclone connected to the cabinet.

2.7 Particle Counting Devices

Two separate devices were used to count and size liquid and airborne particles. The TSI Incorporated LPC 7450 was used for airborne samples and the Malvern Instruments 3600 E type was used for sizing particles in liquid.

2.7.1 TSI Incorporated LPC 7450

The system comprised a vacuum pump, printer and the LPC unit. The vacuum pump draws 5 L min^{-1} into the LPC where it provides a real time count of particles within two size bands, greater than $0.5 \mu\text{m}$ diameter and greater than $5 \mu\text{m}$ diameter. The instrument was set-up to count particles per litre and logged the results over a user defined time interval to the printer. The LPC could be set-up to provide environmental monitoring with definable alarm limits, though this function was not used and the device was used at its most simple level.

2.7.2 Malvern Instruments 3600 E Type

The system comprised the laser, sampling chamber, printer and the controlling computer. The Malvern can be run in an advanced and an easy mode depending on the functions the user requires. For the purposes of the analysis required the Easy particle sizer M3.0 program was run from the control computer. The range of particles sizes that can be quantified by the device is set by the choice of filter, laser focal and beam length. The instrument was set-up with a focal length of 63 mm and a beam length of 14.3 mm, with a filter for particles over the range of $1.2 \mu\text{m}$ to $118 \mu\text{m}$ diameter. The instrument was blanked with SROW that had been filtered through a $0.22 \mu\text{m}$ Whatman cellulose acetate filter. Once blanked the sample was added, via a dropper to the sample chamber until the automatic sample concentration indicator showed that an optimum amount of sample had been delivered into the chamber. The instrument then reads the sample and counts the particles within thirty two size bands spanning the range set by the filter. The results are then sent to the printer together with simple statistics on the diameter of the particle population, such as the Sauter mean diameter (SMD) and the volume mean diameter (VMD).

2.8 Shear Devices

Investigations into the effect of shear on cells passing through small capillaries were carried out using two different devices. These were an Instron capillary rheometer and a rotating disc shear cell.

2.8.1 Instron Shear Device

The design and construction of the capillary rheometer has been described by Thomas and Dunnill (Thomas and Dunnill, 1979). The device consisted of a exchangeable stainless steel capillary tubes (0.2, 0.15 or 0.1 mm ID) 50 mm long and a motor driven stainless steel plunger. 20 mL volumes of *E. coli* RV308 pHKY531 whole cell suspensions were forced through the capillaries at various flow rates (Table 12) and collected in sterile TRS to avoid interfacial effects.

Table 12 Shear rates developed by the Instron shear device for various capillary attachments.

Flow Rate (m ³ s ⁻¹)	Capillary Internal Diameter					
	0.1 mm		0.15 mm		0.2 mm	
	Shear Rate (s ⁻¹)	Reynolds Number	Shear Rate (s ⁻¹)	Reynolds Number	Shear Rate (s ⁻¹)	Reynolds Number
5.96 × 10 ⁻⁸	3.24 × 10 ⁵	966	9.59 × 10 ⁴	644	4.05 × 10 ⁴	483
9.53 × 10 ⁻⁸	5.18 × 10 ⁵	1545	1.53 × 10 ⁵	1030	6.47 × 10 ⁴	772
1.19 × 10 ⁻⁷	6.46 × 10 ⁵	1929	1.92 × 10 ⁵	1286	8.08 × 10 ⁴	964
2.38 × 10 ⁻⁷	1.29 × 10 ⁶	3857	3.83 × 10 ⁵	2572	1.62 × 10 ⁵	1929
4.77 × 10 ⁻⁷	2.59 × 10 ⁶	7731	7.68 × 10 ⁵	5154	3.24 × 10 ⁵	3865
5.96 × 10 ⁻⁷	3.24 × 10 ⁶	9660	9.59 × 10 ⁵	6440	4.05 × 10 ⁵	4830

The samples were collected and particles size analysis and cell breakage quantification performed. The particle size analysis was carried out using the Malvern particle sizer as described in section 2.7.2. To quantify the degree of cell breakage resulting from the shear forces developed in the capillary rheometer, controls and sheared samples were analysed as described in section 2.8.3.

2.8.2 Rotating Disc Shear Cell

The rotating disc shear cell has been used to investigate the effect of shear on plasmid DNA in solution (Levy *et al.*, 1998) and was suitable for the investigation of shear on whole cells. The system was composed of a flat 30 mm diameter 10 mm thick smooth aluminium alloy disc (Durell, Smith Ltd.). The disc was centrally mounted in a cylindrical Perspex chamber which had a removable air-tight flat top. The chamber had an ID of 40 mm ID and was 15 mm high. The shaft attached to the disc was extended through the top via an air-tight PTFE bearing and was connected to a small high speed motor (Grouper Speed 500 BB Race), which was driven by a series of batteries. When operating the batteries could deliver a constant voltage of 2 to 12 volts, which corresponded to disc speeds of 5000 to 30000 rpm in air. When operated with a whole cell solution the maximum speed achievable was 27700 rpm. A standard experimental procedure involved the filling of the test chamber with the cell suspension and stirring the solution at a fixed speed for a defined time in the range of 5 to 25 seconds. The chamber was washed and dried prior to the start of each run. To quantify the degree of cell breakage resulting from the shear forces developed in the rotating disc shear cell, controls and sheared samples were analysed as described in section 2.8.3.

2.8.3 Analysis Of Shear Damaged Cells.

The control cell suspension was filtered (section 2.2.2.2), then the recovered cells were boiled (section 2.2.2.1) to produce a solution of lysed cells with intact DNA for analysis on an agarose gel. The samples of sheared cells were treated in the same manner with a filtration step (section 2.2.2.2) to separate extracellular DNA and whole cells, followed by a boiling stage to lyse the recovered cells so that the total amount of damage may be calculated.

The controls and each samples component parts was run on a 0.75 % agarose gel containing ethidium bromide and electrophoresed at 80 volts for 3 hours, as described in section 2.3.1. The resulting gels were analysed as described in section 2.3.2. The amount of DNA in the control sample was considered to represent 100 % of the DNA present in the original whole cells and the amount of DNA after shearing was expressed as a percentage of this value.

3. Development Of QPCR Assay For *E. coli* RV308 pHKY531

This chapter will detail the development of a QPCR protocol to be used for the detection of *E. coli* RV308 pHKY531. The use of a competitive internal DNA standard (Gilliland *et al.*, 1990a) was selected as the method of quantitation within in the PCR. The method that Noble (1996) followed for the construction of internal standards (Forster, 1994) to enable quantification of DNA in aerosolised samples was used to develop the QPCR protocol. The limit of detection and selectivity of the developed QPCR technique are examined and discussed in light of its application to bioaerosol monitoring. The use of QPCR has been applied to the analysis of bioaerosols by a number of researchers (Mukoda *et al.*, 1994; Alvarez *et al.*, 1995; Noble *et al.*, 1997; Nugent *et al.*, 1997).

3.1 PCR Primer Selection

The selection of primers is important in any PCR protocol as they influence the specificity, efficiency and conditions of the reaction (Steffan and Atlas, 1991). PCR primers generally range in length from 15-30 bases and are designed to flank the region of interest. When selecting primers for a PCR protocol care should be taken to avoid G - C rich sequences which would generate internal secondary structures in the primer. The 3'-ends of the primers should not be complementary to avoid the production of primer-dimers in the PCR. Ideally, both primers should anneal at the same temperature, where they do not the lower melting temperature for the primers should be used.

The pHKY531 plasmid is 6366 bp in size and from a complete sequence primers for the PCR were selected (Table 10). The primer sequences P1 and P2 were both located within the BST insert of the plasmid. The primer BST-Linker was used for a single PCR in the production of the competitive internal standard. These primers were used to generate the internal standard for the QPCR as detailed in section 2.2.6.1 and primers P1 and P2 were used in conjunction with the internal standard in the final QPCR assay.

3.2 QPCR Calibration Curve Generation

Once the internal standard (IS(B)) had been generated and purified, the competitive co-amplification of the plasmid and IS(B) were checked. Details of the purified IS(B) and plasmid used in these studies is given in Table 13. The number of DNA molecules present in 10 μL was used to calculate the appropriate concentrations of IS(B) for use with the plasmid in the construction of the calibration curves.

Table 13 Details of IS(B) and pHKY531 used in co-amplification trials.

Preparation	Concentration ($\mu\text{g mL}^{-1}$)	Length (bp)	MW (Daltons)	Molarity	Molecules μL^{-1}
IS(B)	167	426	0.28×10^6	5.96×10^{-7}	3.71×10^{12}
pHKY531	96	6366	4.13×10^6	2.32×10^{-8}	1.45×10^{11}

By running varying IS(B):pHKY531 ratios the optimum concentration of IS(B) required in the QPCR protocol could be determined. A high concentration of either IS(B) or pHKY531 could out compete the lower concentration component in the PCR. The ideal QPCR will produce products with equal intensities when visualised on an agarose gel. A 1:1 ratio of IS(B) to pHKY531 will not produce this result due to differences in the amplification efficiency of each template and the binding efficiency of ethidium bromide in the gel. The pHKY531 product is approximately 20 % larger than the product generated by the internal standard (527 bp and 426 bp respectively). As ethidium bromide binding to DNA is proportional to size, the plasmid would produce a brighter intensity band than the IS(B), even if the same concentration. Because of these two effects it was important to establish the ratio of IS(B) to pHKY531 in the QPCR.

The experiments on co-amplification ratios showed that a heteroduplex product was formed in the PCR. This could be visualised as a faint band between the pHKY531 and the IS(B) on an agarose gel (lane 4, Figure 14). As the heteroduplex could be easily distinguished from the other products during densitometry analysis the QPCR conditions were not optimised further to remove its presence. A ratio of 1.4:1 IS(B) to pHKY531 was found to give an unbiased co-amplification and visualisation of plasmid and standard products. With this ratio known a series of calibration curves for the plasmid could be produced. Noble (Noble *et al.*, 1997) had shown that any one concentration of an internal standard will allow accurate quantitation within a range of

± 1.5 logs. The concentration of three internal standards was calculated and their anticipated range of quantification determined (Table 14).

Table 14 IS(B) concentrations used to produce calibration curves.

Internal Standard	Concentration (molecules μL^{-1})	Quantification Range (copies pHKY531)
IS(B)1	9×10^3	$2 \times 10^2 - 2 \times 10^5$
IS(B)2	9×10^5	$2 \times 10^4 - 2 \times 10^7$
IS(B)3	9×10^7	$2 \times 10^6 - 2 \times 10^9$

To validate that the competitive internal standard and the QPCR protocol can be applied over the range predicted a series of calibration curves for each IS(B) concentration were prepared with a series of known concentrations of pHKY531 (Figure 14).



Figure 14 Gel showing the co-amplification of IS(B)3 and pHKY531 to generate a calibration curve. Where the pHKY531 concentration (molecules $10 \mu\text{L}^{-1}$) was:

Lane	1	2	3	4	5	6	7	8	9
pHKY531	2×10^6	6.4×10^6	2×10^7	6.4×10^7	2×10^8	6.4×10^8	2×10^9	-	Blank

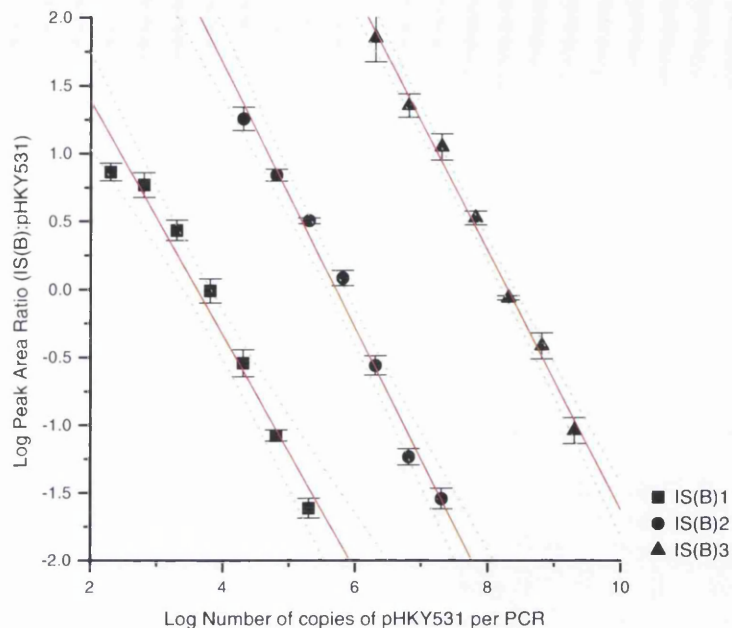


Figure 15 Calibration curves for pHKY531, showing upper and lower 95% confidence limits (dotted lines) of linear regression (solid lines).

When constructing the calibration curve for an internal standard concentration each point plotted was the mean from 5 replicates with the standard deviation of that mean shown. And each replicate had a common sample but a separate PCR. Figure 15 shows that for each internal standard concentration the 3 orders of magnitude range stated by Noble (Noble, 1996) can be applied to the QPCR conditions specified for this strain of *E. coli*. From the linear regression of each line the relationship between peak area ratio and pHKY531 concentration can be determined (Table 15). With this relationship the determination of unknown pHKY531 concentration can be performed.

Table 15 Parameters of IS(B) linear regression analysis.

IS(B)	C	m	R	n
1	3.12	-0.860	-0.985	35
2	5.55	-0.972	-0.993	35
3	7.88	-0.951	-0.997	35

where; $y = c + mx$; R: regression coefficient; n: number of points

3.2.1 Quantification of *E. coli* RV308 pHKY531 Whole Cell Samples

To develop the QPCR protocol further it was important to show a linear response when amplifying plasmid from whole cells compared with the extracted and purified plasmid used previously. To maintain a simple protocol the cells were not lysed to extract the plasmid. When sampling an aerosol it was felt that a high proportion of the cells collected would be stressed due the rapid change in their environment (Cox, 1989). In such a state the rapid increase in temperature produced by the PCR thermal cyclers should give adequate cell lysis (Mahon and Lax, 1993). The data presented in Figure 16 shows good correlation for whole cells used directly in the PCR. From this data it was possible to determine that the copy number of the plasmid pHKY531 in *E. coli* RV308 pHKY531 was 30.8 ± 1.0 plasmid copies per cell. As this was similar to the value (30 copies per cell) reported by Cook (Cook, 1996) the QPCR protocol was proved to work accurately with whole cells. The QPCR data manipulation required to calculate the pHKY531 concentration in an unknown sample is described in Appendix 3.

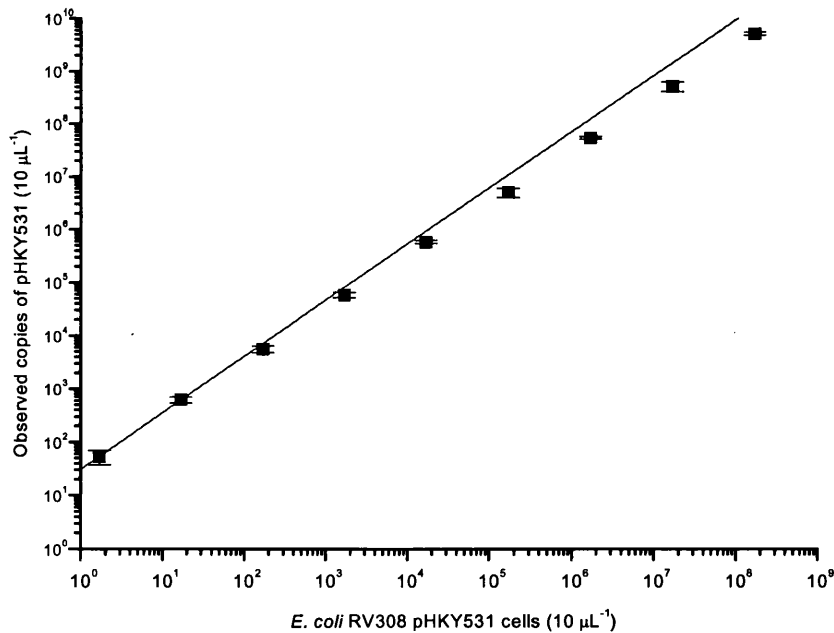


Figure 16 The response of the QPCR protocol to *E. coli* RV308 pHKY531 whole cells. Each point shows the mean of duplicates with their standard deviation.

3.3 Accuracy of *E. coli* RV308 pHKY531 QPCR Assay

The accuracy of the QPCR assay was determined for both for purified plasmid and whole cell samples. A dilution of the purified pHKY531 plasmid and whole cells of *E. coli* RV308 pHKY531 was prepared for each concentration of IS(B). The dilution used was the mid point for each IS(B) calibration curve. At this concentration 5 replicate dilutions were prepared, the plasmid dilution was checked using the DNA quantification method described in section 2.2.6.4 and the cells concentration was checked as in section 2.1.4. Each sample was amplified and analysed under the same conditions. The densitometry data was collated and the values for the copies of plasmid and whole cells calculated by the QPCR were compared with the initial known values (Table 16).

Table 16 Accuracy and error of the QPCR assay.

Sample	IS(B)	[Known] μL^{-1} ①	[Calc'd] μL^{-1} ②	SD ③	Accuracy (%)	Error (%)
pHKY531	1	6.4×10^3	7.7×10^3	4.7×10^2	+ 20.3	± 6.1
	2	6.4×10^5	4.4×10^5	4.2×10^4	- 31.3	± 9.5
	3	6.4×10^7	5.5×10^7	1.7×10^6	- 14.1	± 3.1
Whole Cells	1	200	246	35	+ 23.0	± 14.2
	2	20000	14560	1564	- 27.2	± 10.7
	3	2000000	1435000	172300	- 28.3	± 12.0

where SD: standard deviation; Accuracy = $((\text{②}/\text{①}) \times 100) - 100$; Error = $\pm ((\text{③}/\text{②}) \times 100)$

From a statistical analysis (One-way ANOVA) of the data it was determined that there was no significant difference (0.05 level) in the accuracy of the QPCR with purified plasmid or with whole cells. However the same analysis of the error within each system showed that at 0.05 significance the purified plasmid assays showed less error than the whole cell samples.

The accuracy of the assay appears to be dependant on the IS(B) concentration, with the lowest concentration overstating the actual values and the higher concentrations of IS(B) understating. This accuracy can be improved by a number of approaches:

1. Use two IS(B) concentrations for each sample. As can be seen from the calibration curves (Figure 15) there is a degree of overlap between all of the curves. So it should be possible to get a value for two IS(B) concentrations and combine them to get a more accurate estimate of the number of plasmid copies in a QPCR assay.

2. Use smaller steps of IS(B) concentration over the same range of plasmid concentration. By increasing the number of internal standards and applying them over a shorter plasmid concentration range, accuracy at the high and low ends of each would be increased.

The problem of both these approaches is that they greatly increase the number of assays required to produce quantitative data. This increases the cost of consumables and time required to perform the PCR. During the course of this project where a sample gave a high response with one internal standard it was re-run with the next most concentrated standard.

The increase in error in the whole cell system could be due to uneven cell lysis in the PCR or through the interference of cellular debris and media components. This effect possibly explains that when performing wide range QPCR at high cell concentrations on whole cell samples there is a deviation from the linear trend (Figure 16) of detected plasmid concentration to cell number. To overcome this effect and to reduce sample error a cell lysis step was included prior to the QPCR for high cell concentrations ($> 1 \times 10^8$ cells mL⁻¹). The method of cell lysis adopted was a simple 30 minute boil in sterile TRS as described in section 2.2.2.2. When this approach was used in an experiment all of the samples were treated in the same manner even if it was thought that they were of a low cell concentration.

Noble (Noble, 1996) found that the accuracy of a similar QPCR assay for the detection of *E. coli* whole cells was in the region of ± 30 % and for a purified plasmid (pQR701) ± 24 %. If the data in Table 16 is averaged then for whole cells the mean accuracy is ± 26.2 % and ± 21.9 % for the pHKY531 plasmid. This shows a slight improvement in the overall accuracy of methodology.

3.4 Considerations for bioaerosol samples

The QPCR technique can be used to quantify the microbial load from a variety of environments. The most important factor in the efficiency of the assay is in the preparation of the sample so that there are no inhibitory components present that would interfere with the PCR cycle. As bioaerosols are formed through the transfer of energy to a liquid, sufficient to break it into small particles, it is highly likely that any micro-organisms present will be damaged. The physical stress of release and the airborne factors (Cox, 1989) produce a sample that may contain whole cells, cell debris, enzymes and DNA. As the QPCR is based on the amplification of a specific sequence of DNA it is important that all other extraneous material is present in a relatively low concentration so as not to interfere with the PCR.

The dependence of the QPCR assay on samples that are free from inhibitory compounds places the emphasis on an effective bioaerosol sampling device that can produce a sample that is readily analysable. The aerojet general cyclone does this effectively through a buffered rinsing solution that can concentrate particles into a small volume of liquid. An awareness of the environment being sampled and the type of release enable a prediction to be made on the likely concentration of a sample and whether any pre-treatment would be required. By lysing the cells before the QPCR assay and where appropriate using two or more IS(B) concentrations problems of accuracy and error caused by heterogeneous sample mixes can be overcome. This does show that there is little adaptation to the QPCR technique required for bioaerosol samples, rather an awareness of the sample origin and any problems this may raise.

The result that the QPCR assay will give is a total cell count of the micro-organisms collected in a known volume of air. The advantage of this is that viable and non-culturable cells will be counted, which is an advantage when the damage to cells caused by aerosolisation can be lethal. Bej (Bej *et al.*, 1996) has shown that there are techniques becoming available that allow a viable cell count to be made from the amplification of specific mRNA sequences.

4. Aerosol Sampling Within Contained Cabinets

This chapter details a series of experiments that were performed to show the effectiveness of an aerofet general cyclone for the sampling of bioaerosols and the factors that affect its sampling efficiency. The experiments were carried out in the two cabinets described earlier (section 2.4.1), for reasons of safety and control over the airflow during the course of the experiments. Through the use of standardised bioaerosol generation, collection and quantitation methods enables a thorough investigation of the bioaerosol characteristics that influence sampling strategies and efficiency.

4.1 Cyclone Sampling Optimisation

Earlier research by Ferris (Ferris, 1995) and Noble (Noble, 1996) used the same cyclone system for the collection of bioaerosols efficiently. However with the development of a QPCR assay it was important to establish a clean system for each sample, to prevent cross-contamination and high background levels of DNA. In collaboration with Noble (Noble, 1996) a cyclone cleaning protocol was established and is detailed in section 2.4.3.2. The premise of this cleaning protocol was that the use of a dilute surfactant would ease the removal of cell debris and DNA from the glass walls of the cyclone when rinsed with water. A dilute surfactant, Tego, was used and found to be effective. The water rinse was an essential step to remove any residual surfactant from the cyclone surfaces, as very low levels of surfactant have been shown to inhibit the PCR (Alvarez *et al.*, 1995). The cabinet in which each experiment was performed was also cleaned and flushed with air to remove any residual airborne particles (section 2.4.1).

To increase the collection efficiency of the cyclone it was decided to modify the method of liquid injection into the cyclone so that it could be replicated more consistently. Originally in the work of Ferris (Ferris, 1995) the cyclone was washed by injecting the collecting liquid via a bent catheter angled to spray a jet of liquid down the middle of the cyclone gas inlet connection. As this method was not practicably reproduced, a dedicated liquid injection nozzle was designed. This was attached to the gas inlet via a quickfit joint and produced a jet of liquid that did not impinge on any of the inlet tube

walls. This also enabled the cyclone to be reproducibly set up for each experiment. The dimensions of this attachment are shown in appendix 2.

Cyclone collection efficiency has been related to many parameters such as geometry, airflow and particle size (IoZIA & Leith, 1989; Maunz & Buttner, 1994; Upton *et al.*, 1994). The first factor investigated was the efficiency of the cyclone at collecting micro-organisms released in the form of an aerosol. A suspension of *E. coli* RV308 pHKY531 cells (5×10^7 cells mL⁻¹) was prepared in sterile TRS, 18 mL of this was released into the UCL contained cabinet through the Warren Spring atomiser. The resulting bioaerosol was collected at varying airflow rates by the cyclone. The atomiser and cyclone were opposite each other with a 20 cm gap between them. To attempt to remove any temporal and spatial effects from the sampling another series of bioaerosols were released directly into the cyclone inlet. At high airflow rates, the air pump drew air from the room to make up the required air throughput. The results of this experiment are shown in Figure 17. From this data it can be seen that for the geometry of the Aerojet cyclone used, an airflow of approximately 400 standard litres per minute (SLPM) gives an optimum collection efficiency.

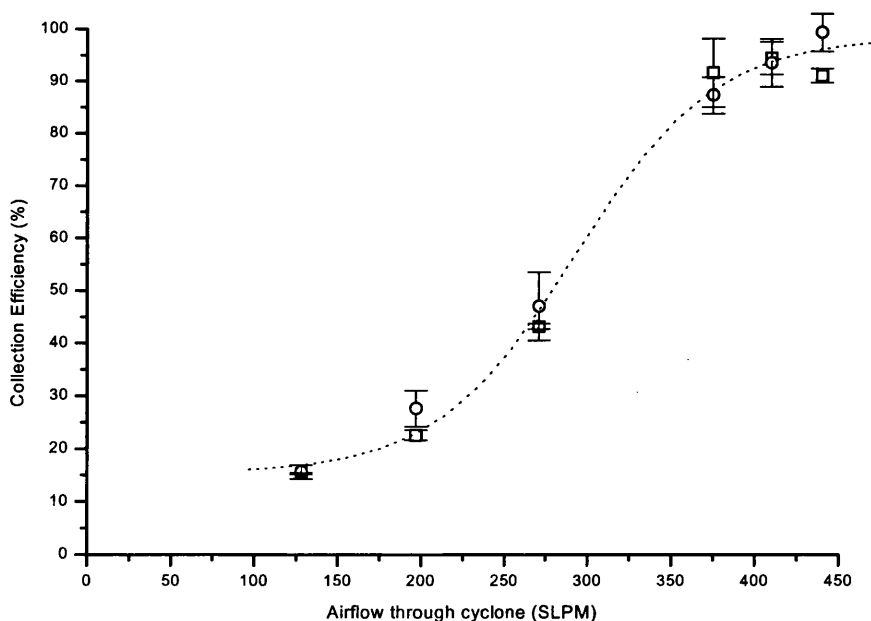


Figure 17 Direct (○) and indirect (□) capture of micro-organisms by an Aerojet general cyclone, where each point is the mean of two samples with their standard deviation.

What the data does not show is that at higher airflows (> 300 SLPM) through the cyclone there is a high degree of entrainment (Errington and Powell, 1969) of the liquid wash. Swift (Swift, 1986) described the use of a serrated edged skirt attached to the top of the cyclone around the vortex finder to decrease losses caused by precession currents. Because of this effect a lower airflow of 375 SLPM was chosen as the optimum balance between collection efficiency and losses due to entrainment. Over a short sampling period those losses would be small, but as the sampling time is extended a higher proportion of the collected sample would be lost as the wash liquid is recirculated through the cyclone. There does not appear to be any difference between the collection efficiency of the direct and indirectly released bioaerosol. This could be due to the effect of the high air throughput that the air pump generates. The airflow generated in turn within the cabinet would appear to transport the bioaerosol over the separating distance of 20 cm between the cyclone and the release point. The effect of spatial separation between the release and collection points is examined further in section 4.2.

Upton (Upton *et al.*, 1994) has reported that the aerojet general cyclone has a high collection efficiency for particles above $2 \mu\text{m}$ diameter. This was confirmed through the use of a particle sizer (section 2.7.1) set to sample the air inlet and exit sections of the cyclone while it was running. The aerosol used was a suspension of *E. coli* RV308 pHKY531 cells (5×10^7 cells mL^{-1}) prepared in sterile TRS, 18 mL of this was released into the UCL contained cabinet through the Warren Spring atomiser. The results (Figure 18) show that the collection efficiency of the micro-organisms follows the same pattern as that of the larger ($> 5.0 \mu\text{m}$ diameter) particles. This trend shows that for the same airflow through the cyclone there is a higher collection efficiency of micro-organisms than the $> 5.0 \mu\text{m}$ diameter particles. From this pattern it is possible to assume that the majority of the particles containing micro-organism collected by the cyclone are larger than $5.0 \mu\text{m}$ in diameter. If this were not the case then the collection efficiency of the $> 5.0 \mu\text{m}$ particles would tend to be greater than that of the micro-organisms for the same airflow. The data on the collection efficiency of smaller ($> 0.5 \mu\text{m}$ diameter) particles shows that above 300 SLPM $> 0.5 \mu\text{m}$ diameter particles are generated within the cyclone, giving the negative collection efficiency shown in Figure 18. This phenomenon can be seen in the cyclone as a more complete dispersal of the TRS wash as it leaves the tip of the injection attachment. This fine spray generated by

higher airflows through the cyclone will increase the relative humidity of the air within the body of the cyclone. This will reduce the effects of surface evaporation from the liquid particles as they travel through the cyclone, making particle sizes more constant.

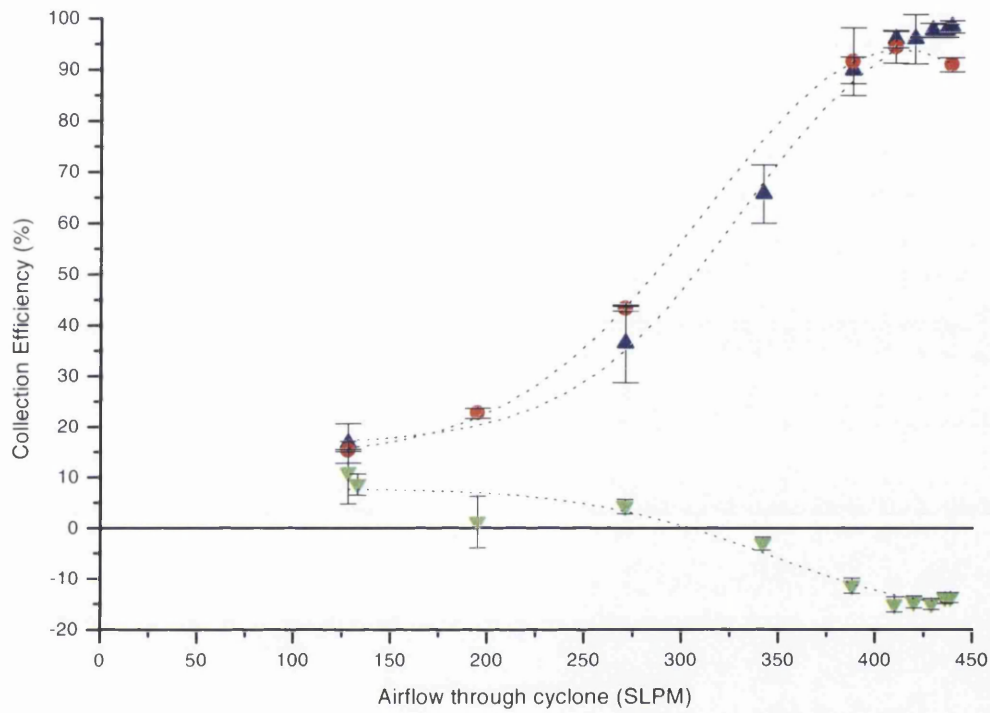


Figure 18 Aerojet general cyclone collection efficiency of micro-organisms (●), particles > 0.5 μm diameter (▼) and particles > 5.0 μm diameter (▲), where each point is the mean of two (●) or thirty (▼, ▲) samples with their standard deviation.

The cut point (d_{50}) for a cyclone is defined as the particle size at which the cyclone will have a 50% collection efficiency. Unfortunately it was not possible to experimentally determine this value for the cyclone set-up used. However by applying the simplest model of cyclone collection a theoretical value for the d_{50} can be made. The static particle theory of Barth (Barth, 1956) as presented by Iozia and Leith (Iozia and Leith, 1990) was used to determine that the d_{50} for the Aerojet general cyclone was 15.1 μm (Appendix 5). From the data shown in Figure 18 a d_{50} of 2 - 3 μm would be expected. This highlights the significant difference between models of cyclone behaviour and their actual performance. The data presented does provide evidence that the Aerojet general

cyclone when operated at 375 SLPM with a TRS spray injection captures approximately 95 % of microbial particles released from the atomiser.

4.2 Particular, Temporal And Spatial Aerosol Effects

Research by Marthi *et al.* (1990) and Hambleton *et al.* (1992) has shown that the medium from which an aerosol is generated can affect the properties of that aerosol. The most likely effect of a change in the liquid properties would be exhibited in the particle distribution of the generated aerosol. Should this produce particles that are very large ($> 100 \mu\text{m}$) or very small ($< 1 \mu\text{m}$) the cyclones collection efficiency is likely to be effected (Maunz & Buttner, 1994). Very small particles are unlikely to be collected by the cyclone and large particles are more likely to settle out in the air before reaching the cyclone, this could produce artefacts in the quantification from a skewed population sample. To establish whether the cyclone and QPCR method would be sensitive to the bulk liquid in an aerosol a series of standardised releases from Luria broth and TRS suspensions of *E. coli* JM107 pQR701 were prepared. 18 mL volumes were released via the atomiser into the Bassaire cabinet.

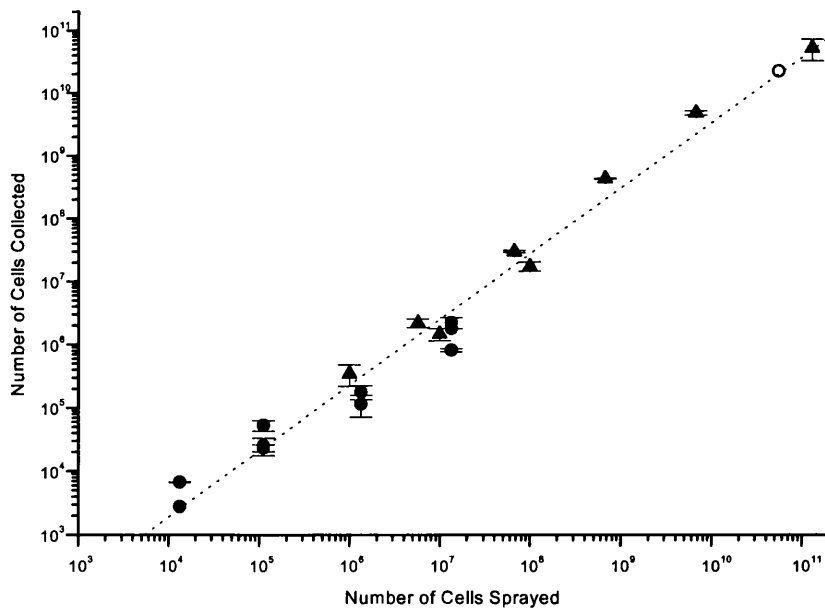


Figure 19 Atomisation and capture of micro-organisms from Luria broth (▲) and TRS (●) within the Bassaire cabinet. The means and \pm standard deviation are shown. Previous data (Ferris, 1995) on TRS suspended bioaerosols is shown (○).

The data presented in Figure 19 shows that there is a relationship between the released micro-organisms and their capture in the cyclone. The data suggests that the collection and quantification system used is insensitive to the bulk liquid of each release. An apparent linear regression can be produced for the range of data giving a very good fit ($R = 0.99$). This is unexpected as the aerosol from nutrient broth will contain a higher proportion media component particles which could act as foci for droplet formation in the aerosol cloud. With these components acting as foci, the particle distribution within the aerosol could be stabilised compared with the TRS aerosol. Therefore the correlation of aerosol release and capture becomes more influenced by the conditions of aerosolisation and the sampling characteristics, rather than the initial liquid properties. For example, aerosolisation at a higher air pressure would also have affected the particle size distribution and the resulting collection efficiencies. This sort of data is very useful for simulating the types of release you might expect within a process environment. An aerosol from the exhaust gas of a bioreactor will have media components in it, contrasted with an aerosol of clarified cells during downstream processing.

Any aerosol released will be diluted by the environment to a low concentration. The release may also be temporally and spatially removed from the sampling device. As any aerosol is composed of suspended particles, it is important to sample them whilst they remain airborne. This would give a window of opportunity during which aerosol sampling would be most effective. Experimentally this was investigated by releasing an aerosol of *E. coli* RV308 pHKY531 (5×10^7 cells mL⁻¹) suspended in TRS into the UCL contained cabinet and allowing it to settle in a stagnant environment, after a period of time the cyclone was connected to the cabinet and a sample of the residual airborne aerosol taken and assayed using QPCR.

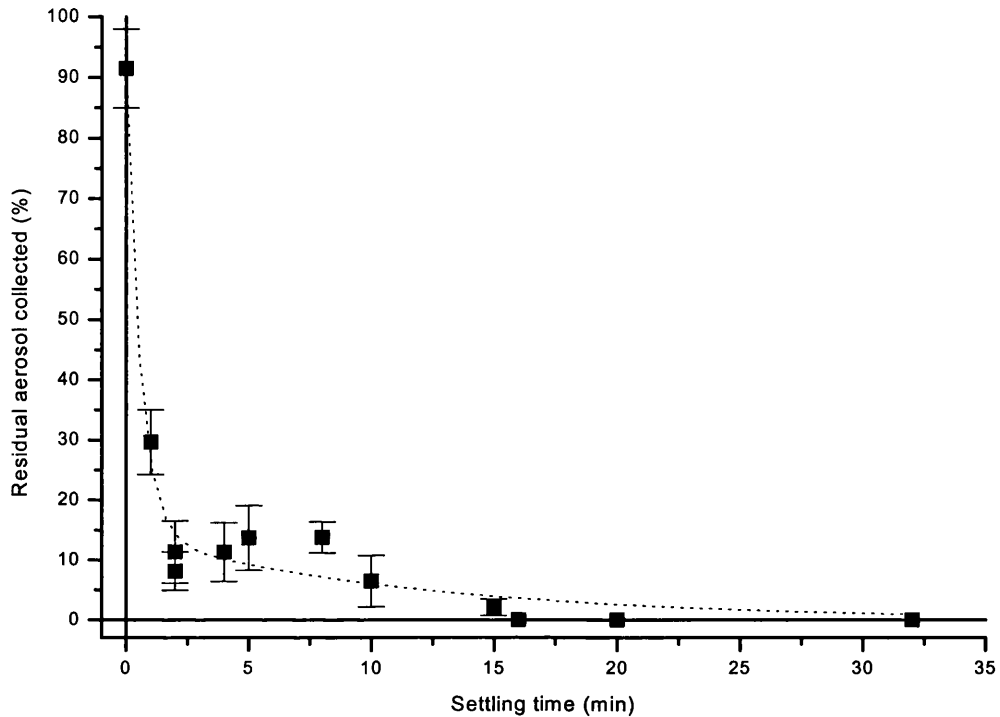


Figure 20 Settling time of an *E. coli* RV308 pHKY531 bioaerosol (5×10^7 cells mL⁻¹) within the UCL contained cabinet, where each point shows the mean of duplicate samples with their standard deviation.

Figure 20 shows that within the space of a few minutes over 90 % of the aerosol released is unrecoverable through the use of the cyclone. And by 15 minutes the cyclone sampling and QPCR can detect no residual aerosol. Any particles remaining airborne after this time will be small and unlikely to contain a micro-organism. From work done by Harari and Sher (Harari and Sher, 1997) it is possible to determine the theoretical Sauter Mean Diameter generated by the atomiser used in this experiment. This gives the diameter of a particle whose ratio of volume to surface area is the same as that of the entire particle distribution. The air blast atomiser used would theoretically produce a particle with a SMD of 28 μm (Appendix 5). The terminal velocity for a particle of this size, assuming it is spherical with unit density, according to Stoke's Law would be 2.4 cm s^{-1} (Hinds, 1982). Within the cabinet used for this experiment this would mean it would have settled out in 12 seconds. After 12 seconds only 75 % of the aerosol would be airborne and still collected. But as the SMD is a single point description of a particle size population it would be more precise to know the whole

particle size distribution for the aerosol and its behaviour. Ferris (Ferris, 1995) used identical conditions for aerosol generation and reported a particle size distribution for nutrient broth and TRS aerosolised cells. This data was used to calculate the settling time of the particles from the TRS aerosolisation. From the particle size data the terminal velocity for each point was determined and the time taken for a particle to drop the 30 cm from the release point to the cabinet floor was calculated. After 5 minutes 76.1% of the TRS aerosol would have settled to the floor of the cabinet. This supports the capture efficiency of the residual aerosol shown in Figure 19 as a drop of approximately 75% is seen in the collection of the residual aerosol within the first 5 minutes. However when Ferris (Ferris, 1995) performed the particle size analysis, the collection efficiency of the particle sizer used was less than 0.1 %, therefore the data reported may not represent the true particle size distribution for that aerosol. Unfortunately, the particle size distribution of the bioaerosols generated in this project were not determined due to equipment limitations. The surface contamination by microorganisms within a bioprocessing environment has been investigated and found that bioaerosol formation was the key cause (Tuijnburg Muijs *et al.*, 1987).

A well-described factor in aerosol sampling is the need to take samples isokinetically (May, 1967; Hinds, 1982). The polydisperse nature of bioaerosols creates different inertial forces on particles of different sizes transported in an moving airstream. When a sampling device such as a cyclone is introduced into the airstream there is a disturbance of the airflow streamlines. Sampling is isokinetic when the inlet of the cyclone is aligned parallel to the aerosol streamlines and the gas velocity entering the cyclone is identical to the free stream velocity approaching the cyclone inlet. When the sampling rate is higher or lower than the bulk air flow, or there is a misalignment of the cyclone, sampling is anisokinetic and the population of particles collected is skewed. These effects arise because particles with sufficient inertia in the region of cyclone inlet do not follow the now distorted streamlines and fail to enter the inlet. When the sampling rate is lower than the bulk air flow, the sampling efficiency will be greater than 100 %, since the larger particles are not carried away from the inlet. And when the sampling rate is higher the sampling efficiency will be less than 100 %, with a sample skewed towards smaller particles sizes. As microbial sampling in a process environment is unlikely to be isokinetic with respect to sampling velocities or orientation, the effect of anisokinetic sampling was investigated. An *E. coli* RV308 pHKY531 bioaerosol (5×10^7 cells mL⁻¹)

suspended in TRS was atomised in the UCL contained cabinet at various points and the cyclone collection efficiency measured (Figure 21).

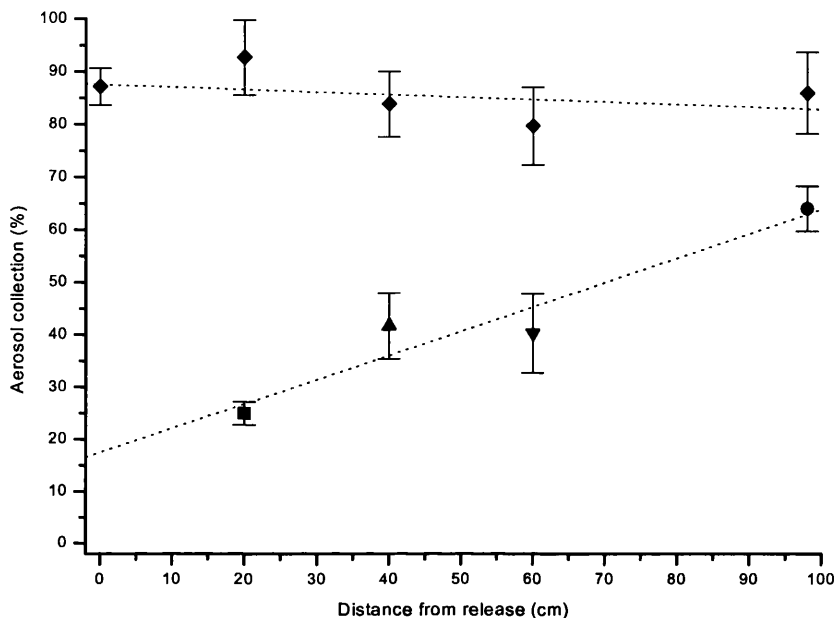


Figure 21 Anisokinetic sampling effects on cyclone collection efficiency, where the angle from the cyclone to the release point was 0° (◆), 5° (●), 25° (▼), 35° (▲) and 55° (■). Each point shows the mean of duplicate samples with their standard deviation.

From Figure 21 it can be seen that when the atomiser is less than 1 m away from the cyclone the collection efficiency is constant, provided it is in-line with the jet released from the atomiser. This plotted trend, though downward is not significant. The data presented for sampling in parallel (Figure 21) does show the effective sampling range of the cyclone under conditions that minimise disturbed streamlines. In the field, a variety of microbial samplers were assessed over a distance of 30 m (May *et al.*, 1976). In this test a cyclone was found to have a collection efficiency of 74 % for 30 µm diameter particles. Research into the dispersal of coliform bacteria has shown detectable levels at 15 m (Fannin *et al.*, 1976) and 1.2 Km from sewage treatment plants (Adams and Spendlove, 1970). The transport and dispersal of micro-organisms over large distances has been investigated by a number of researchers (Lighthart and Mohr, 1987; Lighthart and Kim, 1989; Knudsen, 1989).

From Figure 21 it can be seen that a deviation from the 0°, parallel sampling produces a marked decrease in collection efficiency as the angle from the cyclone to the release point increases. This decrease is seen even when the release point is closer to cyclone and is probably caused by a higher proportion of the generated bioaerosol impacting and adhering to the sides of the cabinet. Upton (Upton *et al.*, 1994) has stated that the cyclone collection efficiency is largely independent of orientation and local air flows. Within a bioprocessing environment high local airflows may be generated by the requirement for high air exchange rates. It has been shown that a high air exchange rates remove particles from the air because of the effect of ventilation and the increased turbulent deposition they generate (Nomura, 1997). Because of these effects the cyclone should be located as close to the process equipment as the physical constraints of the process environment allow. However the data presented here (Figure 21) would suggest that in a process plant when sampling the air it is desirable to position the cyclone within the airflow current, orientated with respect to the suspected release point. This would enable the collection of the highest proportion of airborne particles present. Anisokinetic sampling at a high flow rate will enable a greater total volume of air to be sampled. The effect of process equipment, high volume air exchanges and process operators make isokinetic sampling within a bioprocess plant a difficult target to achieve. The data presented in Figure 18 would suggest that it is not necessary as larger volumes of air can be sampled at a higher collection efficiency when sampling anisokinetically.

4.3 Release Impacts And Its Effect On Secondary Aerosolisation

The release of a liquid from a capillary leak will range in form, from a drop to a jet or an aerosol. Each release form is produced by increasing the amount of energy supplied to the liquid during its release. Lindblad and Schneider (Lindblad and Schneider, 1965) derived the minimum velocity required to form a jet from a capillary based on the surface tension of the fluid. In the following investigation a microbial suspension was released through a 50 mm long 254 μm ID capillary leak at a variety of different shaped targets. The cell suspension (3×10^9 cells mL^{-1} *E. coli* RV308 pHKY531 in TRS) had an applied differential pressure of 1 bar through the model leak system. The set-up of the equipment is detailed in section 2.6.2.4. The release was left for 6 minutes before the cyclone was started to highlight any difference in the particle size distribution generated by the impact of the jet onto the targets. The cyclone was then left to sample the air for a further 5 minutes. The samples collected by the cyclone were analysed by QPCR. The atomiser was used (section 2.4.2) to produce a completely aerosolised sample for comparison with the impacted samples.

Figure 22 and Figure 23 show the results of the particle sizing of the secondary aerosolisation taking place due to the impact of the jet on the target. The results of the particles sizes generated by the impact show that over the first 6 minutes of the release there was a range of particle concentrations generated for each size band. If the mean values are taken for each particle size band it can be seen that a flat target produces a marginally lower number of particles than either a concave or convex target, and the concave target produced slightly more particles than the convex target. The concave target may have been creating particles that collided with the jet as it approached the target and as a result a larger number of particles would have been generated. The convex target shape could be bouncing particles out of the path of the jet and as such reducing any effects of secondary collisions within the air stream. The flat target would appear to fall between the other two target shapes with respect to secondary aerosolisation creating interference with the jet impacting on its surface. When the number of particles generated by the secondary aerosolisation is compared with the number of particles produced by the atomiser it can be seen that the impact of a jet upon a target is a very inefficient method of producing an aerosol.

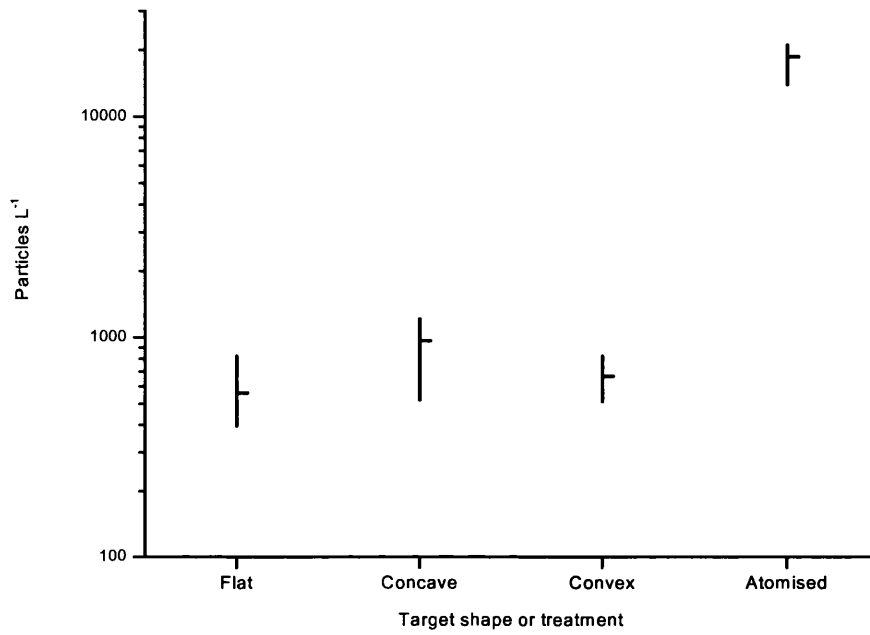


Figure 22 The maximum, minimum and mean number of particles > 0.5 μm in diameter generated by impact with a shaped target or from atomisation.

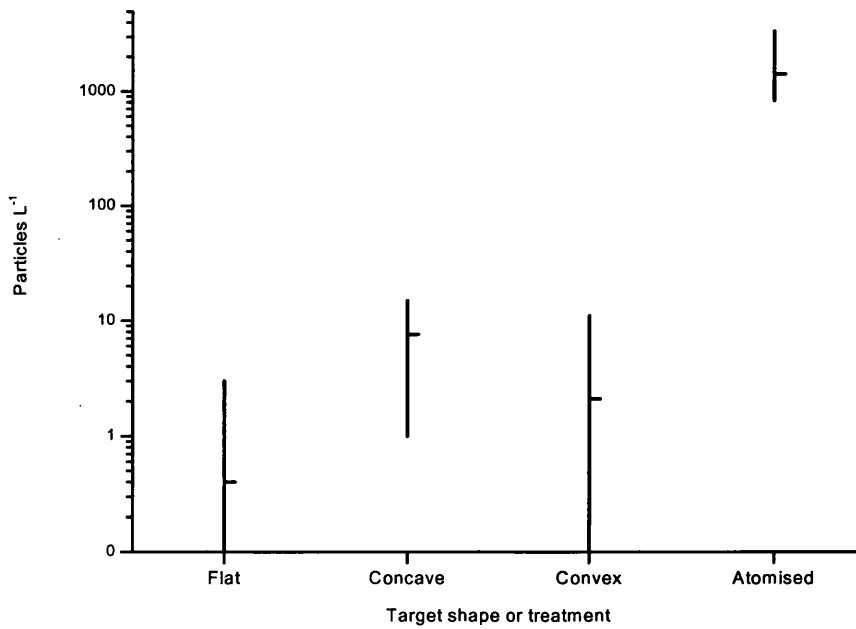


Figure 23 The maximum, minimum and mean number of particles > 5.0 μm in diameter generated by impact with a shaped target or from atomisation.

During the operation of the cyclone it was observed that the average number of particles produced by the impact of the release on each target decreased. This effect was probably due to the large volume of air being sampled by the cyclone disturbing the particle collection by the laser particle counter. When the samples were analysed by the QPCR and the results collected it was found that the concave and convex targets did not produce any particles, carried to the cyclone, that contained micro-organisms. The flat target did produce a signal in the QPCR which equated to 2.7×10^4 cells mL⁻¹, or a collection efficiency of 9×10^{-4} %. This efficiency is low as a result of the poor aerosolisation from the impact and the distance the aerosol must travel to be captured by the cyclone.

Further research into the fate of a release would be desirable, particularly relating to its transmission within a bioprocessing area. As has been shown earlier the most important factor in sampling for a bioaerosol is the correct siting of the cyclone sampler (section 4.2).

5. An Evaluation Of The Turbosep's Microbial Handling

Increasingly fermentation processes are being used to produce bioproducts. Particularly with the use of GMMO's it is important to show containment of the fermentation process. One aspect of fermentations that is frequently assumed to be contained, through the use of filter systems, is the exhaust gas.

Domnick Hunter supply an efficient foam breakage and removal device, the Turbosep, which also allows a more effective use of the tank volume, amongst other secondary benefits. Foam breakage occurs in the Turbosep as a result of the centrifugal forces generated by the spinning exhaust gas stream flowing through it. The similar nature of operation between the Turbosep and a cyclone has lead to some speculation as to whether the Turbosep would be able to remove small particles from the exhaust gas stream in addition to foam.

The objective of the experiment was to use the cyclone and QPCR techniques to investigate the efficiency of the Turbosep's removal of micro-organisms from fermenter exhaust gas.

5.1 Experimental Details

The fermentation used *E. coli* RV308 pHKY531, the BST producing strain developed by Eli Lilly and Company. The inoculation times and growth stage durations are shown in Table 17. The fermenter used was a 6000 L contained vessel and it was run using Speke Operations control strategy EL 4#2. The batch number assigned to the fermentation was B33-FV 039LF6. The addition of peptone at 6.5 hours was used to induce foaming in the vessel. After foam induction the Turbosep was left to control the foam level in the vessel automatically based on the differential pressure across the inlet and outlet of the Turbosep.

The cyclone was connected directly to the exhaust gas pipe, for samples after the Turbosep, and through the control of a valve the air flow through it was regulated at 350 L min⁻¹. The collecting liquid used was 80 mL TRS recirculated at 20 mL min⁻¹ via a peristaltic pump. Sampling was carried out over a 15 minute period. After sampling the volume of collection liquid was measured by weight and the cyclone cleaned. The sample and triplicate 1 mL sub-samples were taken and stored at -20 °C until analysis. All other operating conditions for the cyclone are as previously described in section 2.4.3.

Table 17 Inoculation times and duration of each growth stage.

	Inoculation Time	Duration
1° Veg Flasks	2300 9/7/96	5 hours
2° Veg. Flasks	0400 10/7/96	8 hours
Seed	1200 10/7/96	17 hours
Fermenter	0500 11/7/96	12 hours

A number of samples were taken at different differential pressure values across the Turbosep. An additional sample of the exhaust air after the Turbosep was taken immediately after the fermenter was sterilised. A sample of the foam generated was taken directly from the head space of the fermenter through a spare addition line, without the use of the cyclone. Before killing the fermentation, the foam in the head space was flattened through the addition of an excess of antifoam and a sample of the gas in the head space was taken with the cyclone. The vessel was still aerated and the airflow through the cyclone for this sample was 325 L min⁻¹.

The biomass was monitored on-line through a load cell during the course of the fermentation. Additionally microbial cell counts (section 2.1.3) and optical density measurements (section 2.1.4) were made of each sample for cell concentration calculations.

Samples stored at -20 °C were allowed to thaw at room temperature before being used in the PCR. Culture samples and the foam sample were diluted serially by 100 in TRS. The QPCR protocol was followed as described in section 2.2.5.2 and the products analysed as described in section 2.3.

5.2 Results And Discussion Of Turbosep Performance

The process of aerosolisation of cells from a foaming broth is complex and depends on many variables such as the operating parameters of the bioreactor and the rheological properties of the broth. In this present study the influence of differential pressure on the ability of a Turbosep to remove cells from the exhaust gas of a stirred tank bioreactor was investigated. The differential pressure in a Turbosep is a measure of the amount of foam passing through the device. For the size of Turbosep used in this evaluation a differential pressure of 75 m bar would flood the device and as such this was considered a maximum foam loading. Figure 24 shows that there is little effect of differential pressure on the microbial load present in the exhaust gas after the Turbosep.

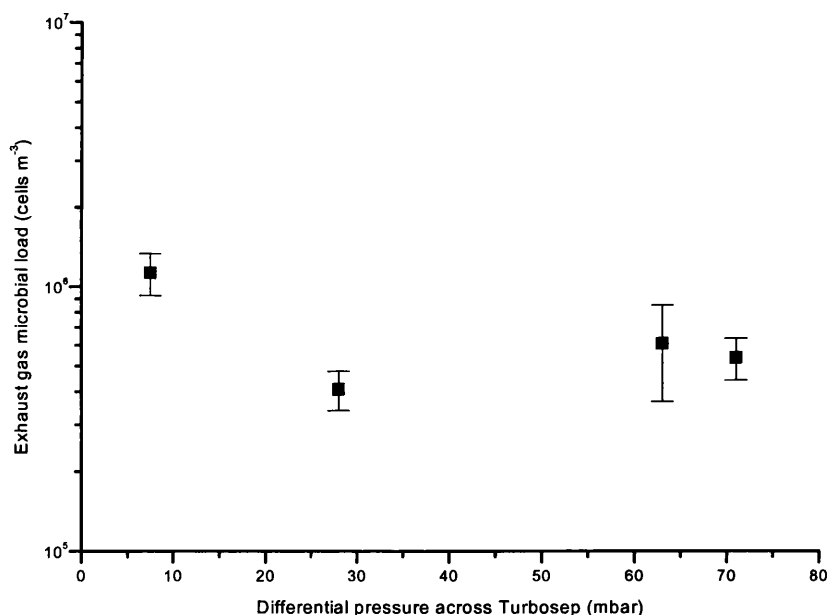


Figure 24 The effect of Turbosep differential pressure on exhaust gas microbial load, showing means and ± 1 SD.

The data presented in Table 18 shows that the fermentation at Speke Operations yielded a final cell concentration of 5×10^{10} cells mL⁻¹ and at this point the concentration of cells in the head space of the vessel was found to be 2×10^9 cells m⁻³. The samples after the Turbosep, whilst recirculating foam, at various stages in the fermentation showed that the average cell count was 7×10^5 cells m⁻³. This shows that the Turbosep is capable of reducing the microbial loading of the exhaust gas by approximately 3½

orders of magnitude. The microbial load present in the exhaust gas after the Turbosep is therefore equivalent to a release of 50 μL of whole cell broth over the course of a 12 hour fermentation.

Table 18 *E. coli* concentration after 12 hours fermentation.

Sample	Microbial Load
Broth	5×10^{10} cells mL^{-1}
Foam	1×10^{10} cells mL^{-1}
Headspace	2×10^9 cells m^{-3}
After Turbosep	7×10^5 cells m^{-3}

The results gathered in this short investigation into the efficiency of a Turbosep at removing micro-organisms from the exhaust gas of a fermentation are very promising. At University College London a small scale study of the number of *E. coli* cells present in the exhaust gas of a 1.5 L bioreactor was undertaken (Nobel *et al.*, 1997). A total cell count of 2×10^{10} cells mL^{-1} were present in the broth and after the condenser there were $5 - 10 \times 10^7$ cells m^{-3} . This showed that a simple condenser decreases the cell count in fermenter exhaust gas.

There are two distinct mechanisms which are probably taking place within the Turbosep. The first is the breakage of foam and its return to the fermenter vessel, which returns any micro-organisms suspended in the foam to an aqueous phase in the main vessel. The second is the removal of smaller airborne microbial particles which are not part of the foam phase and are carried into the Turbosep. It is not clear at the moment which of these is providing the majority of the micro-organism removal. However what is possibly occurring is each mechanism is effective to a degree, with the current Turbosep design favouring the foam breakage mechanism. And the remaining particle removal coming from relatively large particles carried in the gas phase.

There is no simple relationship between cell density in the fermentation broth and the number of cells released into the exit gas. There are a series of factors that might be implicated in the variation of release rate as the fermentation proceeds. Pilancinski and co-workers (Pilancinski *et al.*, 1990) have shown that aerosol formation from a fermentation broth is influenced by several factors such as air flow rate, agitation rate

and the rheological properties of the liquid. Notably, the fraction of particles large enough to potentially carry micro-organisms was found to increase with agitation rate and air flow rate. This work was extended by Szewczyk *et al.* (1992) who also looked at aerosol generation in an industrial pilot scale fermenter, but unlike the Pilancinski work, studied the effects of growth of the micro-organisms (an *E. coli* K12 strain) on the change in aerosol properties. It was found that aerosol particle concentration decreased significantly with increasing cell density and that the change in particle concentration was more pronounced in the size range above 2 μm . Particles at this size and larger are more likely to contain a whole micro-organism.

Additionally, the clumping of cells in fermentation broth is more likely to occur at high cell densities. Larger clumps of cells may not be lifted into an aerosol due to their size not being compatible with the particle distribution of the aerosol. The larger particles will exhibit an increase in settling velocity which occurs according to Stoke's law as the particle diameter increases. This may account for the fall in the number of cells detected.

Expression of the rate of release of cells in terms of the exit gas volume allows a comparison of results with other researchers who have used different methods to measure cell numbers in fermenter head space. The data presented here shows that in the head space there is a cell concentration of 2×10^9 cells m^{-3} . Winkler (1987) has reported that in the fermenter head space there are about 10^6 contaminated particles per cubic meter of gas. Since each "contaminated particle" contains at least one viable cell then this describes only the minimum number of cells present. Additionally, it is well known that a large proportion of viable cells are not culturable (Colwell *et al.*, 1985) and that in the aerosolised state the culturable portion is likely to be very low (Neef *et al.*, 1995).

Other studies on aerosols produced by fermentation have concentrated on aerosol particle characteristics rather than cellular concentration in the aerosol. For instance, Pilancinski *et al.* (1990) measured over 10^8 particles m^{-3} of which between 30 - 40 % exceeded 2 μm diameter above a complex broth stirred at 130 rpm. Szewczyk *et al.* (1992) measured the particle concentration at approximately 15 cm above the fermentation liquid and found that the level decreases from greater than 6×10^8 particles

m^{-3} at inoculation to 2.5×10^8 particles m^{-3} after microbial growth, where the stirrer speed was 450 rpm.

The present use of PCR while sensitive and quantitative does not measure viability. Additionally, in this investigation the exhaust gas has been sampled downstream of a Turbosep, whereas the other researchers have sampled the head space of a fermenter (Winkler, 1987; Pilancinski *et al.*, 1990; Szewczyk *et al.*, 1992).

The exhaust gas monitoring after the Turbosep shows quite clearly that there was a reduction by $3\frac{1}{2}$ orders of magnitude of the microbial load. This research presented here is currently being extended with a view to the redesign of the Turbosep to improve its microbial handling. This preliminary investigation highlights the very low level of incidental release produced from the exhaust gas of a fermentation. The potential release from accidentally spilling a drop of fermentation broth when emptying the fermenter is a release an order of magnitude greater. This type of observation raises the question about the current approach to bioprocess containment.

6. Bioprocess Leak Simulations

Current bioprocesses place high demands on the standard of equipment used, with respect to its performance relative to process goals and to its safety. Equipment is validated to provide documentary evidence that it performs as originally specified. The validation of a processes sterility is easily performed by growth and kill tests. From the results of a sterility test it then may be assumed that a process achieves effective containment. This may not be true for many situations.

A failure in the containment of a piece of equipment will occur when there is a route allowing the transmission of material from the process to the environment, or *vice versa*. This transmission pathway is more commonly called a leak. At present, for the bioprocess industry there is little quantitative data on the size of leaks resulting from normal process operation or accidental events. To effectively validate the containment of bioprocess equipment techniques that enable the quantification of leaks need to be established. With such techniques it should be possible to establish a baseline value for a piece of equipment's containment during the operational qualification of the process validation. This value could later be used as a reference for the performance qualification and normal plant operation. To establish a method for the quantification of leaks within a bioprocess a model leak system was developed.

When testing a piece of equipment for leaks there are three goals that could be achieved during the testing, the detection of a leak, the location of the leak and finally the quantification of the release through the leak. A simple pressure hold test is commonly used for gross leak detection within bioreactors. To compare its efficiency of detection with that of SF₆ tracer gas techniques a set of 50 mm long capillaries of various diameters were attached to a spare port of a 450 L bioreactor (LH) installed at University College London. The vessel was isolated from all but the air system and pressurised to 1 bar. The pressure decay each minute through the attached leaks was monitored for 2 hours using a data logging package (Real Time Data Acquisition Systems). The rate of pressure loss was then calculated from the linear regression of each response and this is presented in Figure 25.

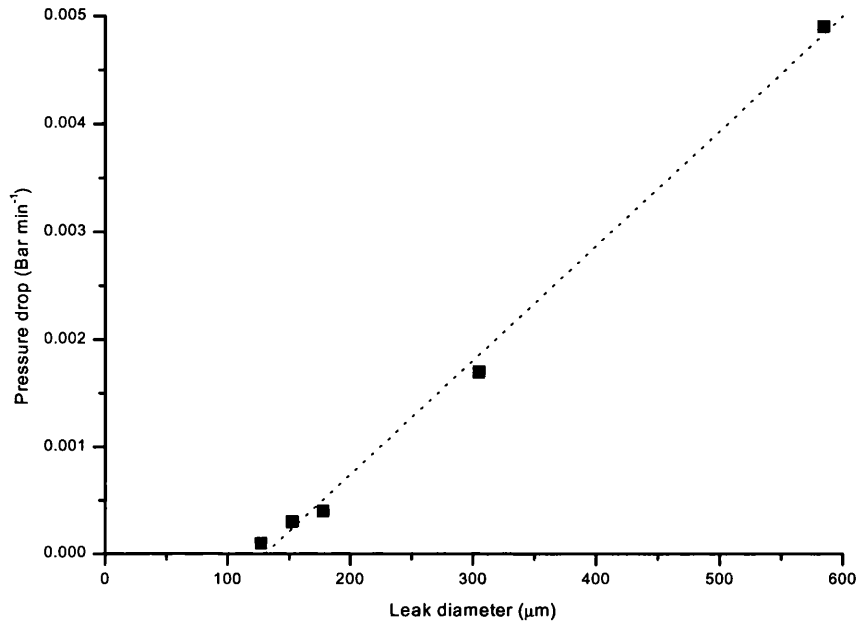


Figure 25 The measured pressure drop in an LH 450 L bioreactor over 2 hours for capillary leaks of various sizes.

A further linear regression of the data was performed to calculate the approximate limit of detection over 2 hours for the pressure hold test. The linear regression was a good fit to the data ($R = 0.998$) giving a value of 132 μm diameter as the limit of detection. This value is specific to the volume of the vessel, test pressure and the duration of the test. Smaller vessels have a much more rapid response to pressure change and as such smaller leaks would be detected as the release of air through the leak forms a high proportion of the total vessel volume. This normally means that pressure hold test are only performed on lab to pilot scale vessels up to approximately 1 m^3 volume. This limits the effectiveness of a pressure hold test to detect, and quantify a leak. It could be said that through a pressure hold test it is not possible to locate a leak, merely prove that there is a drop in pressure, the assumption being that this is the result of a leak.

6.1 Model Leak System Design And Validation

The model leak system design and construction is shown in section 2.6, Figure 10. The system has been designed to be flexible with respect to the size of leak it can simulate and the flow rate through it. Both gaseous and liquid leaks can be produced at various driving pressures, through the use of a pump or a high pressure supply. The most important aspect of the system is its development around needles of defined lengths and internal diameters. By using needles the system becomes much more flexible and easier to modify with respect to the leak path length and diameter. Stainless steel needles can be obtained down to 127 μm ID and these were acceptable for the investigation of gross leaks (Table 11). From the average size of an *E. coli* cell ($1 \times 1.5 \mu\text{m}$) it was assumed that a 1 μm ID orifice would not allow the passage of an intact cell. As it was considered likely that a whole cell could pass through a 127 μm ID orifice a method of producing holes from 1 μm ID was required. The solution to this problem was through the use of hand made borosilicate intracellular sperm injection (ICSI) needles. These can be made with a diameter of a fraction of a micrometer, with extremely high tolerances. As these needles are made of borosilicate glass they are quite fragile and required careful handling and connection to the leak system.

The connections between the components in the model leak system had to be leak tight. Where leak tight is a level of leakage that would be insignificant in the tests to be carried out. This leak rate was defined as a leakage of SF_6 below the limit of detection of the Leakmeter 200 ($0.1 \times 10^{-7} \text{ mL s}^{-1} \text{ SF}_6$). Of equal importance was the proof that the leak system only leaked at a defined point, the tip of a connected needle.

The integrity testing of the model leak system was carried out using the Leakmeter 200 with 1% SF_6 in N_2 as the tracer gas. The Leakmeter 200 was used to sample the entire length of the components in the system with particular reference to junctions between components and the valve body at various valve settings. Table 19 shows the results for the integrity test of the model leak system. Two types of ICSI needles (65 mm long, 250 μm ID) were used; the first had its tip melted closed and the second was left with an unobstructed terminal orifice. From this validation exercise it has been shown that the system does not leak at any of the connections or through the components, at up to 4 bar pressure. When the open ICSI needle was attached to the system a signal from the

Leakmeter 200 was recorded and the detector became saturated with SF₆ in a few seconds. These data shows that the system will give a defined leak at the terminal point of a connected needle and at no other junction, which validates the design of the system.

Table 19 Details of the model leak system integrity validation.

Needle	Test Pressure (Bar)	Test location					
		Valve - Closed	Valve - ½ Open	Valve - Fully open	Pressure gauge	Needle connection	Needle orifice
Sealed	1	< LOD	< LOD	< LOD	< LOD	< LOD	< LOD
	2	< LOD	< LOD	< LOD	< LOD	< LOD	< LOD
	4	< LOD	< LOD	< LOD	< LOD	< LOD	< LOD
Open	1	< LOD	< LOD	< LOD	< LOD	< LOD	Saturated
	2	< LOD	< LOD	< LOD	< LOD	< LOD	Saturated
	4	< LOD	< LOD	< LOD	< LOD	< LOD	Saturated

where LOD = 0.1×10^{-7} mL s⁻¹ SF₆ and Saturated = $> 3.2 \times 10^{-4}$ mL s⁻¹ SF₆

On occasions when the model leak system had to be disassembled all parts were stored in a dry, grease free environment. Upon reassembly the system was checked for leak tightness at 4 bar as described. Due to the simple connections reassembly was not found to introduce leaks into the system.

6.2 The Behaviour Of Leaks

The behaviour of a leak is governed by a combination of its geometry and the fluid/gas passing through it. The mathematical descriptions of fluid flow through tubes and capillaries are well known and described earlier (section 1.6.2). Visible leaks are approximately greater than 300 μm ID and they exhibit viscous flow at close to or above atmospheric pressure. As the dimensions of the leak decrease and they approach the mean free path of the gas the flow regime changes from viscous flow to molecular flow. The mathematics of the transition from viscous to molecular flow has been approximated by an number of empirical relationships (Burrows, 1961; McMaster, 1982). The effect of leak geometry and fluid/gas characteristics are examined in this section.

6.2.1 SF₆ Leaks

The application of theoretical predictions of fluid flow described by equations 1, 2 and 5 can be used to predict the flow of SF₆ through the designed model leak system for different flow regimes (Figure 26). The correlation of actual values with theoretical predictions enables the general flow regime generated within the model leak system to be established.

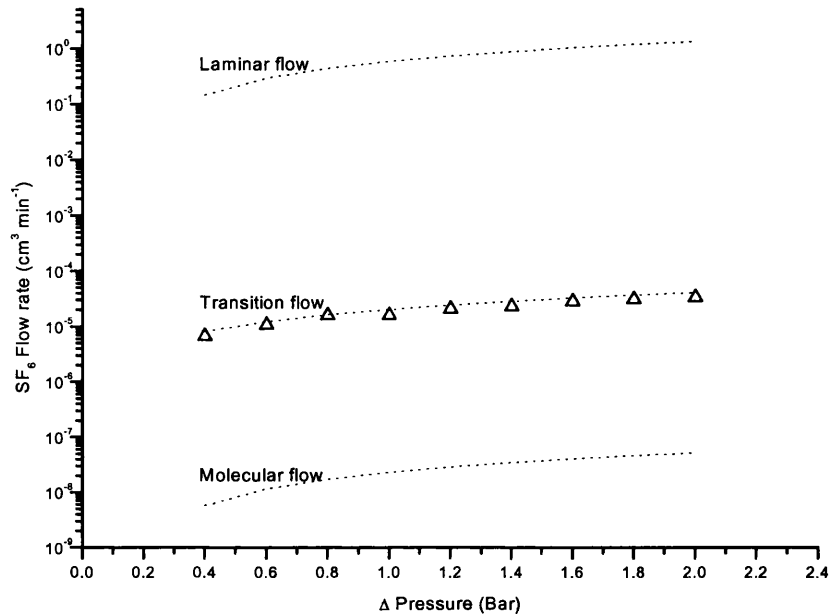


Figure 26 The theoretical 1 % SF₆ flow rates for different flow regimes (---), compared with empirical values (Δ), for a capillary leak 65 mm long and 50 μm ID.

Figure 26 shows that for the leak dimensions given the flow behaviour is most closely described by transitional flow theory. The relationship plotted in Figure 26 is that described by Baram (Baram, 1991) and shown in Equation 2. The mean free path of the SF₆ (34.2 nm (Dobrowolski, 1988)) is smaller than the leak diameter and as such molecular flow does not predominate. Yet neither does laminar flow as the diameter of the leak is not so large that the gas particles do not interact with each other. Hence a proportion of each type of flow contributes to the overall bulk flow characteristic. When a range of leak diameters is examined it can be seen that transitional flow gives a good correlation over the range of sensitivity of the Leakmeter 200 (Figure 27).

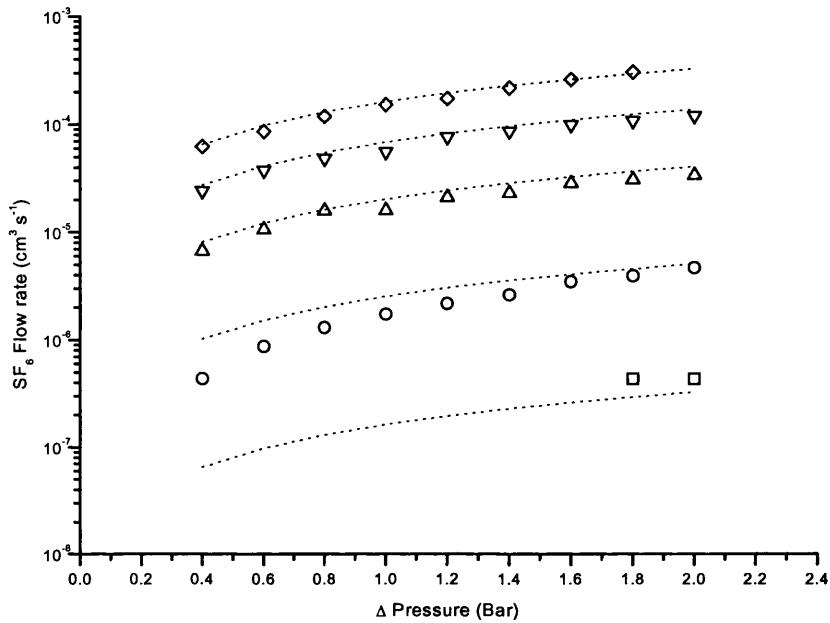


Figure 27 The SF₆ flow rate for 65 mm long leaks of various diameters (10 μm (□), 25 μm (○), 50 μm (Δ), 75 μm (∇) and 100 μm (◇)), correlated with the theoretical transitional gas flow (···) expressed by equation 2 (Baram, 1991).

It should be noted that the missing empirical data for 10 μm and 100 μm diameter leaks in Figure 27 is due to the range of SF₆ detectable by the Leakmeter 200. For the smaller diameter leaks the transitional theory does not give as close a match to the observed values. This may be a result of the tracer gas used being a mixture of 1 % SF₆ in N₂ and as such mean physical values used in the prediction may not necessarily accurately describe the two gas species. In general it can be seen that the empirical values tend to be slightly lower than predicted, suggesting that this factor alone is not responsible. The ICSI needles are manufactured by pulling a glass capillary till it breaks and then flame polishing the tip to the desired size. This technique results in a tapering of the terminal tip and will contribute to a higher pressure drop as the gas exits the capillary. As the capillary uniformly converges there is less turbulence generated as a *vena contracta* does not form and the resistance to flow is reduced (Tilton, 1997). The reduction in flow is not significant in comparison with the overall bulk flow rate and as such in long capillary leaks this effect is ignored.

6.2.2 Aqueous Leaks.

When the flow of a liquid is considered the behaviour of the fluid flow is significantly different than that for a gas. Within the bioprocessing environment it would be expected that the majority of leaks would take place in the aqueous phase. The theoretical flow of water in a variety of capillaries was examined to determine the flow behaviour. The flow rate was calculated by collecting the volume of water leaving dripping from the capillary over a fixed period of time.

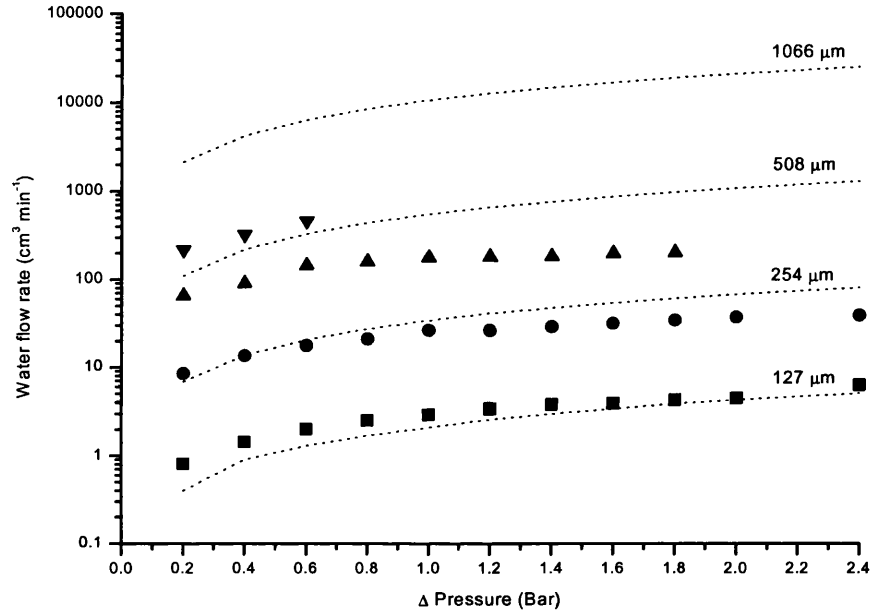


Figure 28 The Water flow rate for 10 mm long leaks of various diameters (127 μm (■), 254 μm (●), 508 μm (▲) and 1066 μm (▼)), correlated with the theoretical laminar liquid flow (---) expressed by equation 5 (Tilton, 1997).

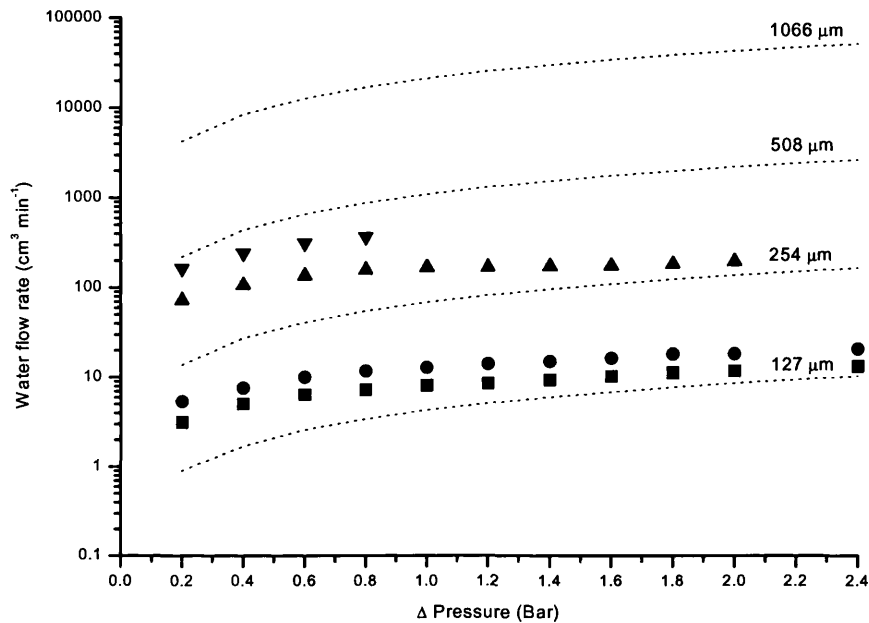


Figure 29 The Water flow rate for 5 mm long leaks of various diameters (127 μm (■), 254 μm (●), 508 μm (▲) and 1066 μm (▼)), correlated with the theoretical laminar liquid flow (···) expressed by equation 5 (Tilton, 1997).

The data presented in Figure 28 and Figure 29 for the flow of water through capillary leaks highlights limitations of a purely theoretical examination of fluid flow. In both figures the trend of the empirical flow is the same as that predicted by the theory of laminar flow. However, as leak diameter is increased the theoretical values begin to diverge from the observed values. To establish a stable flow regime within a length of pipe a commonly stated assumption (Tilton, 1997) is that the pipe should be long relative to its diameter ($25 D$). For the 10 mm long leak path the 508 μm and 1066 μm diameter leaks do not meet this criteria, and only the 127 μm diameter leak has value of $25 D$ less than 5 mm. If this is taken into account then it can be seen in Figure 28 that the 127 μm and 254 μm diameter leaks ($25 D < 10 \text{ mm}$) and the 127 μm diameter leak ($25 D < 5 \text{ mm}$) in Figure 29 show a fair correlation with the predicted laminar flow. Where there is a poor correlation with the predicted flow the leak length is not long enough to establish laminar flow and the high pressure drop to length ratio creates turbulence and a lower flow rate through the leak.

6.2.3 Microbial Leaks

From the data previously shown (section 6.2.1 and 6.2.2) it can be seen that SF₆ will be transmitted through a smaller diameter leak than water. This should allow SF₆ to be used as a tracer gas to detect holes that water will pass through. Fluids within a bioprocess are more than likely to have an aqueous base but they could also contain whole cells, insoluble media components and dissolved salts. The presence of this particulate material within the fluid changes the flow characteristics considerably. This can be seen in Figure 30 where the theoretical flow of water is compared with the actual flow of two concentrations of cell suspensions. The flow rate of the cell suspensions was measured by collecting the volume of fluid passing through the capillary over a defined period of time.

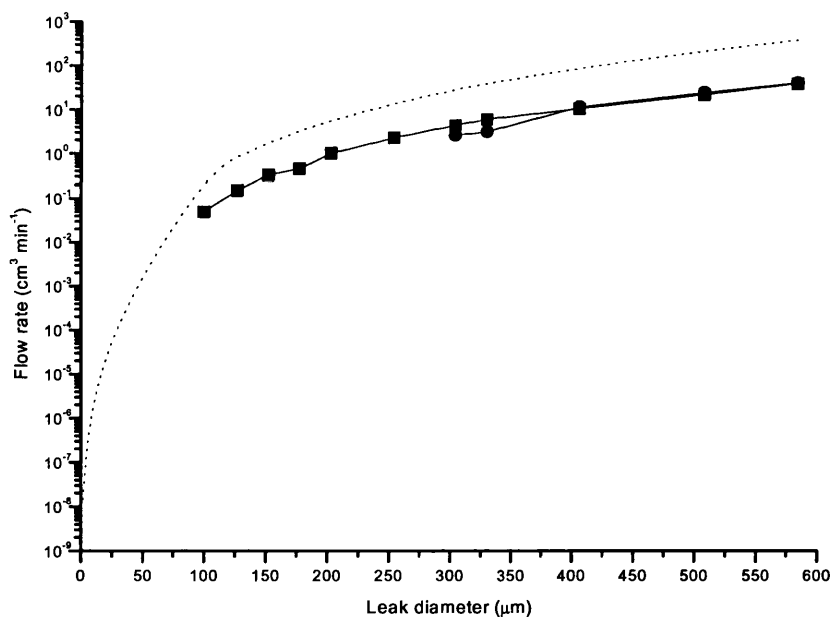


Figure 30 The theoretical flow of water (...) as expressed by equation 5, and the actual flow of *E. coli* RV308 pHKY531 cells (8×10^3 cells mL⁻¹ (■), 8×10^{10} cells mL⁻¹ (●)) through 50 mm long leaks of various diameters at 2 bar ΔP .

The length of the leak was set at 50 mm to ensure laminar flow across the range of diameters. The data presented in Figure 30 shows that water will be transmitted through a leak far smaller than a suspension of *E. coli* cells. The higher cell concentration (8×10^{10} cells mL⁻¹), which is a realistic concentration for an early stage in a fermentation

process, can not pass through a capillary smaller than 330 μm diameter. At a very low cell concentration (8×10^3 cells mL^{-1}) the fluid blocks a capillary 10 times the one blocked by water alone (Figure 29). The difference between the two fluids is the particles they contain. These data show that the presence of *E. coli* cells is enough to prevent transmission, even though the leak diameter is approximately an order of magnitude greater than the diameter of a whole cell.

The flow rate of various concentrations of *E. coli* cells through leaks of various diameters was examined. TRS suspensions of cells were prepared and pumped through the model leak at various pressures. The flow rate of the cell suspensions was measured by collecting the volume of fluid transmitted over a fixed period of time. The results of these experiments are shown in Figure 31, Figure 32 and Figure 33.

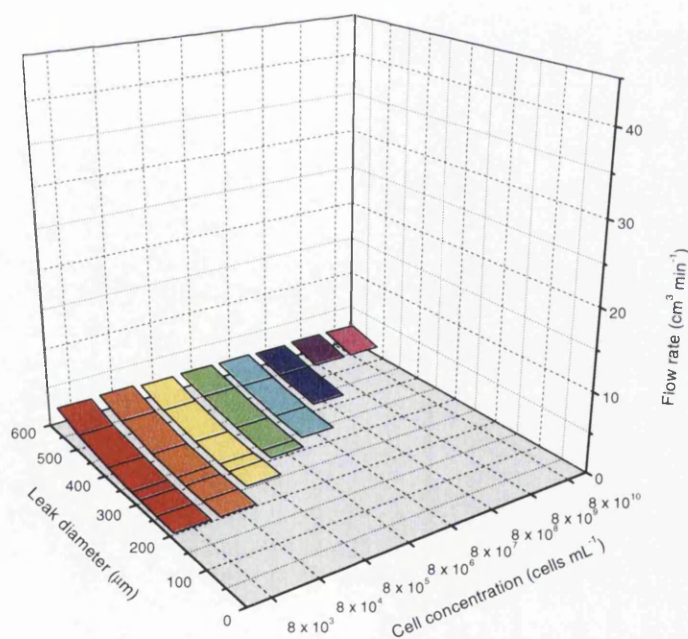


Figure 31 The actual flow of *E. coli* RV308 pHKY531 cells through 50 mm long leaks of various diameters at 0.5 bar ΔP .

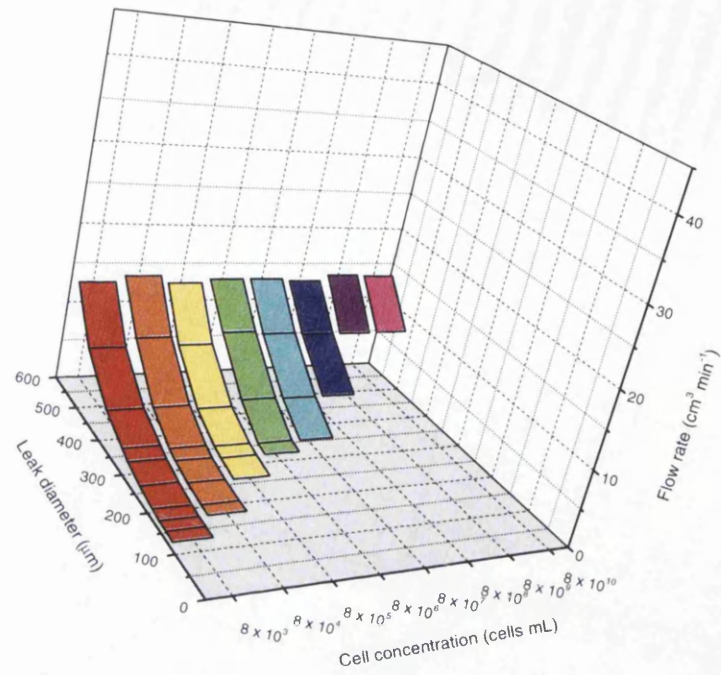


Figure 32 The actual flow of *E. coli* RV308 pHKY531 cells through 50 mm long leaks of various diameters at 1.0 bar ΔP .

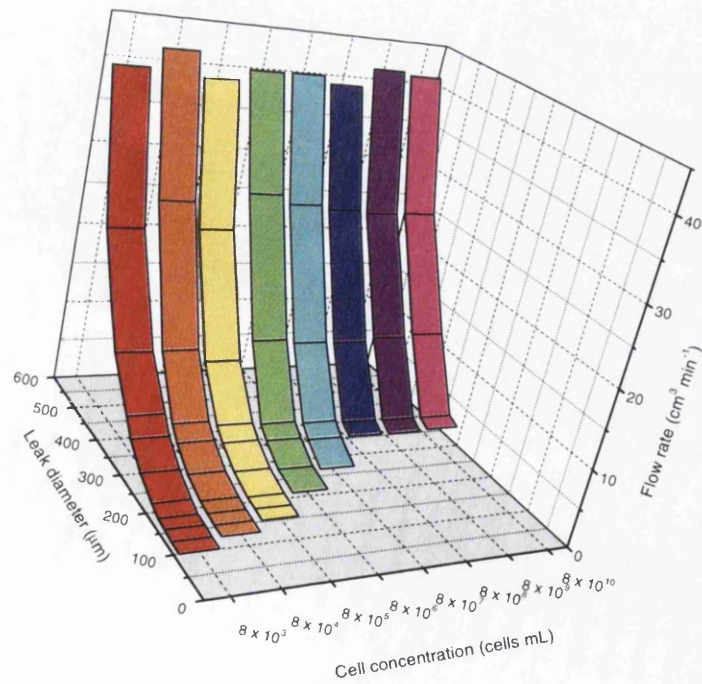


Figure 33 The actual flow of *E. coli* RV308 pHKY531 cells through 50 mm long leaks of various diameters at 2.0 bar ΔP .

From Figure 31, Figure 32 and Figure 33 it can be seen that with an increase in pressure the flow rate of the cell suspension through the capillary leak is increased. Equally at increasing pressures the size of the capillary that the suspension can be transmitted through is reduced. Both of these effects are expected from simple fluid flow. However the suspension of whole cells in the fluid creates blockages in the capillary leaks. The data from the previous three figures (Figure 31, Figure 32, Figure 33) is represented in Figure 34 to show the effect of capillary blockage.

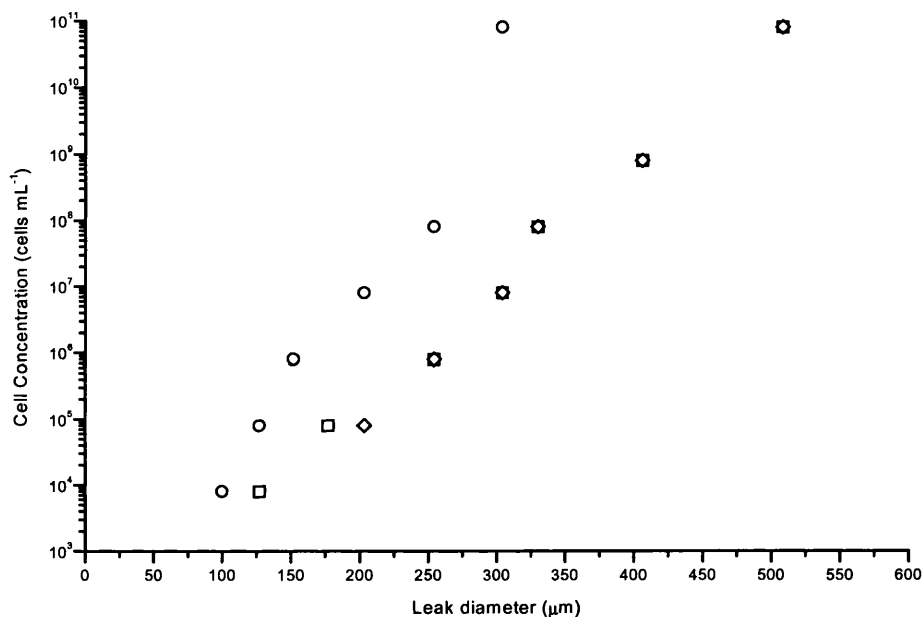


Figure 34 The maximum *E. coli* RV308 pHKY531 cell concentration that can flow through a 50 mm long leak without blocking at various ΔP (0.5 bar (\diamond), 1.0 bar (\square) and 2.0 bar (\circ)).

From Figure 34 it can be seen that the blockage of capillaries at 0.5 and 1 bar is similar for capillaries above 250 μm ID. Below 250 μm ID the effect of the pressure enables a 10^5 cell suspension to penetrate a 203 μm ID capillary at 0.5 bar, and a 177 μm capillary at 1 bar. When the pressure is increased to 2 bar the blockage trend shifts to the left, showing that smaller capillary leaks will be penetrated by the same concentration suspension. At 2 bar a 10^5 cell suspension will penetrate a 152 μm ID capillary. Burrows (Burrows, 1961) investigated the blockage of capillary leaks by liquids. The relationship given for the blockage of a capillary leak is given by the surface tension of

the liquid and the pressure driving the liquid. If it is assumed that the liquid will wet the capillary wall completely then the relationship simplifies to Equation 6. The introduction of suspended material obviously has a marked effect on this relationship. At 2 bar water would flow through a leak with a diameter of 1.5 μm . A microbial suspension will not penetrate such a small capillary and it would block. A liquid with a lower surface tension such as a lubricating oil will have a lower surface tension and will flow through a leak at a lower pressure difference. The flow rate of water through such a small capillary will be very low and that of the oil even lower due to its higher viscosity. As the leaks used were long relative to their diameter laminar flow could be established and as a result particle sedimentation would contribute to capillary blockage. The blockage of capillaries over time is shown in Table 20.

Table 20 The time (s) taken for a 50 mm long capillary to become blocked by a suspension of cells at 1 bar ΔP . Each sample is the mean of duplicates.

<i>E. coli</i> Concentration (cells mL ⁻¹)	Capillary ID (μm)			
	152	203	254	304
8×10^4	300			
8×10^5		150		
8×10^6			240	
8×10^7				180

Table 20 shows that high cell concentrations block capillaries more quickly than lower cell concentrations. The diameter of the capillaries blocked by a given cell concentration were smaller than the capillaries allowing free flow of the same cell concentration in Figure 34. This data shows that there is no clear cut point for the flow or blockage of a cell suspension through a capillary. Above a certain diameter free flow of a cell suspension can be observed and below this there is a region where blockage will occur over a period of time determined by the pressure, cell concentration and capillary diameter. Below this range of diameters the leak would block instantly due to the properties of the fluid, resulting in no detectable flow.

6.2.4 Comparison of SF₆ and Microbial Leaks

Previously it has been shown that a dilute suspension of micro-organisms could penetrate a leak approximately 100 µm in diameter (Figure 34). However it has been shown that simple pressure hold tests are limited in their ability to detect leaks in the region of 130 µm (Figure 25). This then necessitates the use of a method that can detect leaks that do not allow the transmission of micro-organisms.

A comparison of the leak rates of SF₆ and *E. coli* cell suspensions has been made under various conditions to establish the effectiveness of SF₆ as a tracer gas for bioprocess leaks. For each experiment the model leak system was set up as previously described (section 2.6.2) and the release of SF₆ and cell suspension quantified. The quantification of the release of SF₆ was limited by the range of the Leakmeter 200. As such it would appear that there is no flow of the tracer gas above certain leak diameters in the following figures (Figure 35, Figure 36 and Figure 37). There was flow of SF₆ through the larger diameter capillary leaks but the flow rate was greater than the saturation limit of the detector. As such the leak could be located at the tip of the capillary but the release rate through it could not be accurately quantified.

The data in Figure 35 shows the effect of the length of the leak on the release rates of SF₆ and *E. coli* cells. From this it can be seen that the shorter leaks have a higher flow rate of the *E. coli* cell suspension. The smallest SF₆ detectable leak is also effected by the overall length of the leak.

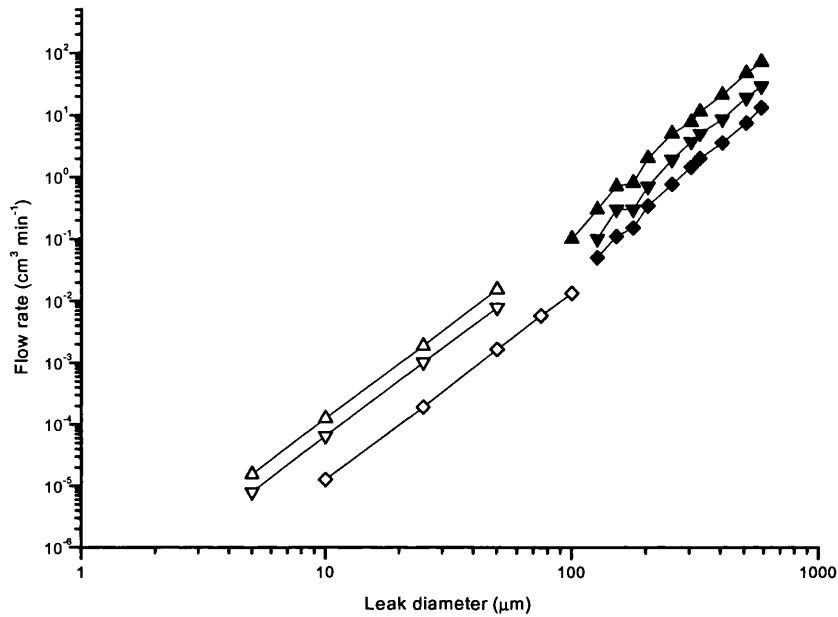


Figure 35 The effect of leak length on the flow of 1 % SF₆ (5 mm (Δ), 10 mm (∇) and 50 mm (◇)) and 8×10^3 cells mL⁻¹ *E. coli* RV308 pHKY531 (5 mm (▲), 10 mm (▼) and 50 mm (◆)) at 1.0 bar ΔP.

In Figure 36 the effect of the differential pressure on the release rate of the cell suspension and SF₆ is examined. It can be seen that as the pressure is increased there is an increase in the flow rate of the cell suspension for a given leak diameter and the largest leak diameter allowing transmission decreases.

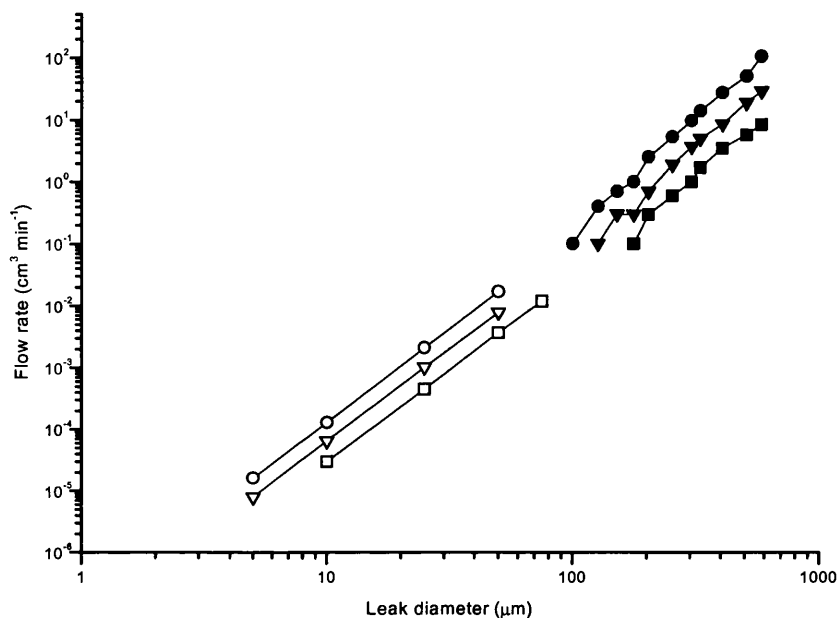


Figure 36 The effect of pressure (ΔP) on the flow of 1 % SF_6 (0.5 bar (\square), 1.0 bar (∇) and 2.0 bar (\circ)) and 8×10^3 cells mL^{-1} *E. coli* RV308 pHKY531 (0.5 bar (\blacksquare), 1.0 bar (\blacktriangledown) and 2.0 bar (\bullet)) through 10 mm leaks.

Both Figure 36 and Figure 37 show a similar pattern of release for the cell suspension and the SF_6 tracer gas. The SF_6 is transmitted through leaks with a diameter far smaller than the cell suspension can penetrate. There is no overlap between the two ranges of quantification for the cell suspension and the Leakmeter 200 used to detect the SF_6 gas. The SF_6 gas used in all of the experiments was a 1 % mix in pure N_2 , due to supply problems it was not possible to obtain 100 % SF_6 to investigate the effect of a higher tracer gas concentration on the resolution of the leak detection. To overcome this the theoretical behaviour of 100 % SF_6 was predicted using Equation 2 (Baram, 1991) and compared with actual flow rates for an *E. coli* suspension and 1 % SF_6 . As the range of detection for the Leakmeter 200 was known the theoretical plots of 100 % SF_6 flow were limited to that range to enable clearer comparison with the 1 % SF_6 results (Figure 37).

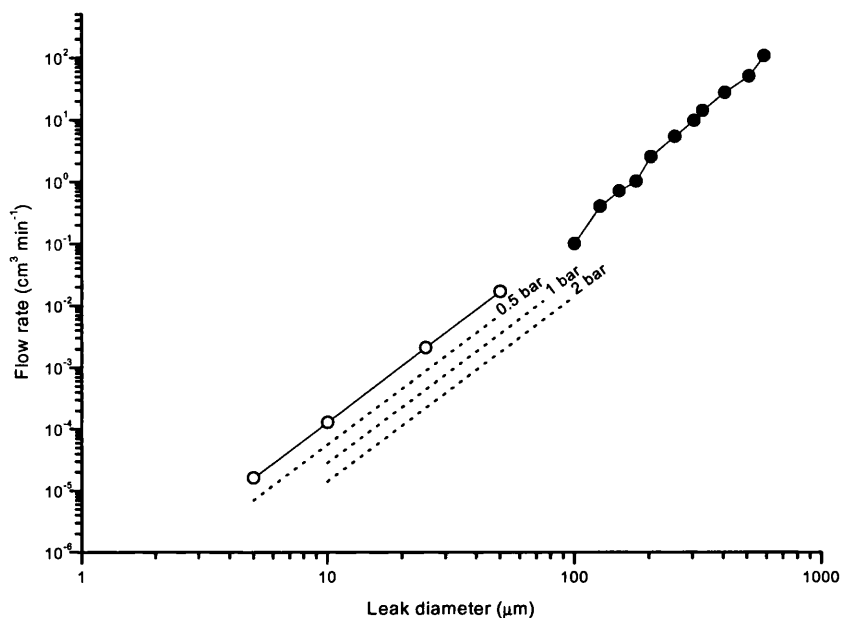


Figure 37 The flow of 1 % SF₆ (O) and 8×10^3 cells mL⁻¹ *E. coli* RV308 pHKY531 (●) through 10 mm long leaks of various diameters at 2 bar ΔP, compared with the theoretical flow of 100 % SF₆ (---) expressed by equation 2 (Baram, 1991) at various ΔP. The theoretical flow data is shown only for the Leakmeter 200 SF₆ range of detection

From Figure 37 it would seem that there is little advantage in switching from a 1 % mix of SF₆ to a 100 % gas. The range of leak diameters quantified is not extended to significantly overlap with the release of the cell suspension. Only at 2 bar differential pressure is there a quantifiable release of cells and SF₆ from the same capillary. Even under 2 bar pressure the Leakmeter 200 would be operating at the extreme of its range. There are other compelling environmental, analytical and economic reasons why 1 % SF₆ should be used instead of 100 % SF₆. As SF₆ is a potent greenhouse gas its release should be minimised wherever possible, this is particularly true when a high background level of SF₆ within the testing environment could mask smaller leaks. There is also the cost of a pure gas over a dilute mixture that should be considered. In favour of 100 % SF₆ there are benefits in the speed of detection and the removal of concerns over homogeneity within the equipment under test. A high concentration of SF₆ will be detected more readily than a low concentration by the detector possibly minimising the downtime of equipment. As SF₆ is denser than air it is preferable to mix the gas within the piece of equipment under test to prevent settling of the gas at the lowest point, and thereby missing the detection of any leaks within the upper surfaces of the equipment.

The combination of the Leakmeter 200 and SF₆ as a tracer gas at 1 % concentration will allow the detection of a leak that a microbial suspension will not be able to pass through. And depending on the size of the leak it will be able to quantify the release upon location. The use of a tracer gas and the Leakmeter 200 enables all the objectives of a leak detection method to be met; detection, location and quantification. Despite the limitation of the range of detection of the Leakmeter 200 it could be stated that if SF₆ was detected and the release rate was quantifiable then there was a leak present that would be too small to allow the transmission of a microbial suspension (Figure 35, Figure 36). If the response of the detector is above its upper limit then the leak could be large enough to allow the transmission of micro-organisms. When defining the criteria for the leak testing protocol of a piece of equipment a reference value for the pass/fail should be set. From the data presented here (Figure 35, Figure 36) a value of $6 \times 10^{-6} \text{ cm}^3 \text{ min}^{-1} \text{ SF}_6$ would be recommended for the pass/fail value for a piece of bioprocess equipment at a differential pressure of 2 bar. For a 5 mm leak this value is equivalent to a 3 μm diameter hole, which has been shown not to transmit a suspension of micro-organisms. The 3 μm diameter is within the range of detection of the Leakmeter 200 and is consistent with the value ($\approx 5 \times 10^{-6} \text{ cm}^3 \text{ min}^{-1}$) Baram cites for the leak testing acceptance of bioprocessing valves (Baram, 1991). Leaks with a diameter *circa* 8 μm have been shown to be the cause of contamination within a bioprocess (Perkowski *et al.*, 1984), and as such 3 μm may still allow the transmission of virus particles. The data presented so far shows that liquid leaks of cell suspensions will block, in effect preventing the transmission of material across the process boundary. A 3 μm diameter hole will be blocked by a capillary of water where the differential pressure is less than 1 bar. However a leak that has become blocked under one set of conditions may not remain blocked. Evaporation of any liquid may occur and biological material may degrade. This could create a leak partially blocked with material which may act as a source of contamination. It is also possible that leak test using a tracer gas may not detect the leak because it has become plugged with particulate matter. It then becomes essential that any cleaning and leak testing standard operating procedure (SOP) can deal with the residue of trapped particulate material within a capillary. To overcome blocked leaks equipment should be dried under a high pressure of air and leak testing should be carried out at as high a differential pressure as possible.

6.3 The Effect of A Surfactant On Leak Transmission.

The rheological properties of a liquid greatly influence its transmission through a pipe (Tilton, 1997). The effect on the flow of a liquid suspension through a capillary leak is as pronounced. It has been shown (Burrows, 1961) that the surface tension of a liquid is a major component in determining whether a capillary will block. To investigate the effect of surface tension a surfactant (Tween 80, BDH) was mixed with a TRS cell suspension and pumped through the leak system. A 50 mm long 254 μm ID capillary was used at 1 bar differential pressure. The TSI laser particle counter (section 2.7.1) was positioned 15 cm below the midpoint of the jet stream exiting needle orifice. The particle counter simply splits detected particles into the two size bands ($> 0.5 \mu\text{m}$ and $> 5.0 \mu\text{m}$ diameter) and records the total every 10 seconds. The results for this series of experiments are shown in Figure 38 and Figure 39.

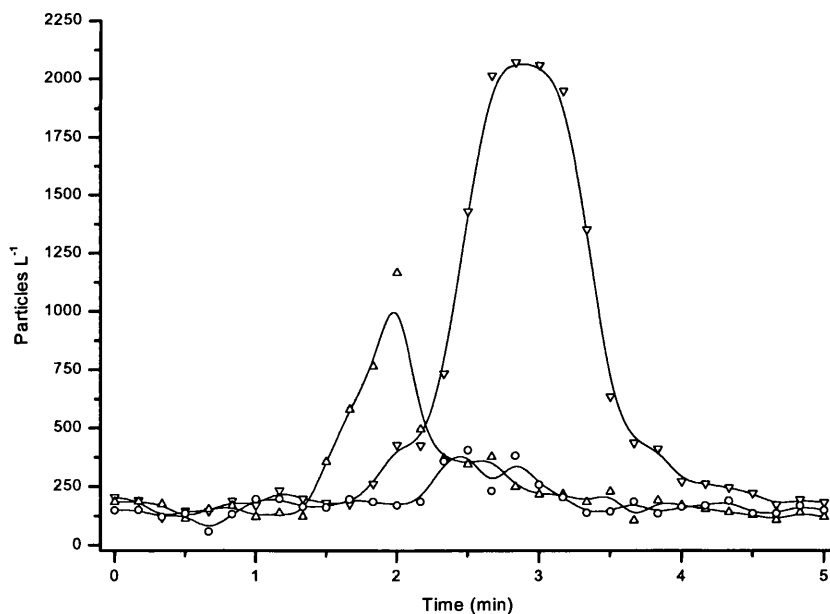


Figure 38 Particles $> 0.5 \mu\text{m}$ diameter of a suspension of *E. coli* RV308 pHKY531 cells (8×10^9 cells mL^{-1}) with 0 % (○), 0.01 % (▽) and 0.1 % (△) Tween 80 (v:v) generated by passing through a capillary 50 mm long and 254 μm diameter.

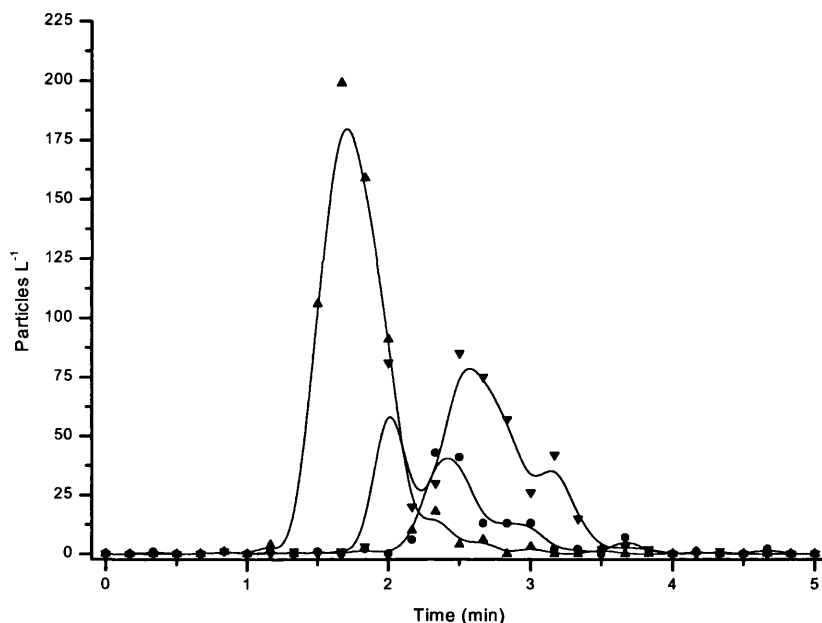


Figure 39 Particles > 5.0 μm diameter of a suspension of *E. coli* RV308 pHKY531 cells (8×10^9 cells mL^{-1}) with 0 % (●), 0.01 % (▼) and 0.1 % (▲) Tween 80 (v:v %) generated by passing through a capillary 50 mm long and 254 μm diameter.

The time trace for each particle size band shows distinct peaks of particle generation. The data from Figure 38 and Figure 39 is summarised in Table 21.

Table 21 The time and relative size of peak particle generation from a suspension of *E. coli* RV308 pHKY531 cells (8×10^9 cells mL^{-1}) passing through a capillary 50 mm long and 254 μm diameter in the presence of Tween 80.

Tween 80 (v:v %)	Particles >0.5 μm diameter		Particles >5.0 μm diameter	
	Time (s)	Size (relative to control)	Time (s)	Size (relative to control)
Control, 0%	150		150	
0.01%	150	200 %	180	650 %
0.10%	90	500 %	120	300 %

The *E. coli* cell suspension passes through a smaller capillary leak than previous data would suggest was possible (Figure 34). The control cell suspension with no addition of Tween 80 did not penetrate the capillary leak but the observed flow was irregular and prone to pulsing more so than the other suspensions. The Tween 80 containing suspensions flowed more freely through the capillary leak over the period of time monitored. A

proposed rationale for the peaks in particle generation for the Tween 80 suspensions is based on their surface tension, viscosity and the settling of particles within the capillary leak. The 0.1 % Tween 80 suspensions will have had the lowest surface tension but it was observed that these suspensions were noticeably more viscous than the others. The 0.01 % Tween 80 suspension would have had a decreased surface tension relative to the control suspension but it was apparently of a similar viscosity. As the cell suspensions are passing through the capillary particles will settle depending on their velocity relative to the bulk fluid flow. This could result in a build up of particles within the capillary creating a constriction and a build up of pressure. This build up particles will occur at different rates depending on the viscosity of the bulk liquid. The data (Figure 38 and Figure 39) shows that the control and 0.01 % Tween suspension generate the most particles after the peak particle generation of the more viscous 0.1 % suspension. The increase in pressure then disrupts any particulate build up and there is a large release of particles over a short space of time; the particle size distribution being influenced by the surface tension of the bulk liquid and the particles within it. The lower surface tension suspensions both generate more particles than the control. The higher 0.1 % Tween 80 concentration produces a higher proportion of larger particles than the 0.01 % suspension. These results could suffer from a loss in accuracy due to particle sedimentation prior to the particle counter, resulting in a skewing of the data.

The implication of these findings is that a low surface tension liquid can generate a more disperse aerosol than a high surface tension liquid. And that a low surface tension liquid will penetrate a smaller leak than a high surface tension liquid. The use of a cleaning agent containing a surfactant could aggravate the problem of small leaks becoming blocked. As the surface tension of the liquid drops the transmission of liquid into a capillary is increased. This highlights the careful design of cleaning protocols prior to leak testing to ensure the removal of residual cleaning agents and the thorough drying of equipment.

6.4 Effect Of Shear On Cells Transmitted Through Capillary Leaks

In this section the effect of the shear forces generated by the flow of a cell suspension through a capillary are investigated. There has been much research published on the effect of shear on biological materials, particularly with a view to minimising shear damage or maximising material recovery. Of particular relevance to this investigation are papers by Bowman and Davidson (Bowman and Davidson, 1972), Zhang (Zhang *et al.*, 1993), Carlson (Carlson *et al.*, 1995) and Levy (Levy *et al.*, 1998). The potential shear damage generated by the passage of cells through a capillary becomes important should an aerosol be produced. The shear forces within the capillary could result in the disruption of the cells to produce a fluid which is predominately cell fragments and DNA. Such a fluid could penetrate smaller orifices and as such present different containment requirements.

To investigate the effect of shear a rotating disc shear cell (section 2.8.2) and a capillary rheometer (section 2.8.1) were used to generate shear forces within *E. coli* cell suspensions. The rotating disc shear cell has been used to investigate the effect of shear on supercoiled plasmid DNA (Levy *et al.*, 1998). In this study a TRS suspension of *E. coli* cells was used in place of a plasmid solution. The results from the shear of the cells can be seen in Figure 40.

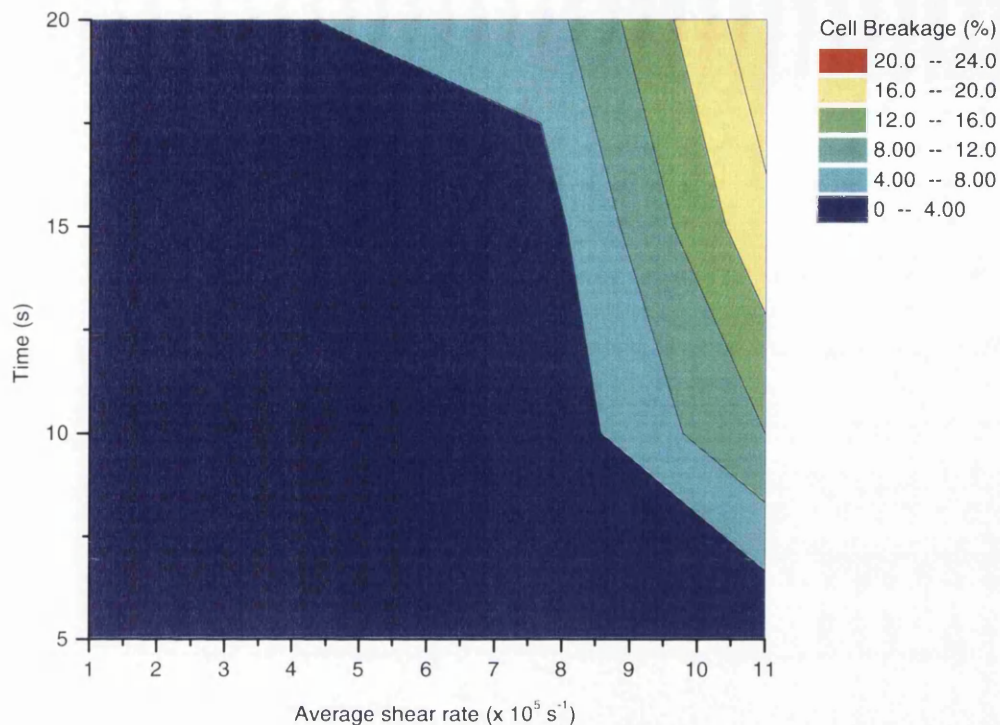


Figure 40 The rotating disc shear-induced cell breakage of an *E. coli* RV308 pHKY531 cell suspension (2×10^8 cells mL⁻¹).

The rotating disc clearly begins to shear the cells open when the average shear rate generated exceeds 8×10^5 s⁻¹. The cell breakage increases with extended exposure to a high shear environment and higher shear rates. The rotating disc shear cell shows clearly that *E. coli* cells will break when subject to shear. The flow field within the device is rotational and although the shear rates may be comparable to those generated within a capillary the local direction of flow is not. To more closely mimic the shear generated within a capillary leak the capillary rheometer was used.

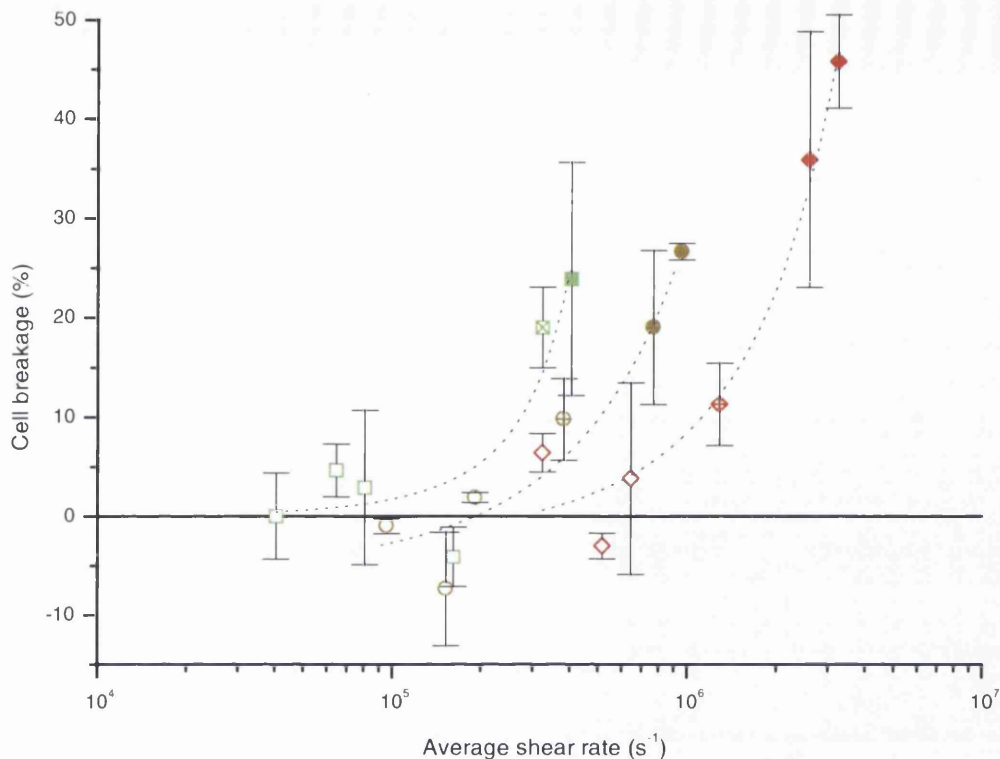


Figure 41 The shear-induced breakage of a suspension of *E. coli* RV308 pHKY531 cells (8×10^5 cells mL^{-1}) passed through 100 μm (\diamond , \blacklozenge , \blacklozenge), 150 μm (\circ , \oplus , \bullet) and 200 μm (\square , \boxtimes , \blacksquare) diameter capillaries. Each point is the mean of triplicate samples with the error bars showing the standard deviation ($\pm 1\text{SD}$) of that mean. The flow characteristic based on Reynolds number is shown as laminar (\diamond , \circ , \square), transitional (\blacklozenge , \oplus , \boxtimes) or turbulent (\blacklozenge , \bullet , \blacksquare). 1st order exponential growth is represented by the dotted lines (...)

From the results shown in Figure 41 it can be seen that the average shear rates generated within a 100 μm diameter capillary are approximately an order of magnitude greater than those generated by the rotating shear cell. The results (Figure 41) for the 200 μm diameter capillary are in good agreement with the results observed in the rotating disc shear cell (Figure 40) where a similar range of shear is generated. From the literature (Carlson *et al.*, 1995) the mechanical breakage of *E. coli* cells follows a 1st order rate model. Figure 41 shows the exponential breakage of cells through lines fitted to the obtained results. These fitted lines show a good correlation with the observed results confirming the model and the behaviour of the system under study. As the shear rate is increased within the capillary rheometer by increasing flow rate and decreasing capillary diameter a high proportion of cells are broken. From the calculation of the Reynolds

number for the fluid passing through the capillary it can be seen that turbulent flow creates the highest cell breakage. This effect has been observed in animal cells (Zhang *et al.*, 1993) and the increased shear damage is thought to occur from the formation of eddies smaller than the cell within the capillary. These can cause localised cell wall deformations and with sufficient energy cell rupture. During transitional flow the eddy formation is reduced and consequently the shear breakage of the cells. Under conditions of laminar flow there should not be any eddy formation and from the results (Figure 41) there can be seen a high degree of scatter around the zero breakage line. The parabolic velocity distribution characteristic of laminar flow could cause shear as fluid streamlines slip over each other during their passage through the capillary. The differential velocity applied to a cell wall could result in breakage.

To investigate the effect of shear on the particle size distribution of the cell suspensions samples of each sheared suspension were analysed by a Malvern particle sizer (section 2.7.2). The results of the particle size analysis summarised in Figure 42, where the highest shear rate for each capillary diameter is shown. The complete particle size analysis data for each shear rate is shown in Appendix 4 (Figure 46, Figure 47 and Figure 48). From the data (Figure 42) it can be seen that the change in particle size distribution is negligible above 2 μm and there is only a deviation from the unsheared sample below this value. The particle size analysis did not show any particles larger than approximately 3 μm , which would rule out the presence of any large agglomerates of cells that were present before or after shearing. This would suggest that there are only single cells being broken by the high shear environment. From data in Figure 41 up to 50 % of the cells are being broken and at the higher shear rates there are significantly more particles less than 1.2 μm diameter present (Figure 42) possibly showing the presence of cell debris.

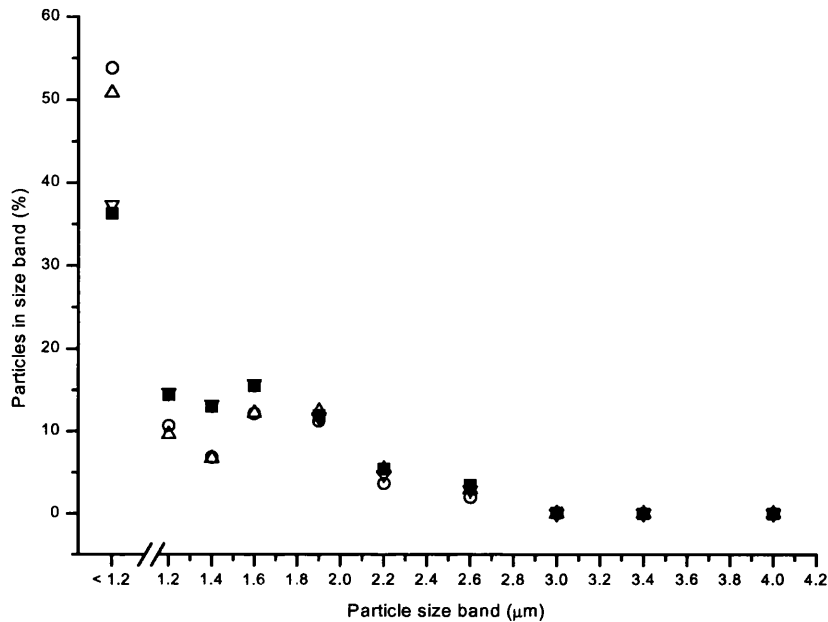


Figure 42 The effect of shear rate (unsheared control (■), $3.24 \times 10^6 \text{ s}^{-1}$ (○), $9.59 \times 10^5 \text{ s}^{-1}$ (Δ) and $4.05 \times 10^5 \text{ s}^{-1}$ (∇)) on the particle size distribution of a suspension of *E. coli* RV308 pHKY531 cells ($2 \times 10^8 \text{ cells mL}^{-1}$).

From the data present in this section it can be seen that shear does have a major effect on material passing through capillary leaks. The damage to cells is considerable and Carlson (Carlson *et al.*, 1995) has found that if cells are subject high shear rates and an air liquid interface such as during nebulisation, complete degradation of any plasmid DNA will occur where high proportions of whole cells are broken. This suggests that any release from a leak will have a degree of shear damage dependent on the differential pressure driving the release and the size of the leak path. As such, a high pressure release is unlikely to generate a bioaerosol with a high microbial viability, rather a bioaerosol of easily inhaled particles (Crook, 1992). This could then be considered an allergenic hazard as opposed to an infectious one. As key pieces of bioprocess equipment have the potential to generate high shear forces, in particular homogenisers and centrifuges, the effect of shear on the components of a release should be considered when designing a contained process.

7. Discussion Of Bioprocess Leak Detection And Containment Validation

In the pharmaceutical and biotechnology industries contamination of processes and products can be the result of poor containment and operating procedures. The primary objective of this thesis was to establish a test method that can generate quantitative data on releases from bioprocess that could then be used to validate their containment. This has been achieved through the correlation of an SF₆ tracer gas leak test with a QPCR assay for the detection of GMMOs. A model system with variable orifice sizes and leak path lengths was developed for the simulation of bioprocess releases and data on the release of a micro-organisms through small orifices has been correlated with the response of the tracer gas detection system. The correlation of this data has been used to define a permissible leak rate of SF₆ above which a leak may be large enough to allow the transmission of a biological particle. From a search of published material there has been little discussion of defining a critical leak size (Perowski *et al.*, 1983; Baram, 1991). The problem that leaks cause has been discussed in relation to vacuum equipment (Beavis, 1970; Reich, 1987; Tison, 1993), where permeation and molecular leaks can be a particular problem. However in the research presented here (section 6.3) an attempt to define a critical leak size for a bioprocess has been made. A leak diameter of 3 µm has been defined as the critical size for the prevention of the transmission of micro-organisms across a process boundary. A leak this size may allow the transmission of a virus particle though this, but is thought to be unlikely due to effects of the bulk fluid that the particle would contained in. Baram (Baram, 1991) uses a critical hole size of 0.41 µm based on the flow of water through a capillary a 7 bar differential pressure. This is approximately an order of magnitude lower than the critical leak diameter assumed from this research and it results from the higher differential pressure used for the leak testing and the difference in tracer gas. For a leak test at 2 bar differential pressure the release of gas through a 5 mm long 3 µm diameter leak would be $6 \times 10^{-6} \text{ cm}^3 \text{ min}^{-1} \text{ SF}_6$ or $2 \times 10^{-6} \text{ cm}^3 \text{ min}^{-1} \text{ He}$ (Baram, 1991). The problem with specifying a critical leak diameter for bioprocess equipment is that the length of the leak and the differential pressure between the two environments are important factors in determining the transmission of a fluid. To overcome this leak detection tests are carried out at a fixed pressure with a defined limit of release for the acceptance criteria of a detected leak. It has been proposed that leak detection for

bioprocess equipment should be carried out at 2 bar differential pressure with an acceptance criterion of less than $6 \times 10^{-6} \text{ cm}^3 \text{ min}^{-1} \text{ SF}_6$. This provides far greater sensitivity than a pressure hold test and it can be applied to most bioprocess equipment. The advantage of using a higher differential pressure is that smaller leak diameter can be identified, but not all bioprocess equipment can be pressurised above 2 bar. As valves are a common source of release (Bello and Sigell, 1997) they are often more highly specified during any *ex situ* test (Baram, 1991) to prove their integrity. A recommended approach to containment validation would be that upon installation each piece of equipment is leak tested and the values for tracer gas release at key points recorded to provide a baseline for future reference. These could be used as indicators of deterioration in valves, connectors and seals, thereby enabling preventative action to be taken prior to a release event occurring.

During the research presented in this thesis the leak geometry has been assumed to be cylindrical. In reality this assumption may not be true and the leak path may be more tortuous and of a non uniform cross section. The effect of leak cross section geometry has been discussed by Rogal (Rogal, 1978) and Steckelmacher (Steckelmacher, 1978). From their research non-cylindrical leaks tend to have lower flow rates due to variations in pressure along the length of the leak. With respect to bioprocesses this can produce leaks that block more easily as particles get trapped at constrictions or the pressure is insufficient to propagate the movement of a capillary of liquid through a tortuous path. During a leak test it is likely that a tracer gas will pass through tortuous leaks far more readily than a liquid, leading Rogal (Rogal, 1978) to advise pneumatic testing of vessels.

At the present time the Biosafety legislation uses qualitative statements to define quantitative events, such as minimising or preventing a release (HSE, 1992). This has resulted in a common approach to containing a piece of equipment through increasing its primary containment, for example by the addition of steam tracing to valves. This additional feature adds another degree of equipment complexity, which in turn could bring with it an increased chance of miss-operation, potentially resulting in an accident (Dowell and Hendershot, 1997). Yet the addition of steam tracing or double seals may do nothing to reduce the occurrence of leaks from a system. Miller and Bergmann (Miller and Bergmann, 1993) put forward a view that the public could perceive the over designing of high containment facilities as exhibiting a lack of confidence in a particular

operation or facility. Whilst it should be acknowledged that some bioprocesses require high containment, more appropriate engineering approaches such as described by Brooks and Russell (Brooks and Russell, 1986) should be advocated. When adopting a unified approach to equipment design it should be noted that a sterile environment is one in which no micro-organisms exist that are capable of growth, compared with a contained system where no transmission of material across a process boundary is possible. This type of unified design can lead to a more economic process as long as the difference between containment and sterility is recognised.

It has been shown (section 5) that the exhaust gas of a fermentation releases micro-organisms equivalent to 50 μL of cell broth in its unfiltered exhaust gas over 10 hours. In a year, assuming a third of the time the bioreactor is operational, the release would be equivalent to 14.6 mL. If it can be assumed that the absolute filter attached to an exhaust gas stream functions correctly then this release should be reduced to zero. The design of bioreactors is crucial to the safety of a bioprocess as it is the bioreactor that is the most likely source of a release of biological material (Leaver and Hambleton, 1992). However accidents do happen and simply dropping a shake flask could result in a larger release of material than the release from unfiltered exhaust gas. This brings into question the need to design processes and equipment for the prevention of incidental and accidental releases. The failure for some industrial activities has been calculated by Israeli (Israeli, 1986) and Jefferis and Schlager (Jefferis and Schlager, 1986), a summary of their findings is given in Table 22.

Table 22 The failure probabilities of some industrial items and operations.

Item or activity	Failure probability (per hour of operation)	Reference
Human error	$10^{-2} - 10^{-3}$	Israeli, 1986
Failure of sensing elements	$10^{-3} - 10^{-5}$	Israeli, 1986
Failure of diaphragm valve	10^{-5}	Jefferis and Schlager, 1986
Failure of mechanical seal	10^{-5}	Jefferis and Schlager, 1986
Failure of steam valve	10^{-6}	Jefferis and Schlager, 1986
Failure of containment	10^{-6}	Jefferis and Schlager, 1986

From Table 22 it can be seen that the biggest source of failure in a process is the human operator. Human error can be split into two groups; those relating to specific operations, and those relating to general activities (Tweeddale, 1992). Where specific activities encompass plant maintenance and general activities relate to management and supervisory weakness which cause mistakes. The subject of risk and risk analysis is vast and has been well discussed by Montague (Montague, 1990), reviewed by Sherif (Sherif, 1991) and applied to industrial biotechnology by Kastelein (Kastelein *et al.*, 1992). Kastelein (Kastelein *et al.*, 1992) concludes that the quantification of risks associated with biotechnology are considerably more complicated than for conventional chemical industries. Predominantly this difficulty stems from a lack of information on the incidental and accidental releases from bioprocess. To generate quantitative information on bioprocess releases the cyclone is considered an ideal device for short term sampling of large volumes of air (Kastelein *et al.*, 1992). Through the generation of quantitative data a hazard can be identified and then the risk it poses assessed and managed. An unidentified hazard can not be managed or is in effect only managed by chance (Schumacher *et al.*, 1997). In a perfectly contained process there is balance between the procedures, training and design that enables containment to be achieved and maintained. This has been described as a biocontainment triangle (Miller and Bergmann, 1993) where a weakness in any of the three sides results in the loss of containment. The development of effective leak detection systems for bioprocesses enables appropriate designs to be used that minimise complexity and reduce the occurrence of errors due to failures in training or supervisory procedures.

8 Proposed Future Research and Recommendations.

The development of a method for the quantification of airborne microbial releases, combined with a tracer gas technique for the detection of leaks, has enabled a proposed maximum release rate of SF₆ to be set for the validation of bioprocess containment. From section 7, SF₆ leak detection for bioprocess equipment should be carried out at 2 bar differential pressure with an acceptance criterion of less than $6 \times 10^{-6} \text{ cm}^3 \text{ min}^{-1} \text{ SF}_6$. This value was established through the use of capillary leaks and as such there is scope to apply the methods detailed in this document to existing bioprocess equipment, with a view to revising this figure. A revision of the maximum tolerated SF₆ release rate can only be made once quantitative data can be gathered. From the application of detailed leak detection studies to bioprocess equipment more specific criteria could be set. For example, a homogeniser, may require a lower limit, because a smaller leak could be penetrated due to the higher operating pressures employed in its use. An aspect of future work should look at the leak testing of bioprocess equipment besides that of simple vessels. With the production of quantitative data steps can be taken to revising containment regulations which are based on qualitative statements. The UK GMO Contained use Regulations are due for revision by 5 June 2000 and a simplified risk assessment is one of the proposals under discussion. With little quantitative data still available it is hard to see how unidentified risks can be effectively evaluated. In such a situation containment regulations will remain qualitative and safety through over engineering will stay common practice.

Within the use of the methods described here, there is scope for technical improvement (Table 23).

Table 23 Potential technical improvements to the methods used in this research project.

Method/Equipment	Potential Improvements
Cyclone air sampling	Use of computational fluid dynamics to improve sampling site selection Cyclone redesign to decrease precession effects Disposable cyclones to prevent residual DNA carry-over
QPCR	Use of generic primers to broaden detection Automation of process (thermal cycling and analysis)
SF ₆ Detection	More accurate / broader detection range

The technical improvements possible would increase the data quality from experimental procedures. By providing automated processes errors that may occur due to manipulation or contamination could be reduced. This would also reduce the skill level required to perform these procedures making them more easily adopted in a production environment.

Aerosolisation of simple liquids is a relatively well understood process. Within a bioprocess most liquids contain particles of various sizes and characteristics, making the aerosolisation more complex. Preliminary experiments have been carried out to investigate the effect of secondary aerosolisation from splashing, but this type of work could be broadened to include the release event. The value of such research would come from a better understanding of what a bioaerosol is made up of (whole cells, cell fragments, naked DNA, media components), and from this a better understanding of the hazard it poses.

Appendix 1 List Of Suppliers

Adolf Kuhner Ag, Basel, Switzerland
Agma plc, Haltwhistle, Northumberland, UK
Ai Cambridge Ltd., Cambridge, UK
Air Control Installations, Chard, Somerset, UK
Anachem, Luton, Bedfordshire, UK
Bassaire Ltd., Swanwick, Southampton, UK
BDH Laboratory Suppliers, Merk Ltd., Poole, Dorset, UK
Beckman Instruments, High Wycombe, Buckinghamshire
Bioengineering Ag, Wald, Switzerland
Biolog Inc., Hayward, California, USA
BOC, Guildford, Surrey, UK
Broadley James Corporation, Santa Ana California, USA
Celsis Ltd., Cambridge, UK
Costar, Cambridge, Massachusetts, USA
Domnick Hunter, Birtley, Co. Durham, UK
Elwyn E. Roberts Isolators Ltd., Market Drayton, Shropshire, UK
Fisons Instruments, Middlewich, Cheshire, UK
Fisons Scientific Equipment, Loughborough, Leicestershire, UK
Gelman, Ann Arbor, Michigan, USA
GeneTrak Systems, Framingham, Massachusetts, USA
GenProbe, San Diego, California, USA
Gibco BRL Life Technologies, Uxbridge, Middlesex, UK
Glen Creston Ltd., Stanmore, Middlesex, UK
Guardine Disposables Ltd., Brandon, Suffolk, UK
Hays Chemical, Leeds, UK
Hybaid, Teddington, Middlesex, UK
Ilford, Mobberley, Cheshire, UK
Incelltech (UK) Ltd., Reading, UK
Malvern Instruments, Cambridge, UK
MDH Ltd., Andover, Hampshire, UK
MSE, Crawley, Sussex, UK
New Brunswick, Edison, New Jersey, USA

New England Biolabs, Beverly, Massachusetts, USA
Nikon, Kingston upon Thames, Surrey, UK
Oxoid, Unipath Ltd., Basingstoke, Hampshire, UK
Perkin Elmer, Foster City, California, USA
Pharmacia, Milton Keynes, Bedfordshire, UK
Promega, Madison, Wisconsin, USA
Qiagen, Chatsworth, California, USA
Research Instruments, Penryn, Cornwall, UK
Sigma, Poole, Dorset, UK
Sigma Laboratory Centrifuges, Osterode, Harz, Germany
Silverson Machines Ltd., Chesham, Bucks., UK
Smith Ltd., London, UK
Soham Scientific, Soham, Cambridgeshire, UK
Stratagene, La Jolla, California, USA
Teledyne Hastings-Raydist, Hampton, Virginia, USA
Testo Ltd., Alton, Hampshire, UK
Th. Goldschmidt Ltd., Milton Keynes, Bedfordshire, UK
TSI Incorporated, Milton Keynes, UK
UVP Ltd., Cambridge, UK
Warren Spring Laboratories, now AEA Technology, Harwell, Didcot, UK
Watson-Marlow, Falmouth, Cornwall, UK
Weber Scientific International Ltd., Teddington, Middlesex, UK
William Pearson Chemicals, Coventry, UK

Appendix 2 Aerojet General Cyclone Dimensions

The Aerojet General Cyclone used during the course of this project is shown in Figure 43.

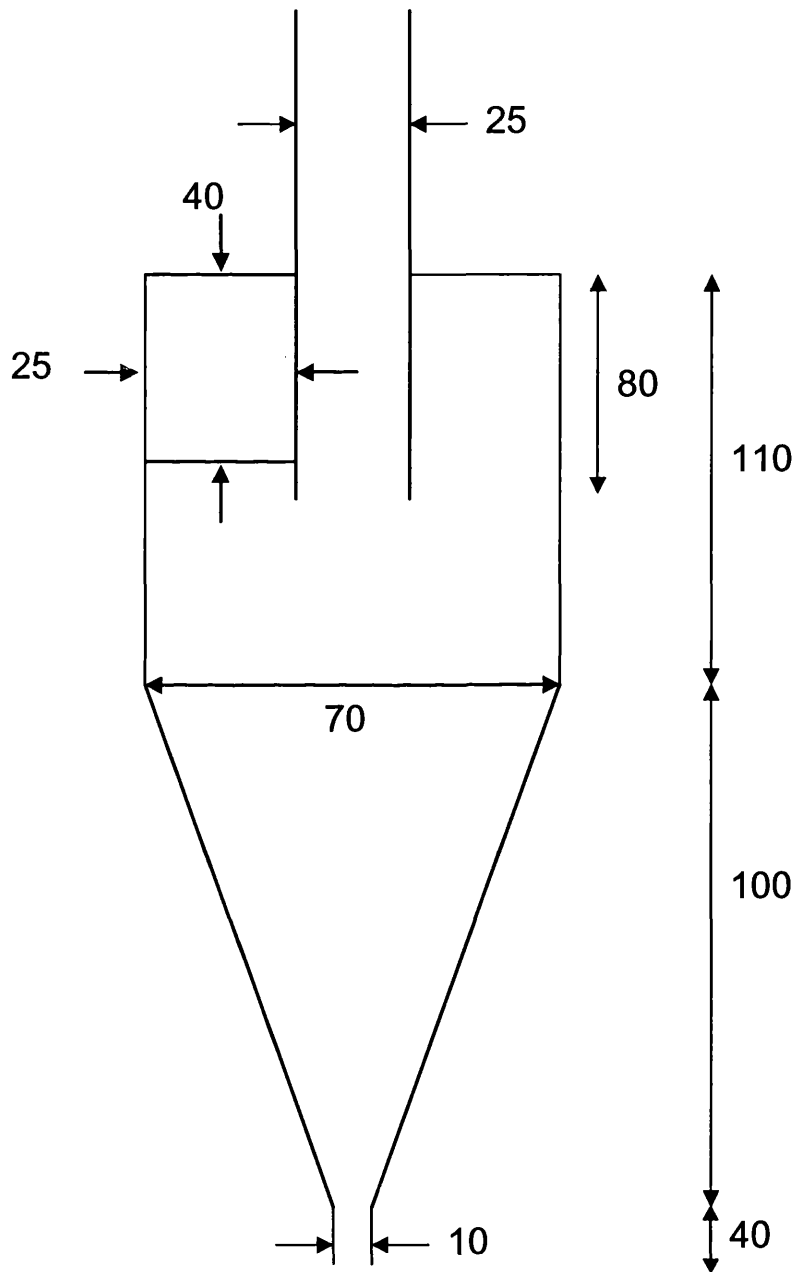


Figure 43 Diagram of an Aerojet General Cyclone (all dimensions in mm). The shading represents the air inlet of the cyclone which rises 50 mm from the plane of the page and terminates with a female BS32/29 quick-fit adapter.

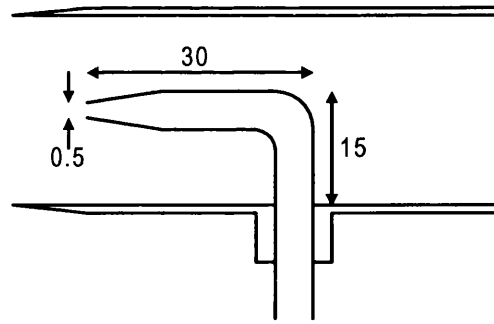


Figure 44 Cross section of the wash liquid injection attachment, connected to the aerojet general cyclone via a male B32/29 quick-fit adapter (all dimensions in mm).

Appendix 3 Calculation Of pHKY531 Concentration

Agarose gel electrophoresis

After the PCR cycle has completed the PCR product mix is run on an agarose gel to separate the products.



Figure 45 Agarose gel showing the results of a QPCR of a sample containing an unknown concentration of pHKY531. Lane 1 contains IS(B) 1 and the sample, Lane 2 contains IS(B) 2 and the sample, Lane 3 contains the molecular weight marker (PCR Marker, Sigma).

From Figure 45 it can be seen that the plasmid concentration in lane 2 is not in the range of IS(B) 2 as there is no distinct band for the internal standard, making quantification from this lane impossible. Lane 1 is chosen for densitometry analysis as two bands are clearly visualised on the gel.

Densitometry Analysis

Densitometry provides a method of analysis of the gel that can give the ratio of pHKY531 and IS(B) 1 band intensities. A spectrum of band intensity for the lane under analysis is produced and the peak area for the bands under analysis can be established (Table 24).

Table 24 Densitometry analysis of lane 1 (Figure 45).

Band Identity	PEAK AREA (ARBITRARY UNITS)
pHKY531	1100
IS(B) 1	235

Calculation of the pHKY531 concentration

The standard IS(B) 1 has a linear range for quantification described by the regression analysis of the standard curve.

$$\text{Log (peak area ratio (IS(B):pHKY531))} = 3.12 - (0.86 \times \text{Log [pHKY531]})$$

$$\text{Therefore the log (peak area ratio (IS(B):pHKY531))} = -0.67$$

Substituting this value into the regression analysis for IS(B) 1 and solving for pHKY531 concentration gives

$$\text{Log [pHKY531]} = (3.12 - (-0.67))/0.86$$

$$\text{therefore Log [pHKY531]} = 4.41$$

therefore [pHKY531] = 2.6×10^4 molecules in 10 μL of sample.

Appendix 4 Particle Size Analysis Of Sheared Cells

The three figures (Figure 46, Figure 47 and Figure 48) presented here show the change in particle size distribution created by the effect of various shear rates. The samples were sheared by passage through capillaries of fixed diameter at various flow rates in a capillary rheometer. A summary and discussion of these figures can be found in section 6.5.

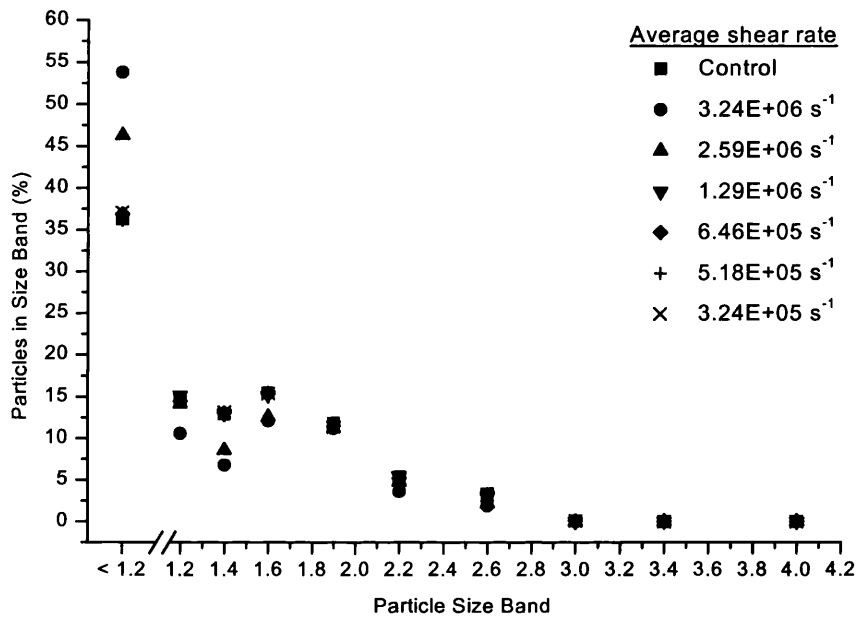


Figure 46 The particle size distribution for an *E. coli* RV308 pHKY531 cell suspension (2×10^5 cells mL⁻¹) passed through a 100 μ m diameter capillary at various flow rates.

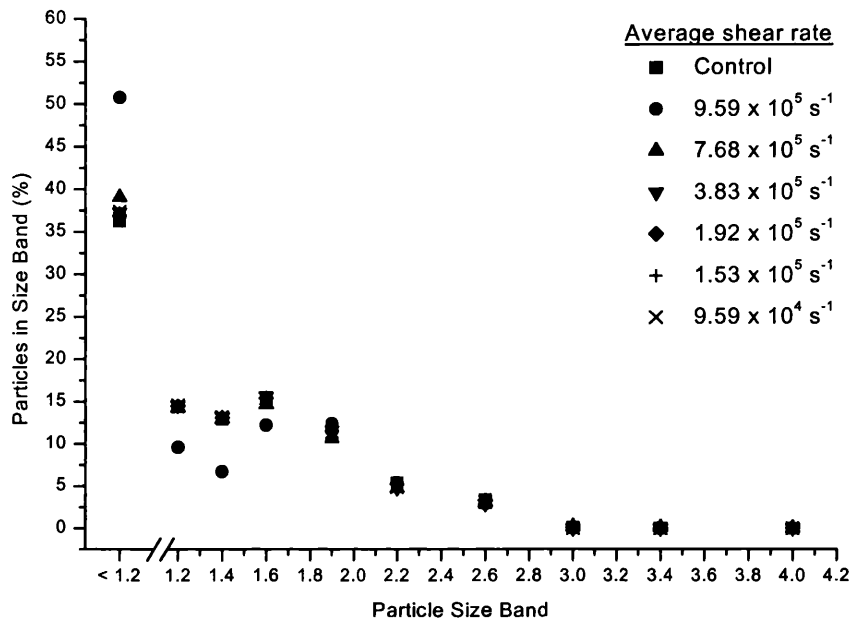


Figure 47 The particle size distribution for an *E. coli* RV308 pHKY531 cell suspension (2×10^5 cells mL^{-1}) passed through a 150 μm diameter capillary at various flow rates.

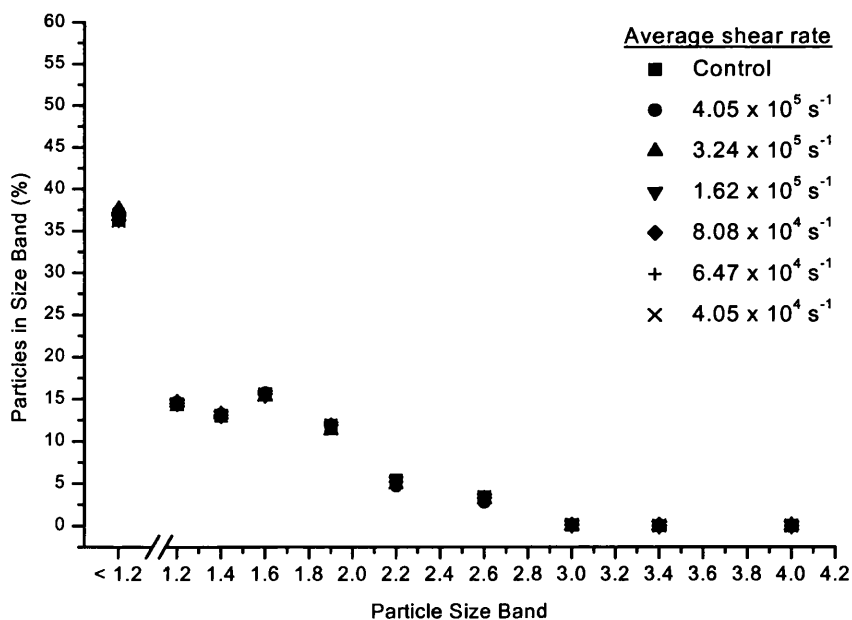


Figure 48 The particle size distribution for an *E. coli* RV308 pHKY531 cell suspension (2×10^5 cells mL^{-1}) passed through a 200 μm diameter capillary at various flow rates.

Appendix 5 Particle Size Calculations

Calculation of the d_{50}

From the static particle theory of Barth (Barth, 1956) Iozia and Leith (Iozia and Leith, 1990) gave the Equation 7 as means of predicting the d_{50} of airborne particles within the body of a cyclone.

Equation 7 Static particle prediction of d_{50}

$$d_{50} = \sqrt{\frac{(9\mu Q)}{(\pi\rho_p z_c Vt_{\max}^2)}}$$

Where:

Q gas flow (ms^{-1})

μ viscosity (Pa s)

Vt_{\max} maximum tangential velocity (ms^{-1})

ρ_p particle density (Kg m^3)

z_c vortex core length (m)

When Equation 7 was evaluated a d_{50} of 15.1 μm was derived.

Calculation of the Sauter Mean Diameter (SMD)

In plain-jet airblast atomisers, a liquid jet is exposed to a high velocity air stream. The high velocity air stream impinges on the liquid as it exits the atomiser nozzle producing an aerosol. Harari and Sher (1997) reviewed the relationship of airblast atomisers to various operational parameters.

Equation 8 Calculation of the SMD from empirically derived parameters

$$\text{SMD} = \left[0.95 \frac{(\sigma_f m_f)^{0.33}}{V_r \rho_f^{0.37} \rho_a^{0.30}} + 0.13 \mu_f \left(\frac{d_0}{\sigma_f \rho_f} \right)^{0.5} \right] \left(1 + \frac{m_f}{m_a} \right)^{1.70}$$

Where:

d_0 orifice diameter (mm)

m mass flow rate (Kg s^{-1})

- V velocity (ms^{-1})
 ρ density (Kg m^3)
 σ surface tension (N m^{-1})

and subscripts are air (a), liquid (f) and relative (r)

This relationship was shown by Harair and Sher (1997) to be accurate ($\pm 8\%$) for water and air in the range of air velocity between 70 and 180 ms^{-1} , m_a/m_f between 1 and 16 and d_0 between 0.4 and 1.58 mm . In the experimental work contained in this thesis the air velocity was approximately 58 ms^{-1} , the mass flow rate ratio 11.8 and the orifice diameter 0.5 mm . The mass flow rate is outside the optimum range for the precise correlation of SMD to the operational parameters, but was considered close enough for a good approximation.

Equation 9 Solution of Equation 8 for typical operational parameters

$$\text{SMD} = \left[0.95 \left(\frac{(0.07 \times 0.000167)^{0.33}}{(57.958 \times 1400^{0.37} \times 1.2^{0.3})} \right) + 0.13 \times 0.72 \times 10^{-6} \left(\frac{0.003}{0.07 \times 1400} \right)^{0.5} \right] \times \left(1 + \frac{0.000167}{0.00197} \right)^{1.7}$$

This resolves to a SMD of $28 \mu\text{m}$ with a flow rate of 1 ml min^{-1} of liquid.

References

ACGM, (1987a). *ACGM/HSE/Note 4, Guidelines for health surveillance of those involved in genetic manipulation at laboratory and large scale.* Advisory Committee on Genetic Manipulation, HMSO, London.

ACGM, (1987b). *ACGM/HSE/Note 6, Guidelines for the large-scale use of genetically manipulated organisms.* Advisory Committee on Genetic Manipulation, HMSO, London.

ACGM, (1988). *ACGM/HSE/Note 7 Guidelines for the categorisation of genetic manipulation experiments.* Advisory Committee on Genetic Manipulation, HMSO, London.

ACGM, (1993). *ACGM/HSE/DOE/Note 7, Guidelines for the risk assessment of operations involving the contained use of genetically modified micro-organisms,* Advisory Committee on Genetic Manipulation, HMSO, London.

Adams AP, Spendlove JC, (1970). Coliform aerosols emitted by sewage treatment plants. *Science*, **169**, 1218-1220.

Alvarez AJ, Buttner MP, Stetzenbach LD, (1995). PCR for bioaerosol monitoring: sensitivity and environmental interference. *Applied and Environmental Microbiology*, **61**(10), 3639-3644.

Anderson AA, (1958). New sampler for the collection, sizing and enumeration of viable airborne particles. *Journal of Bacteriology*, **76**, 471-484.

Ashcroft J, Pomeroy NP, (1983). The generation of accidents which may occur during plant scale production of micro-organisms. *Journal of Hygiene, Cambridge*, **91**, 81-101.

- Bae G, Kinney PD, Liu BY, Pui DYH, (1998). Investigation of aerosol spatial distributions downstream of a critical orifice at low pressure. *Aerosol Science and Technology*, **28**, 479-488.
- Baram D, (1991). Valves for high containment applications. *ASME Bioprocess Engineering Symposium, BED*, **21**, 79-86.
- Barth W, (1956). Berechnung und Auslegung von zyklonabscheidern auf grund neuerer untersuchungen. *Brennstoff warme kraft*, **8**(1), 1-9.
- Beavis LC, (1970). Real leaks and real leak detection. *Vacuum*, **20**(6), 233-245.
- Bej AK, Ng WY, Morgan S, Jones DD, Mahbubani MH, (1996). Detection of viable *Vibrio cholerae* by reverse transcriptase polymerase chain reaction (RT-PCR). *Molecular Biotechnology*, **5**, 1-10.
- Bellow CE, Siegell JH, (1997). Why valves leak: a search for the cause of fugitive emissions. *Environmental Progress*, **16**(1), 13-15.
- Benbough JE, Bennett AM, Parks SR, (1993). Determination of the collection efficiency of a microbial sampler. *Journal of Applied Bacteriology*, **74**,170-173.
- Bennett AM, (1994). Health hazards in biotechnology. In *Biosafety in industrial biotechnology* (Hambleton *et. al.* eds.). Blackie Academic and Professional, Bury St. Edmunds, pp 109-128.
- Berg P, Baltimore D, Boyer HW, Cohen SN, Davis RW, Hogness DS, Nathans D, Roblin R, Watson JD, Weissman S, Zinder ND, (1974). Potential hazards of recombinant DNA molecules. *Science*, **185**, 303.
- Berg P, Baltimore D, Brenner S, Roblin RO, Singer M, (1975). Asilomar Conference on recombinant DNA molecules. *Science*, **188**, 991-994.
- Bloomer RN, (1973). Leaks. *Vacuum*, **23**(7), 231-238.

- Bowman RD, Davidson N, (1972). Hydrodynamic shear breakage of DNA. *Biopolymers*, **11**, 2601-2624.
- Brooks CH, Russell PD, (1986). A unified design approach to fermenter sterility and containment. *Process Biochemistry*, **June**, 77-80.
- Brüel & Kjær Innova, (1997). *Application Note, Monitoring sulphur hexafluoride in the power utility industry*. [Http://www.innova.dk/applikat/sf6mon/sf6mon.htm](http://www.innova.dk/applikat/sf6mon/sf6mon.htm)
- BSI, (1988). BS6755 Part 1 Testing of valves. BSI, London.
- Bürkholz A, (1985). Approximation formulae for particle separation in cyclones. *German Chemical Engineering*, **8**, 351-358.
- Burrows G, (1961). Flow through and blockage of capillary leaks. *Transactions of IChemE*, **39**, 55-63.
- Cameron R, Hambleton P, Melling J, (1987). Assessing the microbial integrity of biotechnology equipment. In *Separations for biotechnology*, eds. Verrall MS, Hudson MJ. Ellis Horwood, Chichester, pp 490-496.
- Carlson A, Signs M, Liermann L, Boor R, Jim Jem K, (1995). Mechanical disruption of *Escherichia coli* for plasmid recovery. *Biotechnology and Bioengineering*, **48**, 303-315.
- Carvell JP, (1992). Sterility and containment considerations in valve selection. *Pharmaceutical Engineering*, **12**(1),
- Chan A, Zhao J, Kraiden M, (1994). Polymerase chain reaction kinetics when using a positive internal control target to quantitatively detect cytomegalovirus target sequences. *Journal of Virology Methods*, **48**, 223-236

- Chexal VK, Quiñones DF, Horowitz J, (1992). Validation of leak-rate model for leak-before-break applications. *Service Experience and Life Management in Operating Plants, American Society of Mechanical Engineers, PVP 240*, 67-74.
- Clarke LV, Bainbridge H, Beck SBM, Yates JR, (1997). Measurement of fluid flow rates through cracks. *International Journal of Pressure Vessels and Piping*, **71**, 71-75.
- Cockshott AR, (1993). *Modelling of recombinant E. coli fermentations at medium and high cell density producing BST*. PhD Thesis, University of London, London.
- Collins N, Lafreniere PJ, (1994). On-line reactor building integrity testing at Gentilly 2 (summary of results 1987-1994). *Proceedings of the Annual Canadian Nuclear Association*, Vol. 1.
- Colwell RR, Brayton PR, Grimes DJ, Roszak DB, Huq SA, Palmer LM, (1985). Viable but non-culturable *Vibrio cholerae* and related pathogens in the environment: implications for release of genetically engineered micro-organisms. *Biotechnology*, **3**, 817-820.
- Colwell RR, Somerville C, Knight I, Staube W, (1988). Detection and monitoring of genetically-engineered micro-organisms. In *The Release of Genetically-engineered Micro-organisms*, eds. Sussman M, Collins CH, Skinner FA, Stewart-Tull DES. Academic Press, London. pp. 47-60.
- Cook W, (1996). Personal Communication, Eli Lilly and company, Speke operations, Liverpool.
- Cox CS, (1966). The survival of *Escherichia coli* sprayed into air and into nitrogen from distilled water and from solutions of protecting agents, as a function of relative humidity. *Journal of General Microbiology*, **43**, 383-399.
- Cox CS, (1989). Airborne bacteria and viruses. *Scientific Progress, Oxford*, **73**, 469-500

Cremer JC, Warner AM, (1982). *Risk analysis of six hazardous industrial projects in the Rijnmond area*. Elsevier, Amsterdam.

Crook B, Cottam AN, (1996). The current status of monitoring for process micro-organisms in biotechnology: results of an industry questionnaire. *Annals of Occupational Hygiene*, **40**(2), 223-232.

Crook B, (1992). Exposure to airborne micro-organisms in the industrial workplace. *Journal of Aerosol Science*, **23**, S559-S562.

Decker HM, Buchanan LM, Frisque DE, (1969). Advances in large volume air sampling. *Contamination Control*, **8**, 13-17.

Dickson A, (1996). Regulatory concerns and prospects in the European Union: an industry view. *Current Opinion in Biotechnology*, **7**, 273-274.

Dirgo J, Leith D, (1985a). Cyclone collection efficiency: Comparison of experimental results with theoretical predictions. *Aerosol Science and Technology*, **4**, 401-415.

Dirgo J, Leith D, (1985b). Performance of theoretically optimised cyclones. *Filtration and Separation*, **March/April**, 119-125.

Dobrowolski ZC, (1988). Low pressure gas flow. In *Fluid Mechanics Source Book*, ed. Parker SP. McGraw-Hill Inc, New York. pp. 89-98.

Dols WS, Persily AK, (1995). A study of ventilation measurement in a office building. In *Airflow Performance Of Building Envelopes, Components And Systems*, ASTM STP 1255, eds. Modera MP, Persily AK. ASTM, Philadelphia. pp. 23-46.

Dowell AM, Hendershot DC, (1997). No good deed goes unpunished: case studies of incidents and potential incidents caused by protective systems. *Process Safety Progress*, **16**(3), 132-139.

Dunnill P, (1982). Biosafety in the large-scale isolation of intracellular microbial enzymes. *Chemistry and Industry*, Nov., 879-881.

Dwivedy KK, (1989). An application of leak-before-break in plant improvement. *High Pressure Engineering and Technology, American Society of Mechanical Engineers, PVP 165*, 85-87.

EC, (1990a). 90/679 EEC Directive on the protection of workers from the risks related to exposure to biological agents at work. *Official Journal of the European Communities*, **33**, 31 Dec. 1990, L374, 1-12.

EC, (1990b). 90/219 EEC Directive on the deliberate release to the environment of genetically modified organisms. *Official Journal of the European Communities*, **33**, 8 May 1990, L117, 1-14.

EC, (1990c). 90/220 EEC Directive on the contained use of genetically modified organisms. *Official Journal of the European Communities*, **33**, 8 May 1990, L117, 15-27.

EC, (1994). 94/51 EC Directive adapting to technical progress Council Directive 90/219/EEC on the contained use of genetically modified micro-organisms. *Official Journal of the European Communities*, **29**, 18 November 1994, L297, 15-27.

Ehrlich R, Miller S, Walker RL (1970). Relationship between atmospheric temperature and survival of airborne bacteria. *Applied Microbiology*, **19**(2), 245-249.

Errington FP, Powell EO, (1969). A cyclone separator for aerosol sampling in the field. *Journal of Hygiene, Cambridge*, **67**, 387-399.

Fannin KF, Spendlove JC, Cochran KW, Gannon JJ, (1976). Airborne coliphages from wastewater treatment facilities. *Applied and Environmental Microbiology*, **31**(5), 705-710.

Ferre F, (1992). Quantitative or semi-quantitative PCR: reality versus myth. *PCR methods and applications*, **2**, 1-9.

Ferris LE, (1995). *Microbial population balancing for containment specification*. PhD Thesis, University of London, London.

Ferris LE, Keshavarz-Moore E, Leaver G, Noble M, Turner MK, (1995). Microbial population balancing as a quantitative aid for evaluating release from a high pressure homogeniser. *Transactions of the IChemE*, **73B**, 182-188

Forster E, (1994). An improved general method to generate internal standards for competitive PCR. *BioTechniques*, **16**, 18-20.

French C, Ward JM, (1995). Improved production and stability of *E. coli* recombinants expressing transketolase for large scale biotransformations. *Biotechnology Letters*, **17**, 247-252.

Gause WC, Adamovicz J, (1994). The use of the PCR to quantitate gene expression. *PCR Method Applications*, **3**, s123-s135.

Gebhardt A, Peters A, Gerding D, Niendorf A, (1994). Rapid quantitation of mRNA species in ethidium-bromide stained gels of competitive RT-PCR products. *Journal of Lipid Research*, **35**, 976-981.

Gilliland G, Perrin S, Blanchard K, Bunn HF, (1990a). Analysis of cytokine mRNA and DNA: detection and quantitation by competitive polymerase chain reaction. *Proceedings of the National Academy of Science*, **87**, 2725-2729.

Gilliland G, Perrin S, Bunn HF, (1990b). Competitive PCR for quantitation of mRNA. In *PCR Protocols: A guide to methods and applications*, eds. Innis MA, Gelfand DH, Sninsky JJ, White TJ. Academic Press San Diego. pp. 60-69.

Grebner H, (1995). Results of a bench mark test on the crack opening and leak rate calculation. *International Journal of Pressure Vessels and Piping*, **65**, 35-39.

Griffiths WD, Boysan F, (1992). An assessment of the application of computational fluid dynamics (CFD) to model the performance of a range of small sampling cyclones. *Journal of Aerosol Science*, **23**, S587-S590.

Griffiths WD, Boysan F, (1996). Computational fluid dynamics (CFD) and empirical modelling of the performance of a number of cyclone samplers. *Journal of Aerosol Science*, **22**(2), 281-304.

Griffiths WD, DeCosemo GAL, (1994). The assessment of bioaerosols: a critical review. *Journal of Aerosol Science*, **25**(8), 1425-1458.

Grinshpun SA, Willeke K, Ulevicius V, Juozaitis T, Terzieva S, Donnelly J, Stelma GN, Brenner KP, (1997). Effect of impaction, bounce and reaerosolisation on the collection efficiency of impingers. *Aerosol Science and Technology*, **26**(4), 326-342.

Hage JHC, Wessels HRA, (1980). In *Naturzkunde van de Atmosfeer*, ed. Wolzers. Noordhof, Crøningen. pp. 42-43.

Hambleton P, Bennett AM, Leaver G, Benbough JE, (1992). Biosafety monitoring devices for biotechnology processes. *Trends in Biotechnology*, **10**, 192-199.

Harari R, Sher E (1997). Optimisation of a plain-jet airblast atomiser. *Atomisation and Sprays*, **7**, 99-113.

Harper GJ, Hood AM, Morton JD (1958). Airborne micro-organisms: a technique for studying their survival. *Journal of Hygiene, Cambridge*, **56**(3), 364-370.

Hinds WC, (1982). *Aerosol technology: properties, behaviour and measurement of airborne particles*. John Wiley and Sons Inc., New York.

Horrell RS, Deem M, Wyckoff P, Shair F, Crawford N, (1989). Ground release SF₆ tracer experiments used to characterise transport and dispersion of atmospheric

pollutants during the southern California air quality study of 1987. *Air and Waste Management Conference Proceedings.*, **8**, 2-25.

HSC, (1988). *Control of Substances Hazardous to Health Regulations 1988, Approved Codes of Practice*. HMSO, London.

HSC, (1994). *Control of Substances Hazardous to Health Regulations 1994, Approved Codes of Practice*. HMSO, London.

HSE, (1992). *A Guide to the Genetically Modified Organism (Contained Use) Regulations 1992*. HMSO, London.

HSW (1974). *Health and Safety at Work etc. Act, 1974*. HMSO, London.

Islam MS, Hasan MK, Miah MA, Sur GC, Felsenstein A, Venkatesan M, Sack RB, Albert MJ, (1993). Use of the polymerase chain reaction and fluorescent-antibody methods for detecting viable but non-culturable *Shigella dysenteriae* type 1 in laboratory microcosms. *Applied and Environmental Microbiology*, **59**, 536-540.

Israeli E, (1986). Biosafety in biotechnological processes. *Advances in Biotechnological Processes*, **6**, 1-30.

Iozia LD, Leith D, (1989). Effect of cyclone dimensions on gas flow pattern and collection efficiency. *Aerosol Science and Technology*, **10**, 491-500.

Iozia LD, Leith D, (1990). The logistic function and cyclone fractional efficiency. *Aerosol Science and Technology*, **12**, 598-606.

Janson JK, (1995). Tracking genetically engineered micro-organisms in nature. *Current Opinion in Biotechnology*, **6**, 275-283.

Jefferis RP, Schlager ST (1986). Using fault tree analysis methods to improve bioreactor safety. *Annals of New York Academy of Sciences*, **469**, 53-62.

- Kastelein J, Logtenberg MT, Stobbelar MF, Boot H, ten Veen J, (1989). *Containment validation of a continuous centrifuge*. TNO report The assessment of risks in scaled-up biotechnological processes.
- Kastelein J, Deans JS, Logtenberg MT, Hesselink PGM, Stewart IW, (1992). Risk assessment in industrial biotechnology. *Agro-Industry Hi-Tech*, **May/June**, 26-28.
- Kim JC, Lee KW, (1990). Experimental study of particle collection by small cyclones. *Aerosol Science and Technology*, **12**, 1003-1015.
- Kricka LJ, (1995). *Nonisotopic probing, blotting and sequencing*, 2nd ed., Academic Press Inc., San Diego.
- Knudsen GR, (1989). Model to predict aerial dispersal of bacteria during environmental release. *Applied and Environmental Microbiology*, **55**(10), 2641-2647.
- König C, Büttner H, Ebert F, (1991). Design data for cyclones. *Particle and Particle Systems Characterisation*, **8**(4), 301-307.
- Lapple LE, (1950). Gravity and centrifugal separation. *Industrial Hygiene Quarterly*, **11**, 40.
- Leaver G, Hambleton P, (1992). Designing bioreactors to minimise or prevent inadvertent release into the workplace and natural environment. *Pharmaceutical Technology International*, **April**, 18-26.
- Leith D, Licht W, (1972). The collection efficiency of cyclone type particle collectors, a new theoretical approach. *Annual IChemE Symposium Series*, **126**(68), 196-207.
- Levy MS, Collins IJ, Yim SS, Ward JM, Titchener-Hooker N, Ayazi Shamlou P, Dunnill P, (1998). Effect of shear on plasmid DNA in solution. *Bioprocess Engineering*, received 5/1/98, accepted for publication.

Lighthart B, Kim J, (1989). Simulation of airborne microbial droplet transport. *Applied and Environmental Microbiology*, **55**(9), 2349-2355.

Lighthart B, Mohr AJ, (1987). Estimating downwind concentrations of viable airborne micro-organisms in dynamic atmospheric conditions. *Applied and Environmental Microbiology*, **53**(7), 1580-1583.

Lighthart B, Shaffer BT, Marthi B, Ganio L, (1991). Trajectory of aerosol droplets from sprayed bacterial suspension. *Applied and Environmental Microbiology*, **57**(4), 1006-1012.

Lindblad NR, Schneider JM, (1965). Production of uniform sized droplets. *Journal of Sci. Instrum.*, **42**, 635-638.

Lundholm IM, (1982). Comparison of methods for quantitative determinations of airborne bacteria and evaluation of total viable counts. *Applied and Environmental Microbiology*, **44**(1), 179-183.

Macher JM, First MW, (1984). Personal air samplers for measuring occupational exposures to biological hazards. *American Industrial Hygiene Association Journal* **45**(2), 76-83.

Mahon J, Lax AJ, (1993). A quantitative polymerase chain reaction method for the detection in avian faeces of salmonellas carrying the *spvR* gene. *Epidemiology and Infection*, **111**, 455-464.

Marthi B, Fieland VP, Walter M, Seidler RJ, (1990). Survival of bacteria during aerosolisation. *Applied and Environmental Microbiology*, **56**(11), 3463-3467.

Matsumoto K, Nakamura S, Gotoh N, Narabayashi T, Tanaka Y, Horimizu Y, (1989). Study on coolant leak rates through pipe cracks: part 2 - pipe test. *High Pressure Engineering and Technology, American Society of Mechanical Engineers, PVP 165*, 113-120.

- Matsumoto K, Nakamura S, Gotoh N, Narabayashi T, Miyano H, Furukawa S, Tanaka Y, Horimizu Y, (1991). Study on crack opening area and coolant leak rates on pipe cracks. *International Journal of Pressure Vessels and Piping*, **46**, 35-50.
- Maunz M, Buttner H, (1994). Particle collection by small cyclones as a function of flow rate, geometric dimensions and particle size. *Journal of Aerosol Science*, **25**(1), s457-s458.
- May KR, Druett H, (1953). *British Journal of Industrial Medicine*, **10**, 142. cited In *Air Sampling Instruments*, 7th edition, ed. Hering SV. American Conference of Governmental and Industrial Hygienists, Cincinnati. pp. 208
- May KR, (1966). A multi-stage liquid impinger. *Bacteriology Reviews*, **30**, 559-570.
- May KR, (1967). Physical aspects of sampling airborne microbes. In *Airborne Microbes*, 17th Symposium of the Society of General Microbiology, eds. Gregory PH and Mantertin JL. Cambridge University Press, Cambridge. pp. 60-80.
- May KR, Pomeroy NP, Hibbs S, (1976). Sampling techniques for large windborne particles. *Journal of Aerosol Science*, **7**, 53-62.
- McCulloch RK, Choong CS, Hurley DM, (1995). An evaluation of competitor type and size for use in the determination of mRNA by competitive PCR. *PCR Method Applications*, **4**, 219-226.
- McMaster RC, (1982). Non-destructive testing handbook, Vol. 1, Leak testing, 2nd edition. American Society For Metals.
- Miller SR, Bergmann D, (1993). Biocontainment design considerations for biopharmaceutical facilities. *Journal of Industrial Microbiology*, **11**, 223-234.
- Montague DF, (1990). Process risk evaluation - what method to use? *Reliability Engineering and System Safety*, **29**, 27-53.

Moore ME, McFarland R, (1993). Performance modelling of single-inlet aerosol sampling cyclones. *Environmental Science and Technology*, **27**, 1842-1848.

Mukoda TJ, Todd LA, Sobsey MD, (1994). PCR and gene probes for detecting bioaerosols. *Journal of Aerosol Science*, **25**(8), 1523-1532.

Narabayashi T, Ishiyama, Fujii M, Matsumoto K, Horimizu Y, Tanaka Y, (1989). Study on coolant leak rates through pipe cracks: part 1 - fundamental test. *High Pressure Engineering and Technology, American Society of Mechanical Engineers, PVP 165*, 121-127.

Neef A, Amman R, Shleifer KH, (1995). Detection of microbial cells in aerosols using nucleic acid probes. *Systemic and Applied Microbiology*, **18**, 113-122.

Nerken A, (1989). History of leak testing. *Materials Evaluation*, **47**, 1268-1272.

Noble M, (1996). *Measurement of bioprocess containment by quantitative polymerase chain reaction*. PhD Thesis, University of London, London.

Noble M, Ward JM, Buss AD, Turner MK (1997). Measurement of bioprocess containment by high flow air rate sampling and quantitative polymerase chain reaction. *Biosafety*, **3**, paper 5, URL:<http://www.bdt.org.br/bioline/by>

Nomura Y, Hopke PK, Fitzgerald B, Mesbah B, (1997). Deposition of particles in a chamber as a function of ventilation rate. *Aerosol Science and Technology*, **27**, 62-72.

Norris KP, (1994). Physical aspects of the uncontrolled release of material in biotechnology operations. In *Biosafety in industrial biotechnology*, eds., Hambleton P, Melling J, Salusbury TT. Blackie Academic and Professional, Bury St. Edmunds. pp. 90-108.

Nugent PG, Cornett J, Stewart IW, Parkes HC, (1997). Personal monitoring of exposure to genetically modified micro-organisms in bioaerosols: rapid and sensitive detection using PCR. *Journal of Aerosol Science*, **28**(3), 525-538.

OECD, (1986). *Recombinant DNA safety Considerations. Safety Considerations for Industrial, Agricultural and Environmental Applications of Organisms Derived by rDNA Techniques*. Organisation for Economic Co-operation and Development, Paris.

Perowski CA, Daransky GR, Williams J, (1983). Detection of microscopic leaks in fermenter cooling coils. *Biotechnology and Bioengineering*, **26**, 857-859.

Pennman I, (1989). Bioreactors: Technical considerations in containment. In *Proceedings of the DTI/HSE/SCI Symposium on Large-scale Bioprocessing safety*, ed. Salusbury TT. Warren Spring Laboratory Report LR746(BT), Stevenage, pp. 63-70.

Podzimek J, (1989). John Aitken's contribution to atmospheric and aerosol sciences - one hundred years of condensation nuclei counting. *Bulletin of the American Meteorological Society*, **70**, 1538-1545.

Radich J, (1996). The promise of gene quantification. *Trends in Biotechnology*, **14**, 145-147.

RCEP, (1989). *The Release of Genetically Engineered Organisms to the Environment*, 13th Report of the Royal Commission on Environmental Pollution, HMSO, London.

Reich G, (1987). Leak detection with tracer gases; sensitivity and relevant limiting factors. *Vacuum*, **37**(8/9), 691-698.

Riffat SB, Cheong KW, (1993). Measurement of ventilation and aerosol particles in buildings. *International Journal of Energy Research*, **17**, 45-55.

Robens' Report (1972). Safety and Health at Work. *Report of the committee 1970-1972 (Chairman Lord Robens)*. HMSO, London.

Rogal VF, (1978). Coarse models of capillary leakages and test leaks. *Soviet Journal of Non-destructive Testing*, **14**(5), 470-472.

Roth A, (1972). The molecular-viscous intersection point and its use in determining the size and density of flow paths. *Vacuum*, **22**(6), 219-224.

Sambrook J, Fritsch EF, Maniatis T, (1989). *Molecular cloning: a laboratory manual*. Cold Spring Harbour Laboratory Press, Cold Spring Harbour.

Sarkar G, Kapelner S, Sommer SS (1990). Formamide can dramatically improve the specificity of PCR. *Nucleic Acid Research*, **18**(24), 7465.

Sarkar G, Sommer SS, (1990). Shedding light on PCR contamination. *Nature*, **343**, 27.

Seliverstov MI, (1992). Use of sulphur hexafluoride as the tracer gas in leak detection. *Soviet Journal of Non-destructive Testing*, **8**, 599-604.

Sherif YS, (1991). On risk and risk analysis. *Reliability Engineering and System safety*, **31**, 155-178.

Shumacher R, Pitblado R, Selmer-Olsen S, (1997). Next generation risk management. *Process Safety Progress*, **16**(2), 69-71.

Singer M, Soll D (1973). Guidelines for DNA hybrid molecules. *Science*, **181**, 1114.

Stairmand CJ, (1951). The design and performance of cyclone separators. *Transactions of the IChemE*, **29**, 256-383.

Steckelmacher W, (1978). The effect of cross-sectional shape on the molecular flow in long tubes. *Vacuum*, **28**(6/7), 269-275.

Steffan RJ, Atlas RM, (1991). Polymerase chain reaction: applications in environmental microbiology. *Annual Reviews in Microbiology*, **45**, 137-161.

Stetzenbach LD, Lighthart B, Seidler RJ, Hern SC, (1992). Factors influencing the dispersal and survival of aerosolised micro-organisms. In *Microbial Ecology*,

Principles, Methods and Applications, eds. Levin MA, Seidler RJ, Rogul M. McGraw-Hill, New York. pp. 455-465.

Stewart GSAB, (1990). *In vivo* bioluminescence: new potentials for microbiology. *Letters in Applied Microbiology*, **10**, 1-8.

Sundfors C, Collan Y, (1996). Basics of quantitative polymerase chain reaction: 2 electrophoresis and quantitation of polymerase chain reaction products. *Electrophoresis*, **17**, 44-48.

Swift P, (1986). An empirical approach to cyclone design and application. *Filtration and Separation*, **Jan/Feb**, 24-27.

Szewczyk KW, Lehtimaki M, Pan MJ, Krishnan U, Willeke K, Elliot DD, Muth WL, (1991). Measurement of the change in aerosol size distribution with bacterial growth in a pilot scale fermenter. *Biotechnology and Bioengineering*, **39**, 243-245.

Thomas CR, Dunnill P, (1979). Action of shear on enzymes: studies with catalase and urease. *Biotechnology and Bioengineering*, **21**, 2279-2302.

Tilton JN, (1997). Fluid and particle dynamics. In *Perry's Chemical Engineering Handbook, 7th Edition*, eds. Perry RH and Green DW. McGraw-Hill, New York. Section 6.

Tinnes R, Hoare M, (1992). The biocontainment of a high speed disc bowl centrifuge. *Bioprocess Engineering*, **8**, 165-172.

Tison SA, (1993). Experimental data and theoretical modelling of gas flows through metal capillary leaks. *Vacuum*, **44**(11/12), 1171-1175.

Tuijnburg Muijs G, Apontoweil P, Harrewijn GA, Houwink EH, Vranck SP, van Sprang H, Tiesjema RH, (1987). Air and surface contamination during microbiological processing. *Swiss Biotechnology*, **5**, 43-49.

Turner MK (1989). Categories of large-scale containment for manufacturing processes with recombinant organisms. In *Biotechnology & Genetic Engineering Reviews, Vol. 7*, eds. Russell GE, Tombs MPs. Intercept, Andover. pp. 1-43.

Tweeddale HM, (1992). Balancing quantitative and non-quantitative risk assessment. *Transactions of the IChemE*, **70(B)**, 70-74.

Upton SL, Mark D, Douglass EJ, Hall DJ, Griffiths WD, (1994). A wind tunnel evaluation of the physical sampling efficiencies of three bioaerosol samplers. *Journal of Aerosol Science*, **25**, 1493-1501.

US Bureau of Mines, (1995). Predictive Capabilities of SF₆ tracer gas in face ventilation analysis. *Journal of the Mine Ventilation Society of South Africa*, **48(3)**, 54-61.

Whaley RS, Ellul IR, (1994). Considerations in choosing a leak detection method. *ASME Pipeline Engineering*, **60**, 39-44.

Willeke K, Lin X, Grinshpun SA, (1998). Improved aerosol collection by combined impaction and centrifugal motion. *Aerosol Science and Technology*, **28(5)**, 439-456.

Young TM, (1993). How well do leak detection methods work? Preliminary results from the EPA test procedures. In *Leak detection for underground storage tanks, ASTM 1161*, eds. Durgin PB, Young TM. American Society for Testing and Materials, Philadelphia. pp. 139-150.

Zhang Z, Al-Rubeai, M, Thomas CR, (1993). Estimation of disruption of animal cells by turbulent capillary flow. *Biotechnology and Bioengineering*, **42**, 987-993.

Zimmerman NJ, Reist PC, Turner AG, (1987). Comparison of two biological aerosol sampling methods. *Applied & Environmental Microbiology*, **53(1)**, 99.